Vol. 65 • No. 9
September 2022

Microwave® Journal

horizon house®
Founded in 1958
mwjournal.com

DC TO 65 GHZ

RF & Microwave Test Solutions

Get More Out of Your Test Setup

Software Controlled Building Blocks and RF Interface Units

Custom Test Systems

Test Accessories

Flexible

- Wide selection of components in stock from DC to 67 GHz
- Start small and expand and reconfigure as your needs change
- Use our software or yours. User-friendly GUI included or develop your own software with LabVIEW®, MatLab®, Python®, C#, C++ or VB.

Reliable

- All components and assembled systems fully tested and characterized in-house
- 50+ years quality, manufacturing and supply chain expertise

Affordable

- High-performance without breaking the bank
- Get more functionality and capacity without heavy investment in additional high-end instrumentation

Fast

- Wide selection of solutions in stock for immediate shipment
- Modular systems allow quick, user-defined hardware configuration
- Industry's fastest turnaround times on custom systems

RF-LAMBDA
THE LEADER OF RF BROADBAND SOLUTIONS
BROADBAND SSPA / EMC BENCHTOP
SOLID STATE POWER AMPLIFIER
0.1-22GHZ
ULTRA BROADBAND SSPA
RFLUPA01M22GA
4W 0.1-22GHZ
RFLUPA0218GB
20W 1-19GHZ
300W 6-18GHZ SOLID STATE BROADBAND
400W 8-11GHZ
SOLID STATE BROADBAND
0.1-6GHZ VHZ,
UHF, L, S, C BAND
RFLUPA02G06GC
100W 2-6GHZ
RFLUPA0706GD
30W 0.7-6GHZ
MADE IN
USA
6-18GHZ C, X, KU BAND
RFLUPA08G11GA
50W 8-11GHZ
RFLUPA0618GD
60W 6-18GHZ
RFLUPA06G12GB
25W 6-12GHZ
18-50GHZ K, KA, V BAND
RFLUPA18G47GC
2W 18-47GHZ
RFLUPA27G34GB
15W 27-34GHZ
RFLUPA47G53GA2
10W 47-53GHZ
RFLUPA27G34GB
30W 18-40GHZ
BENCHTOP RF MICROWAVE SYSTEM POWER AMPLIFIER
RAMP00G06GA- 30W 0.01-6GHZ
RAMP39G48GA- 4W 39-48GHZ
RAMP01G22GA- 8W 1-22GHZ
RAMP27G34GA- 8W 27-34GHZ
www.rflambda.com
sales@rflambda.com
1-888-976-8880
1-972-767-5998
San Diego, CA, US
Carrollton, TX, US
Ottawa, ONT, Canada
Frankfurt, Germany

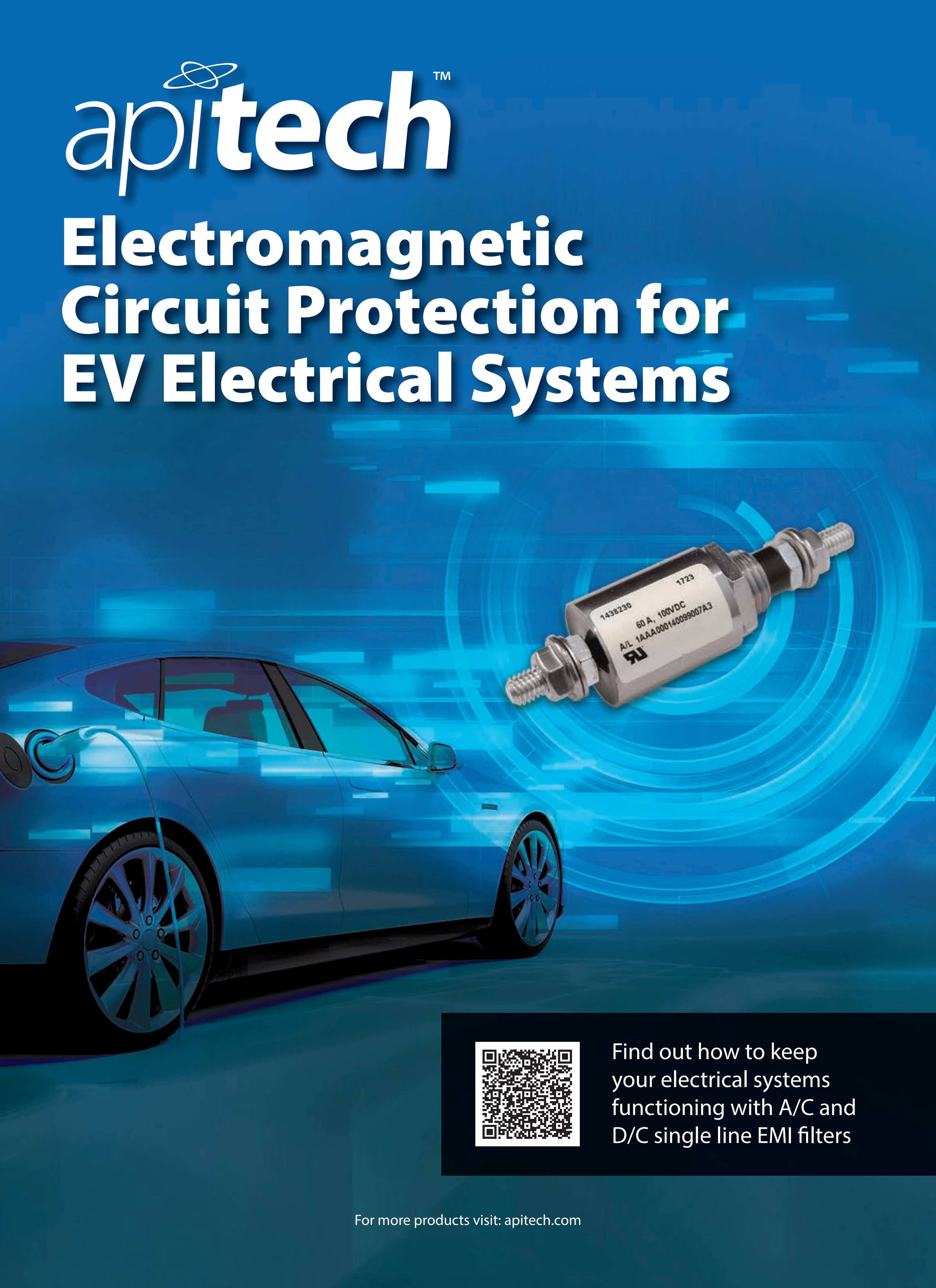
apitech™
Electromagnetic Circuit Protection for EV Electrical Systems
Find out how to keep your electrical systems functioning with A/C and D/C single line EMI filters
For more products visit: apitech.com


Relax
We've got you covered
NOISEWAVE
NW18G-23CS
+28 VDC
OUTPUT
060401
MADE IN USA
NOISEWAVE
NW346B Precision
10M - 18GHz
082399
MAX REV PWR 1W
BIAS
+28VDC
MADE IN THE USA
NOISEWAVE
NW18G-15CS
+28 VDC
OUTPUT
060401
MADE IN USA
NOISEWAVE
NW6G-D
060912
NOISEWAVE
NW2G-15CS
+28 VDC
OUTPUT
060401
GND
MADE IN USA
NOISEWAVE
NW3G-M
OUTPUT
+12 VDC
GND
-12 VDC
MADE IN USA


NOISEWAVE

Quantic PMI
PLANAR MONOLITHICS

- Amplifiers - Solid State
- Attenuators - Variable / Programmable / Fixed
- Bi-Phase Modulators
- Couplers (Quadrature, 180°, Directional)
- Detectors - RF / Microwave
- Filters & Switched Filter Banks
- Form, Fit, Functional Products & Services
- Frequency Converters
- Frequency Sources
- Frequency Discriminators & IFM
- Frequency Synthesizers
- Gain & Loss Equalizers
- Integrated MIC/MMIC Assemblies (IMAs)
- IQ Vector Modulators
- Limiters - RF / Microwave
- Log Amps
- Miscellaneous Products
- Monopulse Comparators
- Multifunction Integrated Assemblies (IMAs)
- Phase Shifters & Bi-Phase Modulators
- Power Dividers/Combiners (Passive & Active)
- Pulse Modulators - SPST
- Rack & Chassis Mount Products
- Receiver Front Ends & Transceivers
- Single Side Band Modulators
- SMT & QFN Products
- Switch Matrices
- Switch Filter Banks
- Switches - Solid-State
- Systems - Radar Sense & Avoid
- Systems - Fly Eye Radar
- Threshold Detectors
- USB Products

COAXIAL MONOPULSE COMPARATORS

- Designs for Beamforming Antenna Applications up to 21.2 GHz
- High power handling with minimum insertion loss
- High Isolation between Channel Ports for Optimum Phase & Amplitude Balance
- Rugged Coaxial Design
- Form, Fit, Function & Custom Package Designs
- Custom Designs for Narrowband & Specified Frequencies
- Military or Aerospace Screening

See more at: https://www.pmi-rf.com/categories/monopulse-comparators


MPC-20R2G21R2G-CD-LNF


PMC-24-7D5-SFF


PMC-2D22D4-6D8-SFF


PMC-3G3D5G-6D8-SFF


PMC-33D7-6D8-SFF

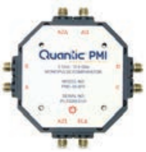
PMC-56-SFF

PMI Model No.	Frequency Range (GHz)	Gain (dB)	Noise Temperature	Phase Balance	Size (Inches) Connectors
MPC-20R2G21R2G-CD-LNF	20.2 - 21.2	0 to +10	100 K	±3°	6.25" x Ø4.8" x 2.0" SMA (F)

PMI Model No.	Frequency Range (GHz)	Insertion Loss (dB)	Isolation (dB)	Phase Balance	Amplitude Balance (dB)	Size (Inches) Connectors
PMC-24-7D5-SFF	2 - 4	7.5	18	±10°	±1.0	3.23" x 3.23" x 0.43" SMA (F)
PMC-2D22D4-6D8-SFF	2.2 - 2.4	6.8	25	±5°	±0.4	3.563" x 3.563" x 0.433" SMA (F)
PMC-3G3D5G-6D8-SFF	3 - 3.5	6.8	23	±5°	±0.4	3.23" x 3.23" x 0.43" SMA (F)
PMC-33D7-6D8-SFF	3 - 3.7	6.8	24	±7°	±0.5	3.23" x 3.23" x 0.43" SMA (F)
PMC-56-SFF	5 - 6	1.0	20	±5°	±0.5	2.60" x 2.60" x 0.43" SMA (F)
PMC-9G10G-7D9-SFF	9 - 10	7.9	18	±6°	±0.6	3.48" x 3.48" x 0.43" SMA (F)
PD-CD-001-1	9.3 - 9.9	8.0	30	±7°	±0.5	2.35" x 1.7" x 0.5" SMA (F)
PMC-9D5G10D1G-7D6-SFF	9.5 - 10.1	7.6	20	±5°	±0.5	3.48" x 3.48" x 0.43" SMA (F)
PMC-9D5G10D5G-7D6-SFF	9.5 - 10.5	7.6	20	±5°	±0.5	3.48" x 3.48" x 0.43" SMA (F)
PMC-12G13G-1D6-SFF	12 - 13	7.6	18	±5°	±0.5	3.48" x 3.48" x 0.43" SMA (F)
PMC-16G17G-SMA	16 - 17	1.6	18	±10°	±0.8	3.125" x 3.125" x 0.440" SMA (F)


PMC-9G10G-7D9-SFF


PD-CD-001-1


PMC-9D5G10D1G-7D6-SFF


PMC-9D5G10D5G-7D6-SFF


PMC-12G13G-1D6-SFF


PMC-16G17G-SMA

Quantic PMI
PLANAR MONOLITHICS

West Coast Operation:
4921 Robert J. Mathews Pkwy, Suite 1
El Dorado Hills, CA 95762 USA
Tel: 916-542-1401, Fax: 916-265-2597

East Coast Operation:
7311-F Grove Road
Frederick, MD 21704 USA
Tel: 301-662-5019, Fax: 301-662-1731

sales@pmi-rf.com • www.pmi-rf.com

ITAR Registered International Traffic in Arms Regulations

ISO 9001 International Organization for Standardization

Microwave Journal

CONTENTS

September 2022
Vol. 65 • No. 9
Automotive and Connected Vehicles
mwjournal.com

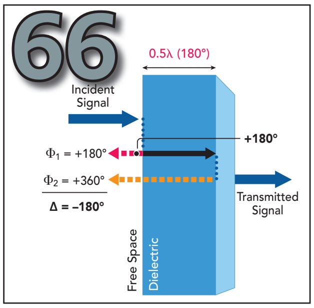

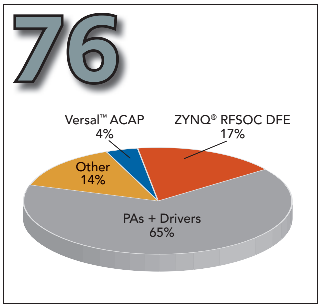

online spotlight

Look for this month's exclusive article online at mwjournal.com

RF Data Converter Performance and Evaluation Methods

Steven Norsworthy of RF2BITS

Cover Features

Technical Features

65 YEARS OF PUBLISHING EXCELLENCE

Qorvo® Ultra-Wideband

Enabling Seamless & Secure Ecosystems

Ultra-Wideband has been adopted into

40+

verticals across mobile, consumer, automotive & industrial

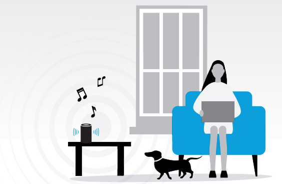

Spatial Awareness

Safety

Secure Transactions

Location Services

Why Qorvo?

- **We can help you** with expertise across 100s of applications in mobile, automotive, consumer and industrial
- **We have turnkey solutions and software** including low-latency/low power chips
- **We will take you to the next level,** investing in UWB R&D to enable your future applications and use cases
- **Join our tech forum,** the largest UWB technical community, with 3500+ engineers

Resources

Brochures & Ebooks

- Ultra-Wideband Brochure
- Ultra-Wideband For Dummies® Ebook

Blogs

- How Does Ultra-Wideband Work? Learn from Qorvo Experts
- Lights, Camera, Action! UWB is the Star Supporter in Le Premier Royaume
- Bringing the Bible to Life with Ultra-Wideband
- Location, Location, Location: The Road to Ultra-Wideband

Videos

- A Future Enabled by Ultra-Wideband
- UWB for Automotive: An Engineering Primer
- The Future is Ultra-Wideband

White Papers

- Getting Back to Basics with Ultra-Wideband

To learn more, visit **www.qorvo.com/go/uwb**

CONTENTS

mwjournal.com

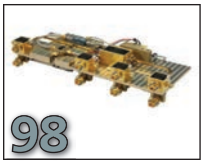

Tech Briefs

Departments

Microwave Journal (USPS 396-250) (ISSN 0192-6225) is published monthly by Horizon House Publications Inc., 685 Canton St., Norwood, MA 02062. Periodicals postage paid at Norwood, MA 02062 and additional mailing offices.

POSTMASTER: Send address corrections to Microwave Journal, PO Box 1028, Lowell, MA 01853 or e-mail mwj@e-circ.net.com. Subscription information: (978) 671-0446. This journal is issued without charge upon written request to qualified persons working in the RF & microwave industry. Other subscriptions are: domestic, $120.00 per year, two-year subscriptions, $185.00; foreign, $200.00 per year, two-year subscriptions, $370.00; back issues (if available) and single copies, $10.00 domestic and $20.00 foreign. Claims for missing issues must be filed within 90 days of date of issue for complimentary replacement.

STAFF

Publisher: Carl Sheffres
Associate Publisher: Michael Hallman
Editorial Director: Patrick Hindle
Editor: Gary Lerude
Managing Editor: Jennifer DiMarco
Associate Technical Editor: Cliff Drubin
Editorial & Media Specialist: Kelley Roche
Associate Editor: Emma Lutjen
Multimedia Staff Editor: Barbara Walsh
Electronic Marketing Manager: Chris Stanfa
Senior Digital Content Specialist: Lauren Tully
Digital Content Specialist: Alice Barry
Audience Development Manager: Carol Spach
Director of Production & Distribution: Edward Kiessling
Art Director: Janice Levenson
Graphic Designer: Ann Pierce

EUROPE
Office Manager: Nina Plesu

CORPORATE STAFF
CEO: William M. Bazzy
President: Ivar Bazzy
Vice President: Jared Bazzy

EXECUTIVE EDITORIAL OFFICE
685 Canton Street, Norwood, MA 02062
Tel: (781) 769-9750
FAX: (781) 769-5037
e-mail: mwj@mwjournal.com

EUROPEAN EDITORIAL OFFICE
16 Sussex Street, London SW1V 4RW, England
Tel: Editorial: +44 207 596 8730 Sales: +44 207 596 8740
FAX: +44 207 596 8749

SUBSCRIPTION SERVICES
Send subscription inquiries and address changes to:
Tel: (978) 671-0446
e-mail: mwj@e-circ.net

www.mwjournal.com

Printed in the USA

Microwave Journal ONLINE .COM

E LEARNING CENTER

5 Ways Our Filters Are Extending the Norm for Peak Performance
Sponsored by: RFMW and Knowles 9/13

Impacts of Solder Reflow on High Bandwidth RF Connectors: Everything's great until you apply solder!
Sponsored by: Samtec 9/14

Matching mmWave Radar Software Models to PCB Antenna Measurements
Sponsored by: Rogers Corp. 9/20

Catch *Frequency Matters*, the industry update from *Microwave Journal*,
microwavejournal.com/FrequencyMatters

WHITE PAPERS

- ABRACON — Why Use Planar Inverted-F Antennas (PIFA) for Compact IoT Devices
- ALTAIR — Electromagnetic Simulation for Electronic System Design in Aerospace and Defense
- ANALOG DEVICES (AHEAD OF WHAT'S POSSIBLE™) — Hybrid Beamforming Receiver Dynamic Range Theory to Practice
- CPI Communications & Power Industries — 4 kW X-Band Amplifier and Receiver Protector
- qorvo — 5G RedCap: RF Implications for IoT Devices
- MVG Microwave Vision Group — 5G BTS Advancing Technology and Hardware Dimensions Driving Test Lab Reconfigurations
- ROHDE&SCHWARZ Make ideas real

Executive Interviews

Signal Hound's new CEO, **Harrison Osbourn,** and president, **Tom Lane,** discuss the recent change in ownership, how they plan to build on the legacy of founder Bruce Devine and Signal Hound's new products.

Harrison Osbourn

Tom Lane

Jim Nevelle, president of **Prose Technologies North America**, describes the long lineage behind this new spin-off, its product and market focus and how it aims to stand out in a consolidated wireless market.

Jim Nevelle

Visit us @ mwjournal.com

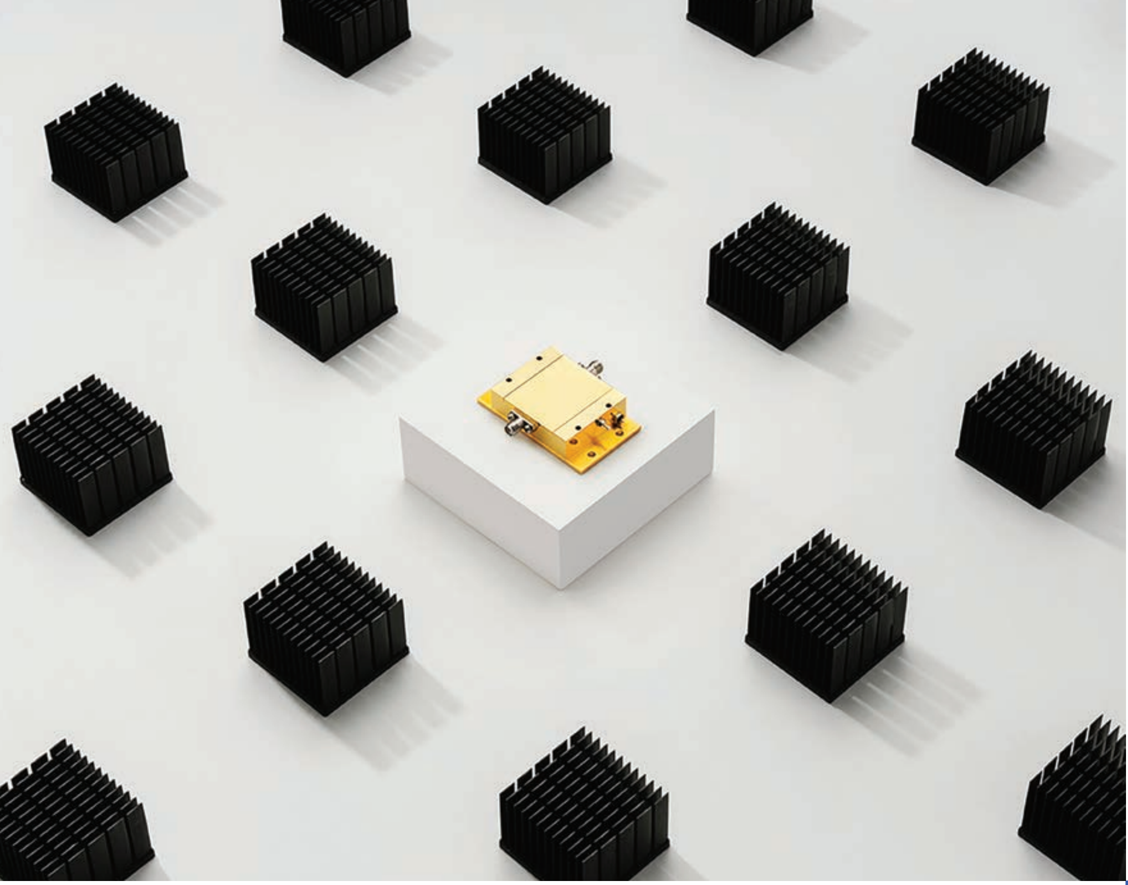

0.05 MHz TO 86 GHz

High-Frequency Amplifiers

Ultra-Wideband Performance

Features for Almost Any Requirement Now up to E-Band

- High gain, up to 45 dB
- Noise figure as low as 1.7 dB
- Output power up to 1W
- Rugged designs with built-in protections
- Wide DC input voltage range

NEW TO MARKET

ZVA-50953X+
- 45 to 95 GHz
- ±0.5 dB Gain Flatness

ZVA-543+
- 18 to 54 GHz
- ½W Saturated Output Power

Mini-Circuits®

MARK YOUR CALENDAR

STAY CONNECTED TO COMING EVENTS

SEPTEMBER

19-21
ECOC 2022
Messe Basel, Switzerland
www.ecocexhibition.com

19-23
IEEE HPEC 2022
Online
https://ieee-hpec.org

25-30
EuMW 2022
Milan, Italy
www.eumweek.com

25-30
International Test Conference
Disneyland, Anaheim, Calif. and Online
www.itctestweek.org

28-30
MWC Las Vegas
Las Vegas, Nev.
www.mwclasvegas.com

OCTOBER

9-14
AMTA 2022
Denver, Colo.
https://2022.amta.org

11-14
IEEE International Symposium on Phased Array Systems and Technology
Waltham, Mass.
https://array2022.org

16-19
BCICTS
Phoenix, Ariz.
https://bcicts.org

25-27
AOC International Summit
Washington, DC
www.crows.org/mpage/2022HOME

NOVEMBER

8-10
Global MilSatCom 2022
London, U.K.
www.smi-online.co.uk/defence/uk/conference/global-milsatcom

15-17
Space Tech Expo Europe
Bremen, Germany
www.spacetechexpo.eu

15-17
Mobility Connectivity Conference
Bremen, Germany
www.spacetechexpo.eu

Call for Papers Deadlines

9/23 GOMACTech 2023

10/14 IEEE Aerospace Conference 2023

12/6 IMS2023

Online Panel

9/21
Taking Automotive/Vehicle Radar Sensors to the Next Level for Safety and Sensing

FOR DETAILS VISIT MWJOURNAL.COM/EVENTS

Cover Feature
Invited Paper

Advanced Multi-Mode Multi-Mission Software-Defined mmWave Radar for Low Size, Weight, Power and Cost

Peter Fox
aiRadar Inc., Vancouver, Canada

Erik Ojefors
Sivers Semiconductors AB, Kista, Sweden

A series of advanced electronically scanned phased array (AESA) mmWave radars are designed with a multi-mode multi-mission software-defined radar (SDR) capability. These research radars address a variety of markets including advanced driver assistance systems (ADAS), fixed or mobile ground deployed small unmanned aerial vehicles (sUAVs) drone detection and tracking systems, sUAV air-to-air and air-to-ground radars and sUAV deployed airborne synthetic aperture radar (SAR). The radars are designed to facilitate radar research and development from early stage concept-of-operations through requirements definition and validation to system design, verification and deployment.

The radars are designed and manufactured by aiRadar Inc., using highly integrated, state-of-the-art RFICs from Sivers Semiconductors AB for the transmit/receive modules (TRMs). All are multi-mode multi-mission. They can switch seamlessly between a sector scanner covering 90 degrees in azimuth with better than 0.5 degrees angular resolution with triple baseline interferometric positioning in elevation, to a sUAV deployed single pass interferometric SAR (InSAR) with range and azimuth resolution better than 5 cm generating digital surface models (DSMs) with up to 16 channels of along track interferometry for high-resolution unambiguous moving target indication (MTI).

The InSAR configuration provides a multi-aperture SAR capability with displaced phase center antenna (DPCA) micronavigation. The radars range in size from the smallest model, with a mass of 3,850 grams comprising three transmit (Tx) and three receive (Rx) 64-element arrays, to the largest model, with a mass of less than 10 kg comprising 1,536 active elements in an identical array layout but with 256-element arrays.

The target customers are commercial, military and academic researchers who seek to advance the state-of-the-art in radar using a ruggedized reconfigurable

instrument rated to IP-67 and Mil-Std-810. Deploying these research radars with a simple but powerful compiled radar programming language (aiRPL), which executes on a field-programmable gate array based multi-mode radar processing unit (aiRPU), eliminates the risks associated with developing AESA radar systems based on analysis and simulation, either computer simulation or over-the-air validation using radar target simulators.

An ADAS developer might wish to perform an operational real-world comparison of various AESA configurations with different array sizes and with virtual or real array elements. These research radars permit, for example, the direct co-located and co-temporal comparison of a two Tx and four Rx MIMO array to a 12 Tx and 16 Rx MIMO array. Similarly, the 12 Tx and 16 Rx MIMO array (with 192 virtual channels) may be compared to a 256 Tx and 512 Rx array (with 512 real channels arranged as a long or medium baseline elevation interferometer). A simple script in aiRPL manages the complexity, enabling these three (or more radar configurations) to be cycled on a PRI-by-PRI basis, providing an objective comparison of radar performance under the same operating conditions.

Once the requirements and AESA configurations are validated for a specific application, the commercial, military or academic radar developer may proceed, based on the risk assessment, the economics or the urgency of time-to-market, with an in-house radar design or an aiRadar customized application specific radar. This can be done with or without the licensing of the aiRadar programming language compiler and the radar processing unit IP Core.

The aiRPU IP Core provides real-time bidirectional interfaces, up to 48 Gbps, to the lowest level in-phase and quadrature raw radar data channels, and to the aiRPU IP Core. This interface is provided for researchers and developers of cognitive adaptive (CA) radar allowing an external artificial intelligence (AI) processor, perhaps based on GPU arrays, to modify any or all of the radar configurations from transmit pulses to beamforming/steering directions on a PRI-to-PRI bases.

An example application is adaptive pulse code modulation (PCM) for ADAS in the inevitably congested radar environment that will exist as more radars are deployed in ever more advanced systems. The CA loop facilitates the analysis of received signals to determine if an interfering source (another vehicle) is present and select the PCM codes to reject that interference. This CA loop has applications in low probability of intercept (LPI) radars for military applications as well. A key feature of the CA physical and API interfaces is that the algorithms in the CA loop remain the exclusive intellectual property of their developers.

To facilitate the granting of experimental and research licenses, the first offering of these research radars has a center frequency at 66 GHz, where there is little commercial activity at this stage. The research radars are architected in such a manner that the digital control and RF interfaces to the TRMs enable hardware reconfiguration to 24 GHz with existing Sivers Semiconductors technology or reconfiguration to 76 to 81 GHz with future Sivers Semiconductors technology. The generalized TRM interfaces anticipate the emergence of new allocated mmWave frequency bands, should they arise.

ADAS

Given the ability of radar sensors to operate in conditions such as rain, fog and snow, which impairs or disables the operation of LiDAR sensors and visual cameras, it is inevitable that radar will become a fundamental element of ADAS.

Most radars currently deployed in automotive applications have very coarse resolution. While lower resolution radars may detect an object, a motorcycle, person or a truck, the object is represented by little more than a "blob." The task of object recognition is largely offloaded to an AI/machine earning (ML) algorithm, where advances in AI hardware and software algorithms are tasked with providing that one crucial step closer to a fully autonomous, safe vehicle.

There may be several reasons for this allocation of functionality and performance, but one likely contender may be that the requirements definition and validation, followed by the design and manufacture of advanced modern radar with complex AESA antennas is difficult. This difficulty translates into technical, performance, schedule and cost risk. Availability of low-cost and low risk advanced AESAs may enable changes to this allocation and, perhaps, advances in autonomy levels.

In addition to the design and manufacture of complex advanced AESA radars, verification and ongoing product assurance is not trivial and requires well-defined metrics. A simple requirement such as integrated sidelobe ratio (ISLR) impacts the angular resolution of two targets and the angular measurement accuracy of a single target, as well as having a significant impact on image quality. This lack of resolution and image quality may have a very negative impact on the AI/ML interpretation of the scene.

MILITARY AND COMMERCIAL RADAR SYSTEMS

A growing number of radar applications have emerged recently where current radars perform poorly or are not suitable. These applications include ground deployed (and human portable) real aperture radar for detecting and monitoring small drones which pose security and military threats as well as small UAV-deployed high-resolution imaging with SAR and/or real aperture radar (RAR).

A good example is InSAR deployed at the site of a flooding disaster where the desired product is high-resolution scenes superimposed on DSMs, captured in real time as riverbanks and slopes subside, with the identification of objects of interest with overlays of velocity vectors (MTI) attached to those objects.

Military applications are highlighted by the ongoing conflict in the Ukraine. Hostile drones are

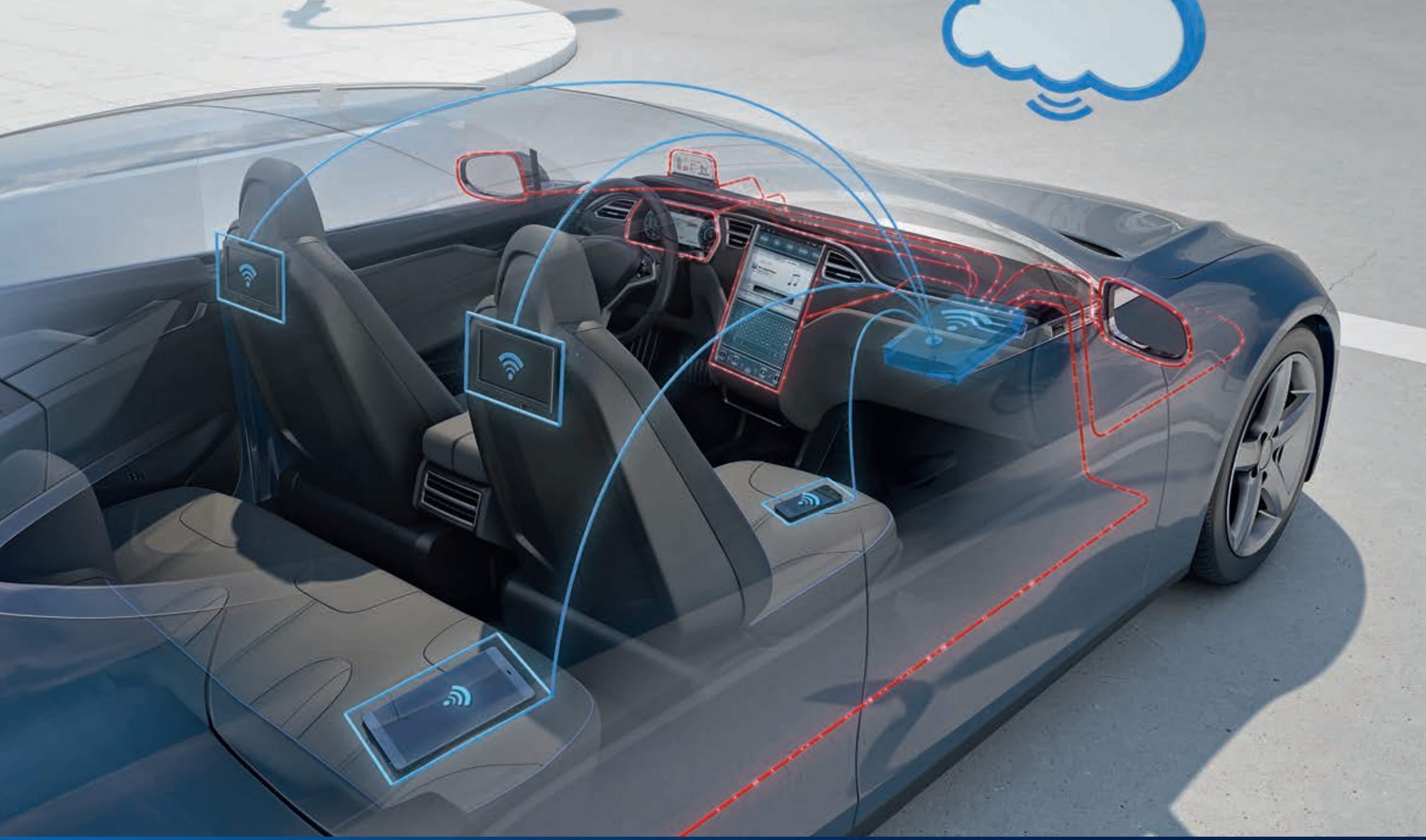

extremely dangerous: locating forces, providing intel on those forces, directing artillery fire with devastating accuracy and assessing damage. While the open literature shows many sUAV detection systems, these do not appear to have been effectively deployed as evidenced by multiple videos from loitering drones eliciting no evasive responses when artillery is spotted onto a target or when improvised weapons, such as modified rocket propelled grenades are dropped vertically onto targets from sUAVs.

SAR offers extremely high-resolution but requires motion, while RAR provides excellent image quality from a stationary position. A sUAV deployed SAR with 3D InSAR DSMs might be the preferred instrument for pre and post operation high-resolution threat and damage assessment, while an sUAV deployed RAR with an AESA may be better suited for real-time target spotting.

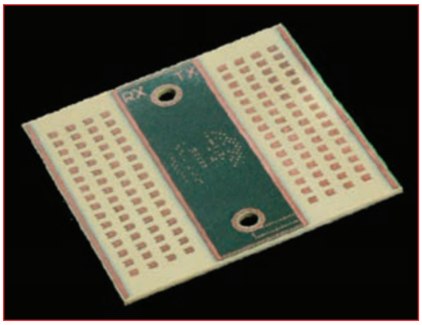

Fig. 1 **Antenna side of the Sivers Semiconductors transceiver.**

Fig. 2 **RRI-100 research radar interferometer.**

ARRAY ARCHITECTURE AND TRANSMIT RECEIVE MODULES

Addressing multiple applications, multiple modes and multiple missions with a SDR on a single hardware platform with a common interface as an economic and affordable solution is challenging. An early decision to implement a hybrid beamforming architecture, with analog beamforming at the level of 16 antenna elements and digital beamforming at a higher level, reduced the number of ADCs and data rates.

An investigation of available multi-channel mmWave technologies suitable for this hybrid architecture led to Sivers Semiconductors AB. Sivers Semiconductors develops, among other things, MMICs, modules and subsystems based on advanced semiconductor technology for WiGig mmWave networks.

The Sivers TRXBF01 RFIC is integrated into a module with a 16-element Tx and 16-element Rx arrays that covers 14 GHz of bandwidth from 57 to 71 GHz. The Sivers module has a transmit power of +11 dBm per channel and a receive noise figure of 7 dB in a 90-degree horizontally scanned AESA. ***Figure 1*** shows the front of the Sivers BFM01 module. These RFIC modules are supported by evaluation kits.

A customized version with interfaces for coherent multi-module AESAs with wide bandwidth modulation has been developed specifically for aiRadar. This device, the BFM06012-RFM, has a modulation input with 4 GHz of transmit bandwidth, enabling 5 cm range resolution. The vertical beamwidth is modified with tapering to produce a 30-degree beamwidth with sidelobe levels below -20 dB. aiRadar has integrated these modules into research radars, the smaller RRI-100 is shown in ***Figure 2***, the larger RRI-400 in ***Figure 3***.

In both figures, the Tx/Rx row pairs are visible in the radome window recesses, with a pair at the top of the radome, a pair in the middle and a pair at the bottom.

Has Amplifier Performance or Delivery Stalled Your Program?

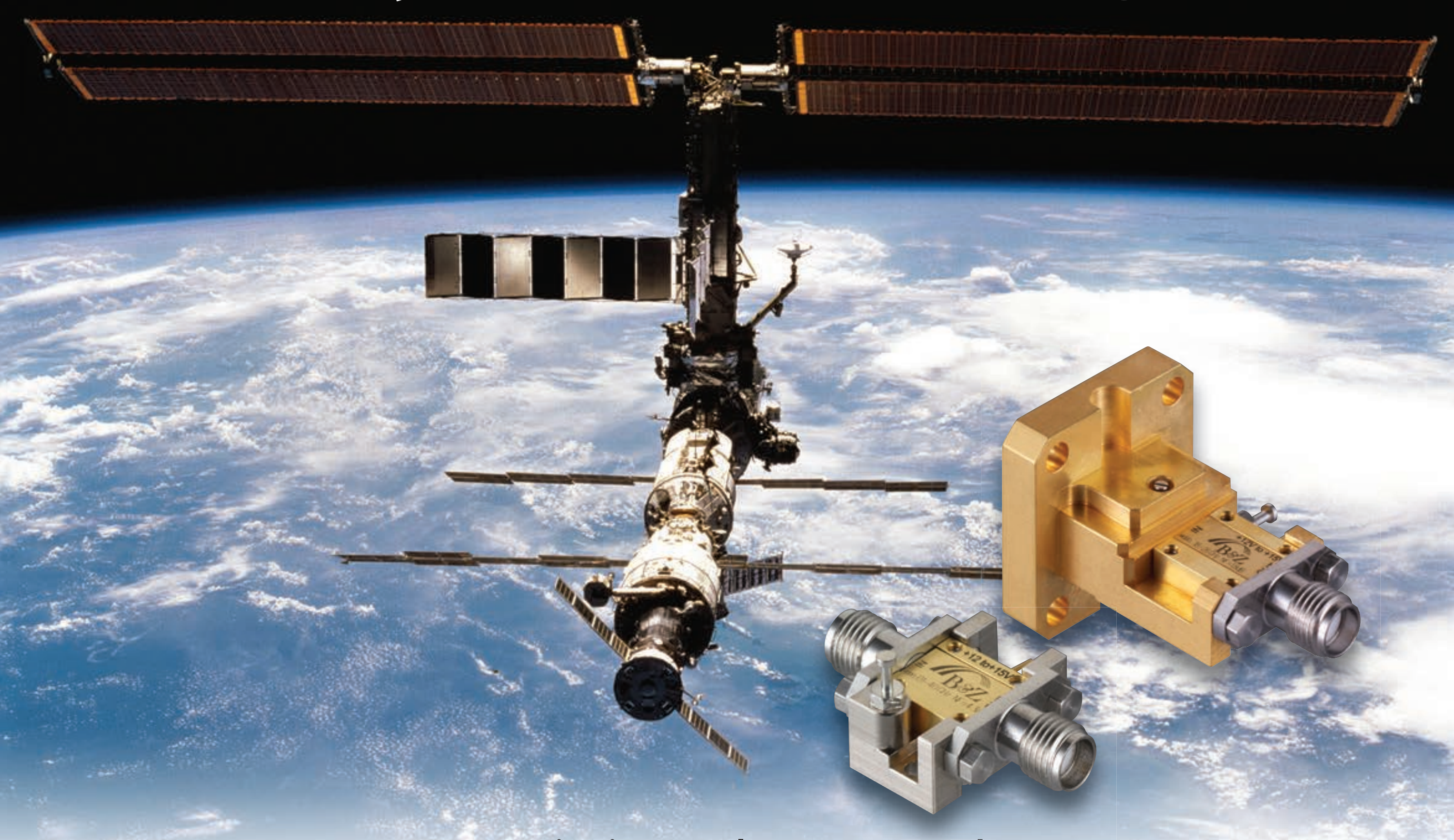

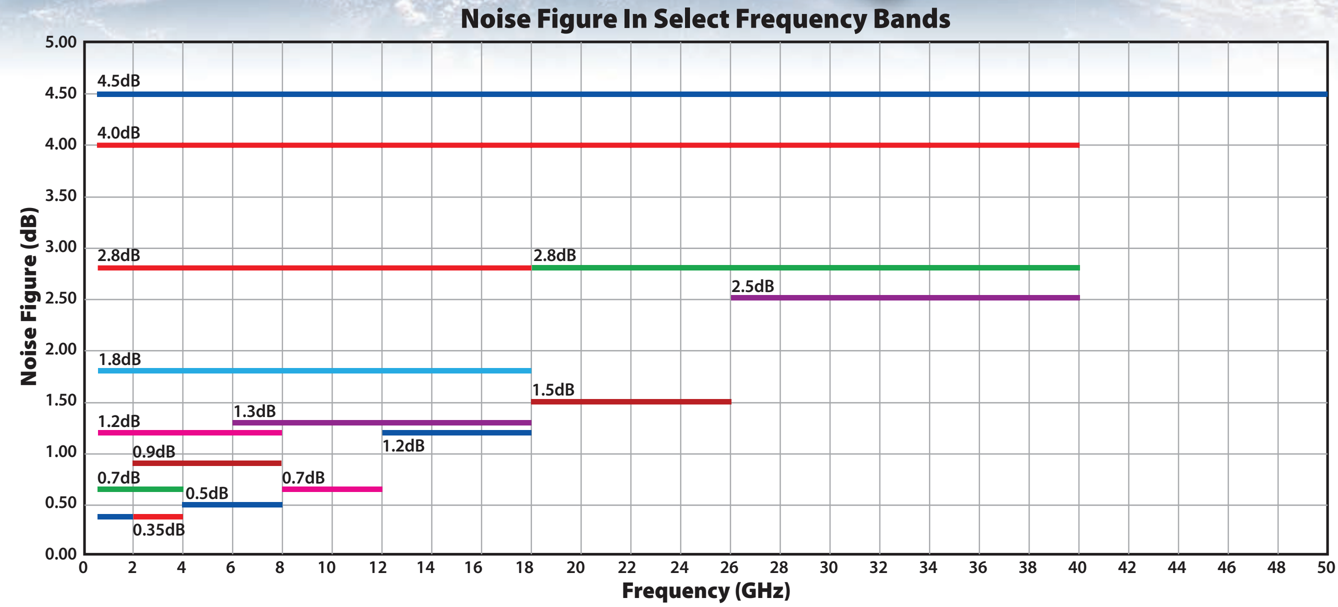

B&Z TECHNOLOGIES
Innovating to Excel

www.bnztech.com

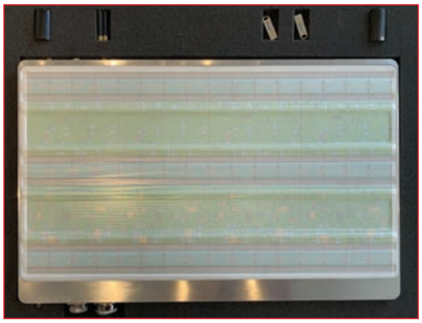

Fig. 3 **RRI-400 research radar interferometer.**

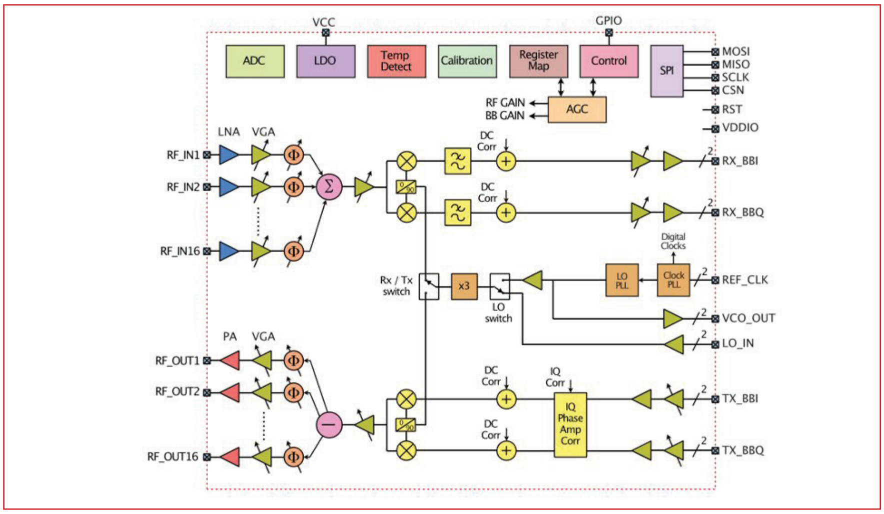

Fig. 4 **Transceiver RFIC architecture.**

The spacing from top to middle is slightly different from the middle to bottom spacing. A double difference interferogram may be formed resulting in a virtual short baseline interferometer.

The aiRadar sensor electronics modules (SEMs) are configurable in frequency. A SEM can be mechanically modified to use a customized version of the Sivers Semiconductors BFM02801 for operation in the 24 GHz band, albeit with reduced bandwidth to comply with the frequency allocation. aiRadar and Sivers are currently evaluating a 77 to 81 GHz band TRM for migration from a research 66 GHz ADAS to an operational 77 to 81 GHz version.

Figure 4 shows the internal architecture of the Sivers TRM, and ***Figure 5*** shows a functional block diagram of the radar. The digitized raw Rx outputs from the radar that appear in the radar data packets may be configured (in the RRI-400) as 16 digitized in-phase and 16 quadrature (I/Q) channels from each of the three azimuth Rx arrays, or a single digitally beamformed receive signal from each of the Rx arrays.

The 16 channels of Rx I/Q data provide the multi-aperture (16) SAR capability for 5 cm along track strip map imaging, the multi-baseline MTI capability using along track interferometry and the data for the DPCA micronavigation system.

The Sivers module provides zero IF Rx bandwidth to the aiRadar SEM with multiple control interfaces: a general purpose interface (GPIO), a serial programmable interface and a beamforming control interface. The aiRadar customized Sivers module has an external 22 GHz local oscillator (LO) interface with an internal 3× multiplier to the 4 GHz wide 66 GHz transmitter.

The Sivers RF LO interface, with a 1.33 GHz bandwidth at 22 GHz, and the Tx IQ interface are driven from the dual direct digital synthesizer (DDS) in the SEM, with modulation at two levels, on both the LO and the Tx IQ. This interface providers linear frequency modulated (FMCW) and arbitrary pulse modulation supporting LPI operations.

The high bandwidth arbitrary transmit signal is generated with a multistage RF lineup from the DDS in-phase and quadrature (I/Q) components, through a quad DAC with quadrature modulator cor-

RF-LAMBDA

MADE IN USA

THE LEADER OF RF BROADBAND SOLUTIONS

EMC Broadband RF Power Amplifier

High Power Solid State

HUNDREDS IN STOCK

FAST SHIPPING

FREQUENCY UP TO 90GHZ

POWER UP TO 2KW CW

REMC06G18GG

6-18GHZ 300W

- AUTOMATIC BUILT IN SELF CALIBRATION AND BIAS ADJUSTMENT.
- OVER TEMPERATURE, CURRENT, INPUT POWER PROTECTION.
- VSWR MEASUREMENT AND OPEN CIRCUIT PROTECTION.
- USER FRIENDLY CONTROL INTERFACE.
- REMOTE ETHERNET CONTROL AND FIRMWARE UPDATE.
- HIGH POWER EFFICIENCY AND LIGHTWEIGHT.

RAMP42G47GA 42-47GHZ 8W

RAMP18G40GB-U 18-40G 20W

RAMP05M80GC 0.5-80GHZ

REMC02G06GE 2-6GHZ 500W

REMC08G11GE 8-11GHZ 400W

rection and group delay correction enabling IQ compensation for gain, offset, phase and group delay between channels, a quadrature upconverter to 5.5 GHz and then a multi-channel multiplier to 22 GHz for distribution to the Sivers BFM devices.

Coherence, phase noise and Allen variance are critical in a radar at this frequency, particularly when used in a SAR mode. The primary reference is an ultra-low jitter oscillator. This reference is provided to an ultra-low noise clock jitter cleaner with dual-loop phased-locked loops to distribute the multiple coherent clocks to various subsystems.

SAR systems are typically deployed on larger drones or aircraft. SAR has been demonstrated by researchers on small drones (< 50 kg), but space varying errors due to aerodynamic turbulence and flight path position and attitude errors degrade resolution and are an obstacle to deployment on sUAVs. The aiRadar InSAR has an innovative solution to this, using the multi-aperture SAR capability, DPCA micronavigation, dual GNSS (GPS) receivers, nine-axis attitude sensors and time domain back projection to support unsupervised SAR processing.

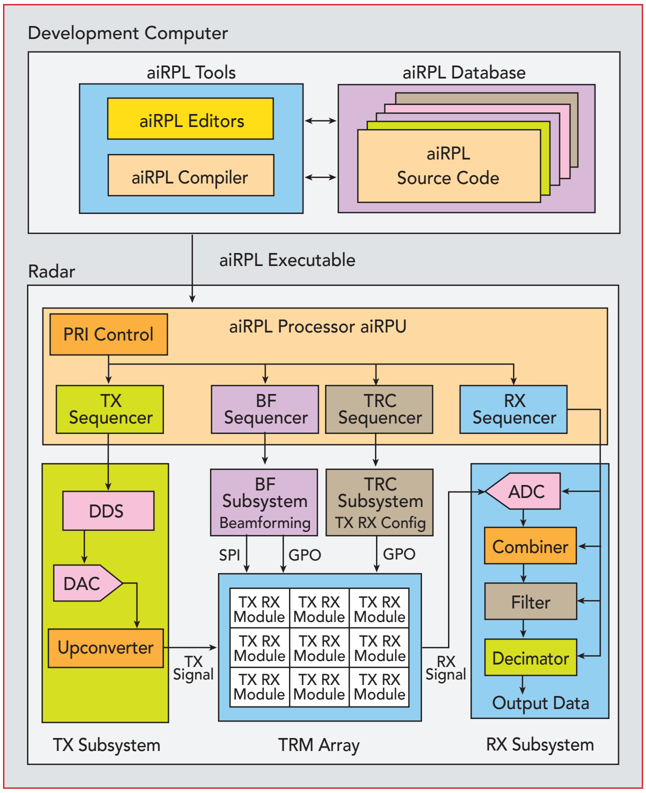

Fig. 5 Software-defined radar block diagram.

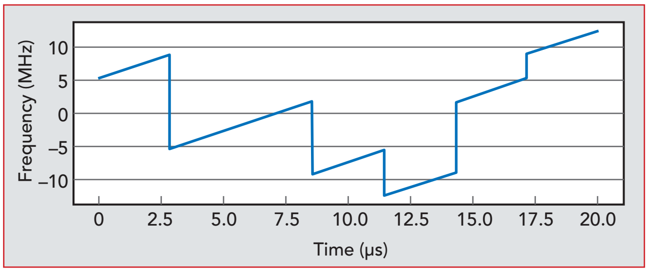

Fig. 6 Typical LPI frequency vs. time code, spanning 25 MHz within a 20 μs period.

COMMAND AND TELEMETRY; THE AIRPL ECOSYSTEM

The SEM is controlled by the aiRadar aiRPL, a compiled language with a syntax like C, which runs on the aiRPU. This language provides sophisticated multilevel looping and calls to the transmit pulse modulations, the beamforming and the receive data processing. This system is a powerful yet simple tool for the programming of radar configurations and almost arbitrarily complex operational modes.

The aiRPL ecosystem is composed of an integrated software development environment with compiler, databases, a command processor and a radar precision timing processing unit. The integrated software development environment consists of two main parts:

- The radar programming language—tools for the generation and sequencing of PRI bursts, sequences and frames.

Data structure creation and maintenance tools, including:

ERAVANT
FORMERLY **SAGE MILLIMETER**

100 to 330 GHz
TERAHERTZ PRODUCTS

Eravant THz components cover the frequency range of 100 to 330 GHz and include antennas, antenna accessories, low noise amplifiers, power amplifiers, mixers, frequency multipliers, and many other waveguide components.

Amplifiers
Traditional configurations with sturdy waveguide construction offer high isolation and good broadband performance. Ideal for general-purpose use on test benches and in subassemblies.

Frequency Converters
Mixers translate THz frequencies with low conversion loss. Frequency multipliers driven by swept or synthesized sources produce THz signals over wide bandwidths.

Passive Waveguide
Power dividers and magic tees offer low insertion loss, good return loss, and high power-handling capability over full waveguide bands.

Compact Ferrite Devices
Novel configurations with precision machined housings offer the smallest package size available. Highly resistant to stray magnetic fields and ideal for subassemblies where space is a premium.

WWW.ERAVANT.COM

www.eravant.com 501 Amapola Avenue Torrance, CA 90501
T: 424-757-0168 F: 424-757-0188 support@eravant.com

Adapters • Amplifiers • Antenna Feeds • Antennas • Attenuators • Bias Tees • Cable Assemblies • Corner Reflectors • Couplers • DC Blocks • Detectors • Ferrite Devices • Filters • Frequency Converters • Frequency Multipliers • Limiters • Magic Tees • Mixers • Noise Sources • Oscillators • Phase Shifters • Power Dividers • Radar Sensors • Subassemblies • Switches • Termination Loads • Test Equipment • Test Hardware & Accessories • TX/RX Modules • Uni-Guide™ • Waveguide Sections

- Transmit Pulse Design
- Receive Configuration Design
- Beamforming Design
- TRM Hardware Configuration
- Radar Constraint Definition
- Image Quality Analysis
- Test and Maintenance.

Built into the aiRPL are source methods for invoking radar operations and for sequencing these operations, for example, the PRI command. A PRI could be:

PRI (5e−3, " tr0rx12," " bfwide7," " txfmcw4," "rxfmcw1")

In this example, a 5.0 msec PRI is programmed, accessing four structures, "tr0rx12," "bfwide7," "txfmcw4" and "rxfmcw1." The first structure defines the Tx/Rx and interferometric configuration, the second controls the beamformer, the third defines the transmit pulse and the fourth defines the receive mode, digital filtering and decimation.

LPI RADAR

A fragment of radar programming code is shown below to demonstrate the programming of an LPI mode in which the radar transmitter has an LPI code hopping from PRI-to-PRI, with a triplet of pulses (two Frank codes and one Costas code) transmitted in each burst.

REPEAT(16) {
// PRI sequence is executed 16x per burst

PRI(1.00E-03, "f_trcconf1," "f_bfnoop0," "f_txlpi0," "f_rxconf0") // Frank Code N = 3

PRI(1.00E-03, "f_trcconf1," "f_bfnoop0," "f_txlpi1," "f_rxconf0") // Costas Code array size = 10

PRI(1.00E-03, "f_trcconf1," "f_bfnoop0," "f_txlpi2," "f_rxconf0") // Frank Code with N = 4

}

A typical encoded LPI pulse in the frequency/time domain referred to in the code above as "f_txlpi0" is shown in ***Figure 6*** (parameters have been chosen for graphics clarity) and ***Figure 7***.

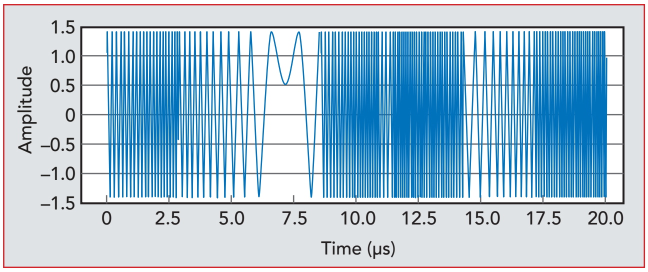

Fig. 7 **DDS output waveform with the typical LPI code.**

IMAGE TEST RESULTS AND IMAGE QUALITY

aiRadar instruments provide ongoing image quality assessment tools to monitor performance by measuring quantitative performance parameters such as impulse response function, peak sidelobe ratio and ISLR.

Figure 8 is a screenshot from the aiRadar image quality analysis tool captured during preliminary calibration of the RRI-100 radar. It shows a point scatterer in a clutter rich short-range environment. Annotations on the image are added for clarity.

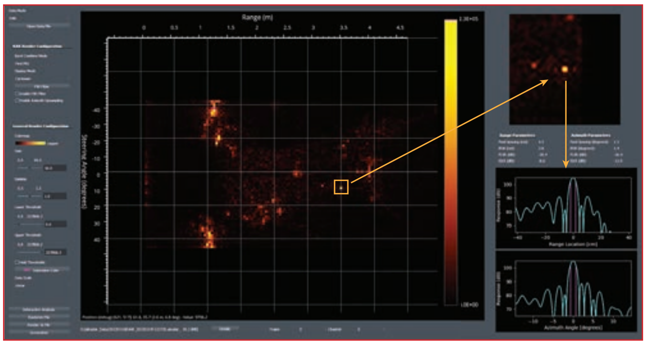

Fig. 8 **Screenshot from the image quality analysis tool.**

Figure 9 shows an image of two parking lots with vehicles, dump-

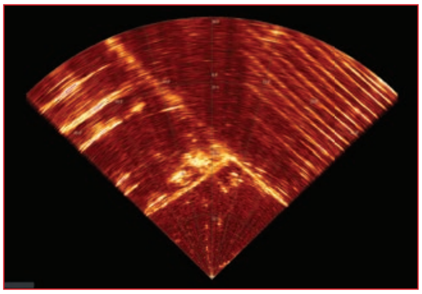

Fig. 9 **Image of parking lots and rail yards.**

Nxbeam

Ka-Band Power

27 TO 31 GHz

Maximized performance for linear power applications

GaN MMIC's to 40W

Nxbeam's suite of Ka-band PA MMICs offers customers an unparalleled combination of power, gain, and efficiency with proven reliability.

PRODUCTS:
NPA2001-DE
NPA2002-DE
NPA2003-DE
NPA2030-DE

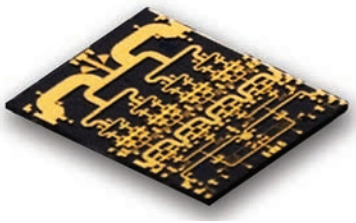

Packaged MMICs to 35W

Nxbeam offers its Ka-band MMICs in leaded flange packages for easier system integration

PRODUCTS:
NPA2001-FL
NPA2002-FL
NPA2003-FL
NPA2030-FL

Module Products to 60W

For higher levels of power and integration, Nxbeam offers modules that combine multiple Nxbeam MMICs to achieve higher performance in an easy-to-use form factor. Custom designs available

PRODUCTS:
NPM2001-KW
NPM2002-KW
NPM2003-KW

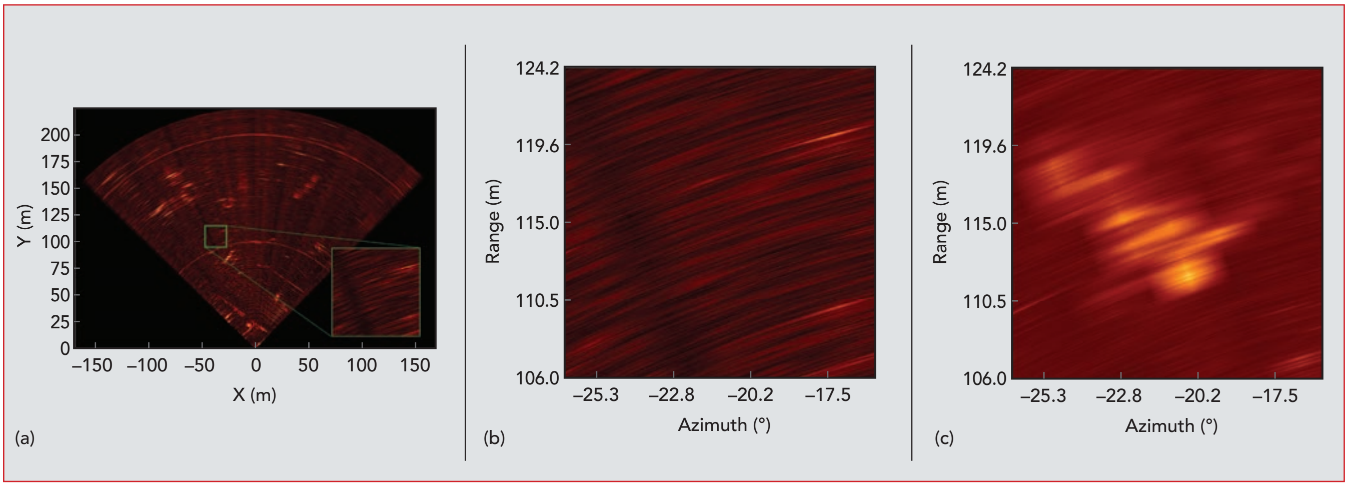

Fig. 10 **Stationary radar image with normal processing (a), expanded view of highlighted area (b) and highlighted area with MTI processing (c).**

sters and a railway switching yard. A relatively shorter range of 50 m is selected to demonstrate filtering and down-sampling of the 20,000 range samples at 5 cm resolution. The radar was deployed at an elevation of 20 m with the elevation boresight horizontal.

MTI

ADAS requires excellent MTI processing to separate stationary infrastructure, such as buildings and traffic signs, from moving or stationary objects, such as cars, trucks, cyclists and pedestrians. V- and W-Band provide excellent sensitivity and resolution of moving objects. A stationary radar image with normal processing is shown in ***Figure 10a***, the outlined area expanded in ***Figure 10b***. The expanded area processed with 32 chirps in a frame and reprocessed with a 32-bin Doppler filter (i.e., 32-point FFT) clearly shows the moving target (see ***Figure 10c***), which was invisible in the normally processed image.

CONCLUSION

aiRadar research radars facilitate the definition of validated requirements and AESA configurations for emerging commercial, military and academic radar applications. These research instruments provide the tools to validate requirements and develop sophisticated radar systems reducing time-to-market and offering a low risk path to commercialization and deployment. aiRadar offers in-house radar design for a customized application-specific radar or licensing of the aiRadar programming language (aiRPL) compiler and the radar processing unit IP Core (aiRPU). Developing compact low size, weight, power and cost, AESA radars with RAR, SAR, InSAR, multi-baseline MTI, LPI and CA has never been easier. ■

3D Waveguide Metallized Plastic Antennas Aim to Revolutionize Automotive Radar

Ulf Huegel, Alejandro Garcia-Tejero, Rafal Glogowski, Eugen Willmann, Michael Pieper and Francesco Merli
HUBER+SUHNER, Herisau, Switzerland

Today, the 3D waveguide antenna metallized plastic technology, first introduced by HUBER+SUHNER more than a decade ago, plays an integral role in several industries, particularly in automotive radar for advanced driving systems. This article provides insight into the technology and products and how the products meet the technical demands of the automotive industry. The article recounts on the technology journey from antennas for mmWave backhaul through fixed wireless communications to automotive radar, establishing HUBER+SUHNER as a 3D metallized plastic antenna supplier.

In the search for highly efficient and compact radiators that can be produced at an attractive manufacturing cost, engineers at HUBER+SUHNER have worked on metallized plastic technology since the early 2000s. Through multiple innovation steps, lightweight 3D waveguide antennas with compact form factors have been successfully designed, manufactured and validated.

Thanks to improved efficiency, pattern stability and large bandwidth, these products are becoming increasingly sought after in the automotive world. This work reviews the journey HUBER+SUHNER has taken to become the supplier of 3D radar waveguide antennas.[1,2]

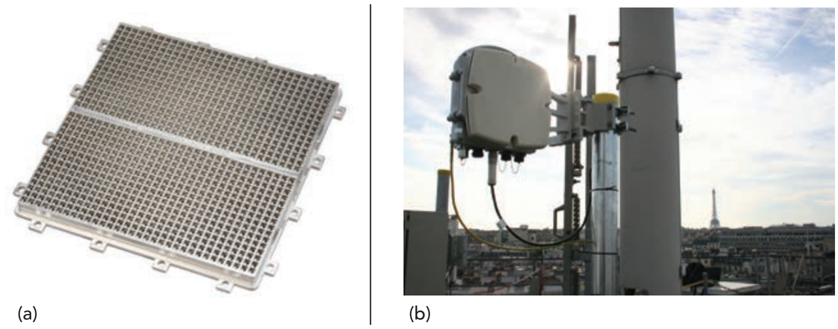

(a) (b)

▲ Fig. 1 **HUBER+SUHNER mmWave backhaul antennas: 38 dBi (a) and 43 dBi (b).**

THE ORIGIN: MMWAVE BACKHAUL

The first 3D waveguide metallized plastic antennas (see ***Figure 1***) were designed by HUBER+SUHNER and have been manufactured there since 2006.[3,4] These products provide high gain and small form factor for mmWave backhaul at V- and E-Bands (57 to

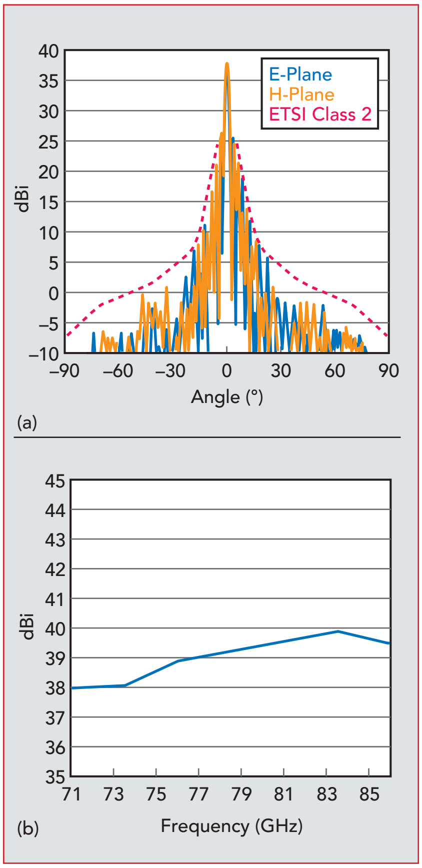

Fig. 2 **HUBER+SUHNER mmWave backhaul antennas measured radiation pattern at 73.5 GHz (a) and boresight gain over frequency (b).**

66 GHz and 71 to 86 GHz, respectively) while remaining compliant with international regulations.[5]

For this purpose, several designs incorporating 1024 to 4096 radiators are fed with the same amplitude and phase and are combined into a single input. This approach results in a radiation pattern with a very focused pencil beam (directivity ranging from 38 to 43 dBi, respectively), controlled sidelobe levels and stable gain over frequency (see ***Figure 2***).

Filters and diplexers with high Q factors were also built with the same technology. This led to further advantages, including compact mechanical housing and fixation concepts which enabled the realization of a fully integrated point-to-point mmWave radio backhaul system, the 'SL60' (see ***Figure 3a***).[3] A more recent version of the V-Band antenna and the diplexer combination is shown in ***Figure 3b***.

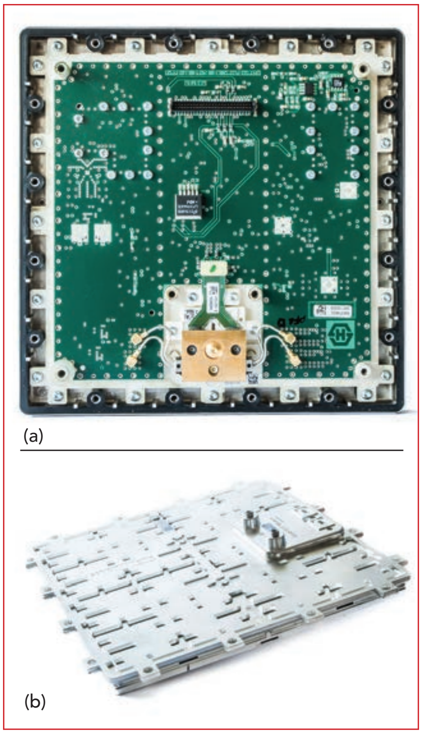

Fig. 3 **SL60 RF front-end (a) and integrated V-Band antenna-diplexer (b).**

SOLVING THE URBAN BANDWIDTH CHALLENGE

The next phase of the metallized plastic antenna evolution occurred with the shift from point-to-point links to multipoint-to-multipoint wireless distribution network applications within the Terragraph[6] program. This project seeks to provide more people with access to fast internet, deploying gigabit connectivity quicker and more efficiently in markets where fiber trenching is expensive. The solution developed by HUBER+SUHNER, given its broadband characteristic covering the frequency spectrum from 57 to 66 GHz, formed the backbone of the first technology demonstrators for sustained, reliable connectivity (see ***Figure 4***).

THE MULTI-CHANNEL EVOLUTION

The multipoint-to-multipoint wireless distribution network called for HUBER+SUHNER metallized plastic antennas to evolve from single to multi-channel; a 36-input antenna with vertical polarization was designed and manufactured.

The combined use of all channels makes it possible to steer the main radiation beam to point the communication link to where it is most needed. ***Figure 5*** shows how full coverage over ±35 degrees in the horizontal plane is achieved while maintaining a realized gain above 29 dBi.

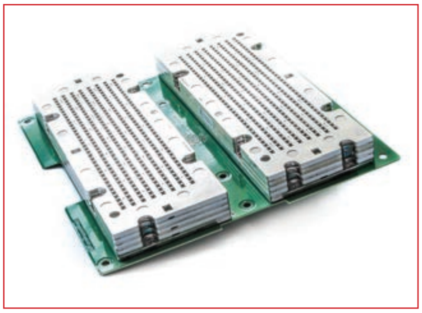

Fig. 4 **Terragraph RF front-end board. Two antennas were used for transmitting (Tx) and receiving (Rx), respectively.**

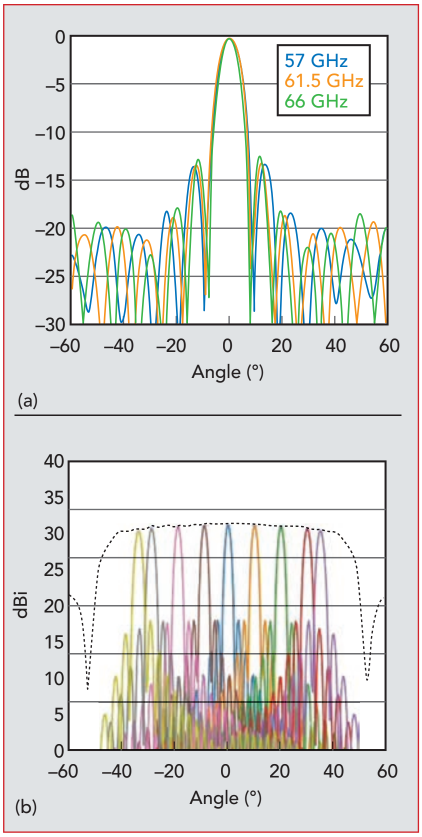

Fig. 5 **36-channel antenna module normalized elevation pattern vs. frequency (a) and azimuth beam steering at 61.5 GHz (b).**

Designing and manufacturing a multi-channel antenna dramatically impacted its testing as well. As early as 2016, HUBER+SUHNER engineers designed a semi-automated system to test all channels and ensure the quality of the delivered products.

Finally, the simultaneous use of several channels called for higher

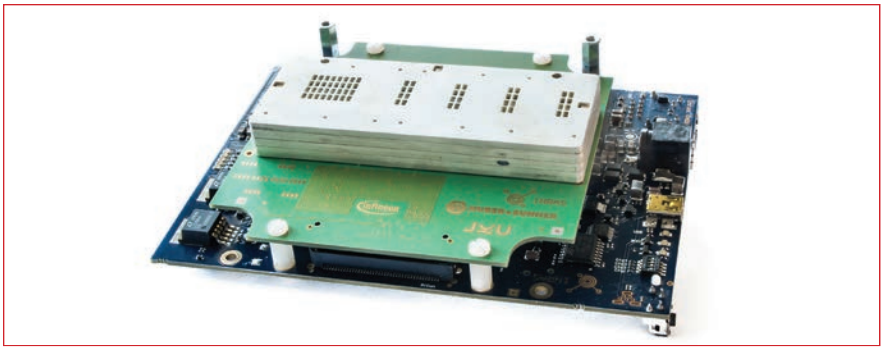

Fig. 6 **Demorad radar developed with Infineon.**

integration between the antenna and the active electronics. A dedicated, and proprietary, RF interface solution was developed to directly mount the antenna onto the printed circuit board (PCB) with no waveguide flanges required to increase overall product compactness and achieve higher performance.[7]

77 GHZ AUTOMOTIVE MIMO RADAR: A SWEET SPOT

After the implementation of HUBER+SUHNER metallized plastic antennas into the communication market, the use of this technology was introduced for automotive radar applications in 2016,[8] with its first demonstration in 2018.[9] Since then, several antenna solutions and sensors have been designed, manufactured and validated, focusing on both product development and their integration into the ecosystem.

As most original equipment manufacturers (OEMs) and Tier-1 suppliers require dedicated and customized antenna designs pro-

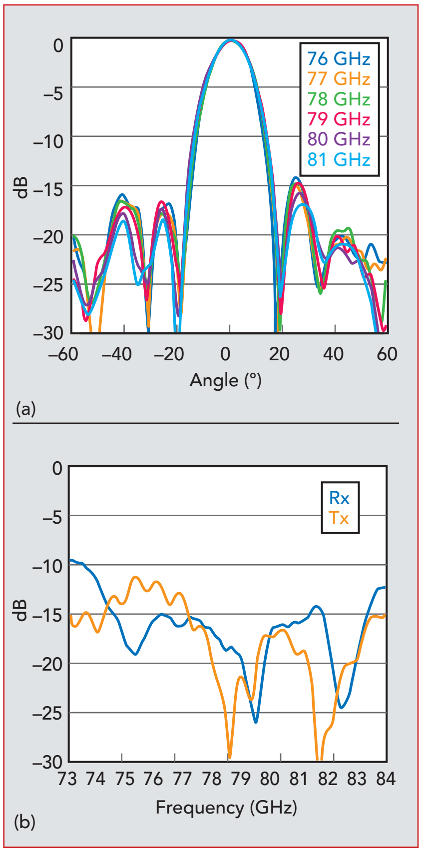

Fig. 7 **Measured Demorad normalized antenna pattern from 76 to 81 GHz (a) and |S11| of the Rx and Tx antenna elements (b).**

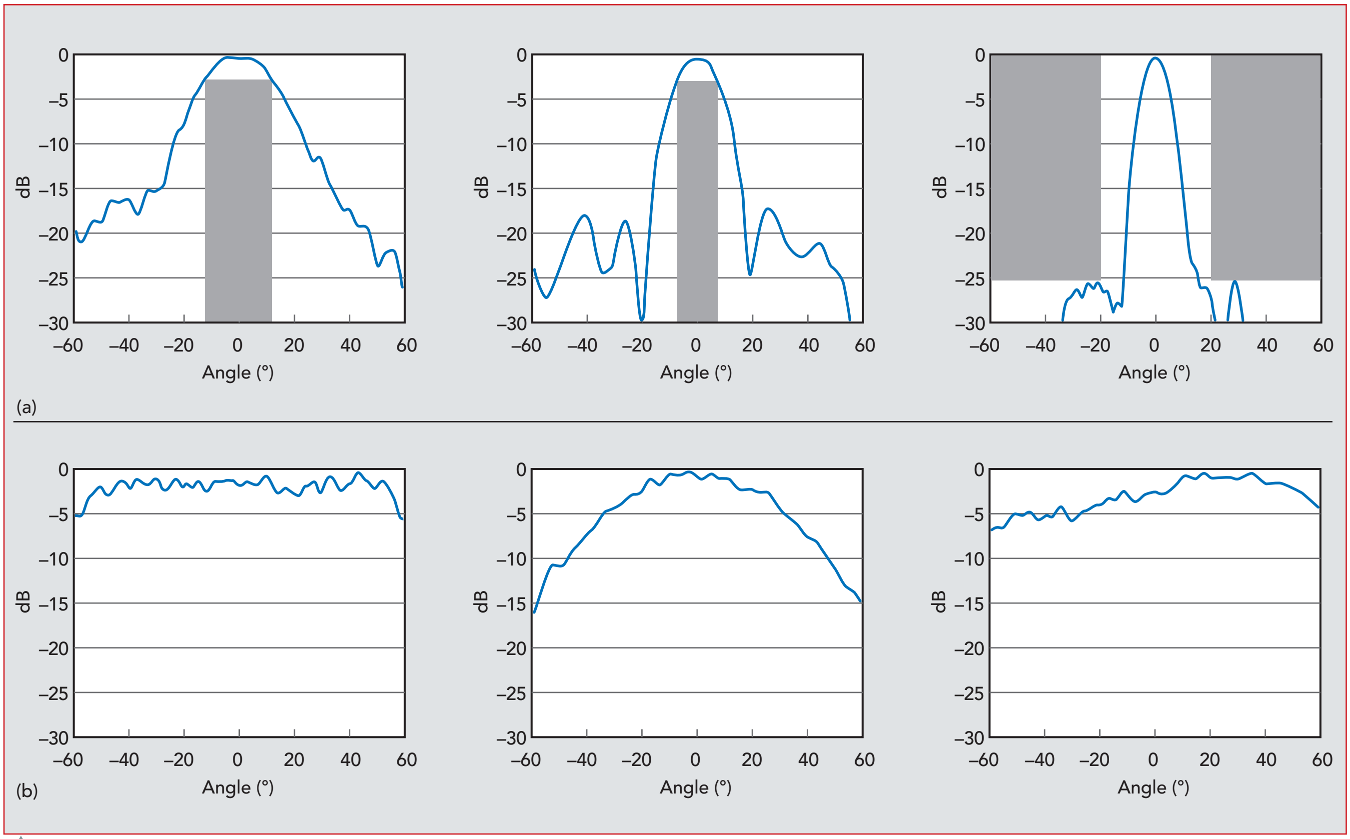

Fig. 8 **Measured automotive radar antenna patterns: elevation (a) and azimuth (b) planes.**

tected under confidentiality, this article describes antennas and systems that are the result of internal HUBER+SUHNER development for different radar applications (long-, mid- and short-range, corner and side-looking radars).

THE 3D ANTENNA AND ITS ECOSYSTEM

The antenna developed for the first system demonstrator—'Demorad' (see ***Figure 6***)—comprised four 3D-printed layers, standard microstrip-to-hollow waveguide launchers on a low loss RF PCB substrate and an almost uniformly corporate-fed antenna array. Lambda over two and lambda over four spacings were selected for receive (Rx) and transmit (Tx) elements, respectively, to establish a virtual linear array (8 Rx, 4 Tx).

Figure 7 shows some of the measured characteristics of the manufactured prototype. The technology demonstrates a broadband behavior (12 percent relative bandwidth), enabling use of the entire 76 to 81 GHz automotive radar frequency band. Such performance is matched by a stable radiation pattern over frequency with -15 dB sidelobe levels and a high efficiency of 90 percent (0.5 dB loss).

These characteristics outperform the state-of-the-art PCB-based antennas traditionally used within the industry.[10] While this initial demonstration was developed in collaboration with Infineon, the technical solution finds application with all MMIC suppliers.

Today, the design and the technology have taken several steps forward. The first step is product miniaturization. 'Demorad' offered exceptional RF performance but, due to the use of four plastic layers, the product was bulky. With technological evolution, the number of layers is now reduced to two, with the overall thickness reduced to less than two lambdas.

The second step is the introduction of advanced feeding techniques with both amplitude and phase tapering for complex radiation pattern shaping. With just two plastic layers different performance characteristics are achieved, from broad azimuth pattern coverage through a tilted beam to narrow elevation patterns with extremely low sidelobe levels, as shown by the measured radiation characteristics in ***Figure 8***. All the typical automotive radar requirements for long-, mid- and short-range radar can now be fulfilled. As a further result of modern advancements, diverse polarizations such as horizontal, vertical, slant or circular can be easily obtained, allowing for polarimetric radar applications as well.

The third step comes in the form of integration with the rest of the sensor and the MMIC. The first demonstrator employed a low loss RF substrate to route and launch signals from the MMIC to the antenna; however, this requires the presence of high performance/high-cost RF substrate material that still generates noticeable loss-

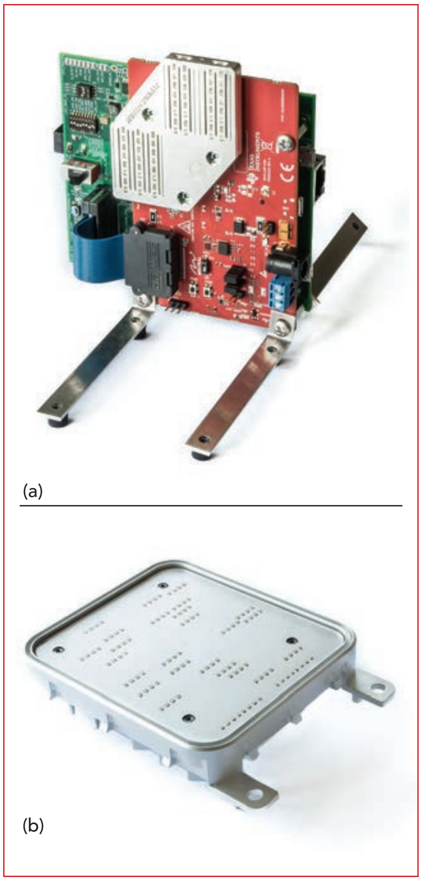

▲ Fig. 9 **Mid-range demonstrator developed with Texas Instruments (a) and Uhnder digital imaging radar using HUBER+SUHNER 3D antennas (b).**

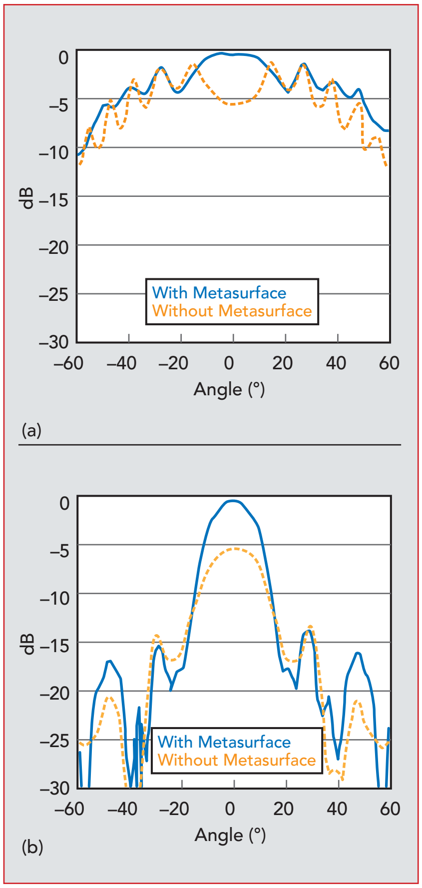

▲ Fig. 10 **Simulated effect of a metasurface to minimize antenna-bumper reflections: azimuth (a) and elevation (b) planes.**

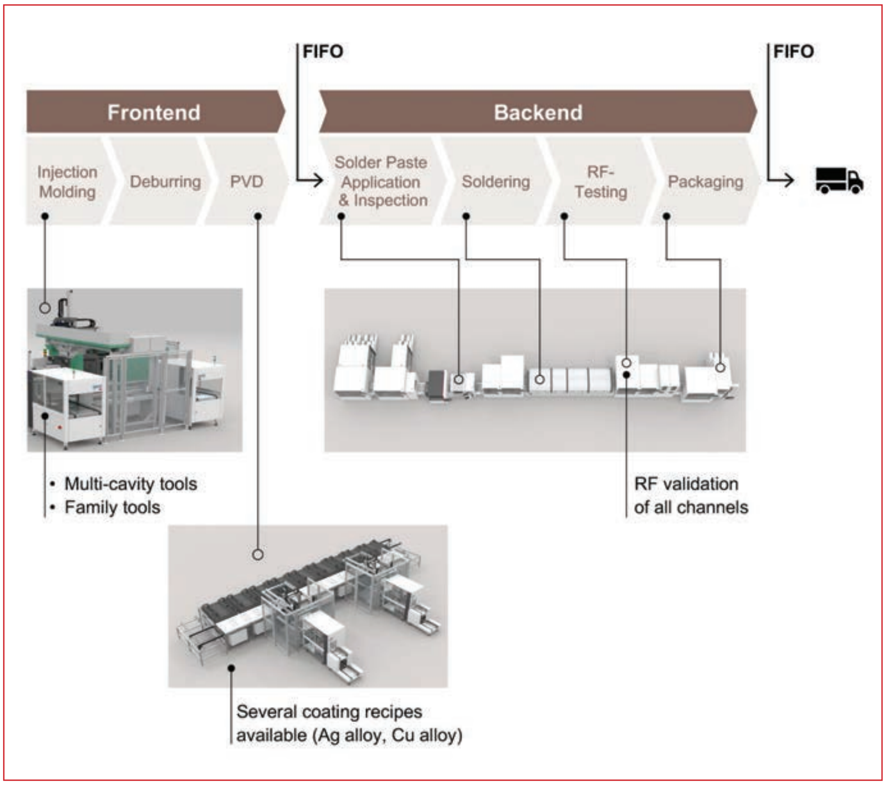

▲ Fig. 11 **Antenna production flow showing main manufacturing steps.**

es within the substrate and fails to use the full potential of the low loss waveguide technology.

Thanks to the latest joint development with Texas Instruments,[11,12] a highly integrated sensor has been realized (see ***Figure 9a***). Direct coupling from the MMIC, through plated holes in the PCB, to the antenna dedicated RF interface enables efficient power transmission without the need for a low loss substrate. This provides an RF substrate independent solution and a dramatic benefit in terms of both performance (because there is no need for PCB launchers that easily add 2 to 3 dB loss to the link budget) and cost (by avoiding the need for a high performing RF material).

Figure 9b is another example of integration showing a HUBER+SUHNER 3D metallized plastic antenna as part of the next generation of digital imaging radars. Its low loss characteristics are crucial to providing an antenna array with a highly sparse location of elements over large apertures.

Finally, using a 3D antenna with a large area allows for novel design features to be added to mitigate—if not cancel—radiation pattern distortion introduced by the radome and/or the bumper placed in front of the radiator.[13]

The orange traces in ***Figure 10*** show the result of multiple reflections when simulating a simple case of antenna-bumper radiation interaction using a flat bumper model with dielectric constant of 3.0, 3.5 mm thickness and an antenna to bumper distance of 18 mm. By introducing periodic elements (i.e., a metasurface) on the antenna top layer, the desired main beam radiation performance is substantially recovered and pattern ripples are noticeably reduced (blue traces).[14,15]

TECHNOLOGY: MEANT FOR MASS PRODUCTION...

Since its inception, HUBER+SUHNER metallized plastic technology has incorporated large volume, low-cost and well-established manufacturing technological steps, such as injection molding (IM), physical vapor deposition

coating (PVD) and soldering (e.g., reflow soldering including solder paste application and inspection). Due to complete ownership of the three technologies and their joint optimization, HUBER+SUHNER could revise all its core manufacturing steps when moving from the communication segment to the automotive market with its stringent lifetime and reliability requirement (e.g., extended temperature and humidity ranges, increased number of cycles).

This level of expertise is matched by a proprietary design for manufacturability.[16,17] To ensure the use of the manufacturing technologies mentioned above, the complex 3D RF geometries are separated into several different layers, paying close attention to both RF performance and the manufacturability.

For example, the waveguides, designed to support the TE10 mode and created by joining different layers, are split across at the maximum of the E-field, corresponding at the null of surface current.[18] This enables a high performance, robust, easy to implement and energy leakage-free assembly. This design approach, together with a proprietary coating, leads to losses as low as 8 to 10 dB per meter with no cross coupling between adjacent channels.

Finally, drawing on its experience, as previously described, HUBER+SUHNER developed a complete RF testing station that can verify all RF channels in a matter of seconds.

Figure 11 shows the process flow of a typical manufacturing line for metallized plastic technologies that provides a modular approach to fit different customer needs.

TECHNOLOGY: ...WHILE BEING AGILE

The availability and the use of mass production equipment may endanger the agility required in a product development program, especially when introducing the latest technologies into a new market. Indeed, validating complex and challenging product design iterations requires fast and simple manufacturing technologies.

HUBER+SUHNER masters 3D printing technology and rapid IM (i.e., using aluminum tools) to produce individual plastic layers while maintaining an in-house dedicated prototype shop for coating and soldering. Such know-how and capability enables the production of individual samples for concept studies and validation purposes,

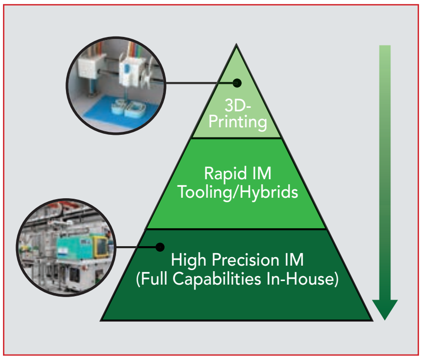

Fig. 12 **Available technologies to support product development.**

along with small series production, to match product development requirements, timing and cost. The challenge, thus the art, lies in the implementation of a solution that is as close as possible to series production, even at the earlier stages of product development. HUBER+SUHNER controls the complete value chain from polymer granulates to final validated product (see ***Figure 12***).

MASS PRODUCTION: TODAY AND BEYOND

The demand for automotive radar antennas shows no signs of slowing. Driver assistance functions are increasingly coming to the fore, whether it is an emergency brake assistant, adaptive cruise control or even autonomous driving. To meet this increasing demand, HUBER+SUHNER implemented high volume production technologies that incorporate a high degree of automation from the start.

In addition to the first highly automated production line for long-range radar antennas in Switzerland, a short-range radar production line was recently set up at the HUBER+SUHNER premises in Poland. As a next step, matching customer and market requirements, production lines could be implemented at HUBER+SUHNER locations in other key markets such as China and America. Doing so allows production close to customers' sites, minimizing the product-related CO_2 footprint.

CONCLUSION

HUBER+SUHNER metallized plastic technology is revolutionizing the automotive radar world for all radar applications (long-, mid- and short-range, corner and side-looking radars) as it enables the achievement of very low insertion loss, improved efficiency, pattern stability and impedance bandwidth. It offers overwhelmingly higher performance compared to PCB antennas, with competitive manufacturing costs. Particularly, very low routing losses (less than 8 to 10 dB per meter) enable the distribution of antenna arrays quite freely over a large aperture, enabling high angular resolution and increased virtual array possibilities.

Based on more than a decade of experience and applications into multiple markets, HUBER+SUHNER 3D antennas for radar applications are meeting the demands by major OEMs and Tier-1 suppliers for increased waveguide antenna performance.[1,2] ■

References

1. "HUBER+SUHNER Becomes Supplier of Radar Antennas to Leading Tier 1 Automotive Supplier," *HUBER+SUHNER AG*, September 2021, Web: https://www.hubersuhner.com/en/company/media/news/2021/09/2021-09-30-en.
2. "Advanced Radar Sensor – ARS540," *Continental Automotive*, Web: https://www.continental-automotive.com/en-gl/Passenger-Cars/Autonomous-Mobility/Enablers/Radars/Long-Range-Radar/ARS540.
3. "Wireless Ethernet Bridge SENCITY ®LINK SL60," *HUBER+SUHNER AG*, 2010, Web: https://www.hubersuhner.


INTRODUCING
STATIONMAX
The Most Powerful Rigol Oscilloscope Ever
DS70000 Series
Digital Oscilloscope with Real-Time Spectrum Analysis
• 3 & 5GHz Bandwidths
• 20 GSa/s Sample Rate
• 2Gpts Memory Depth
• 1 Million wfms/s
• 8 to 16 Bit Resolution
• 15.6" Multi-Touch Display
• New UltraVisionIII Platform
NEW Multi-Pane Display
Check Out STATIONMAX & Our High Performance
MSO5000 & MSO8000 Scopes
RIGOL
www.Rigolna.com/DS70000

com/en/documents-repository/markets/pdf/automotive/wireless-ethernet-bridge-sencity-link-sl60.aspx.

4. "SENCITY® Matrix Flat Antennas," *HUBER+SUHNER AG*, July 2017, Web: https://5.imimg.com/data5/NE/EW/KK/SELLER-948981/huber-sencity-matrix-directional-wave-outdoor-antenna.pdf.
5. "Fixed Radio Systems; Characteristics and Requirements for Point-to-Point Equipment and Antennas; Part 4-2: Antennas; Harmonized EN covering the essential requirements of article 3.2 of R&TTE Directive," *ETSI*, Final draft ETSI EN 302 217-4-2 V1.4.1, November 2008, Web: https://www.etsi.org/deliver/etsi_en/302200_302299/3022170402/01.04.01_40/en_3022170402v010401o.pdf.
6. Terragraph, Web: https://terragraph.com/.
7. U. Hugel, R. Glogowski, M. Thiel and F. Merli, "Adapter with Waveguide Channels and Electromagnetic Band Gap Structures," European Patent Office, Patent No. EP3430685, 2020.
8. A. Post, "An Antenna Concept that Addresses the Challenges with Automotive Radar," *IWPC Trends in Automotive Radar and Impact on System Architecture*, Workshop Presentation, March 2016.
9. F. Merli and A. Post, "Injection Molded Radar Antennas," *IWPC 2018 New Features for Automotive Radars*, Workshop Presentation, January 2018.
10. J. Hasch, E. Topak, R. Schnabel, T. Zwick, R. Weigel and C. Waldschmidt, "Millimeter-Wave Technology for Automotive Radar Sensors in the 77 GHz Frequency Band," *IEEE Transactions on Microwave Theory and Techniques*, Vol. 60, No. 3, March 2012, pp. 845–860.
11. F. Merli and A. Post, "Injection Molded Radar Antennas," *IWPC 2021 In Search of Optimum Automotive Sensor Solutions*, Workshop Presentation, May 2021.
12. F. Merli, A. Garcia-Tejero and M. Kagelmann, "3D Waveguide Antenna Radar Systems - an RF Independent Substrate Solution," *IWPC 2022 Which Direction is Automotive Radar Heading?*, Workshop Presentation, April 2022.
13. R. Schnabel, D. Mittelstrab, T. Binzer, C. Waldschmidt and R. Weigel, "Reflection, Refraction, and Self-Jamming," *IEEE Microwave Magazine*, Vol. 13, No. 3, May 2012, pp. 107–117.
14. J. Kowalewski, A. Garcia Tejero, P. Romano, M. Pieper, E. Willmann, M. Notter, F. Merli, A. Freni and A. Mazzinghi, "Antenna Device for Radar Applications," European Patent Office Patent 2022/063535, 2021.
15. A. Garcia-Tejero, J. Kowalewski, F. Rodriguez Varela, A. Freni, A. Mazzinghi and F. Merli, "Three Advances in Metallized Polymer mmWave Waveguide Antenna Design," *2021 IEEE APS/URSI*, Workshop Presentation, December 2021.
16. A. Garcia-Tejero, P. Romano and F. Merli, "Antenna Device," European Patent Office Patent 2021/081922. 2020.
17. R. Glogowski, "Array Antenna," CH Patent 00825/16, 2016.
18. H. Butterweck, "Mode Filters for Oversized Rectangular Waveguides," *IEEE Transactions on Microwave Theory and Techniques*, Vol. 16, No. 5, May 1968, pp. 274–281.

DefenseNews

Cliff Drubin, Associate Technical Editor

Demo Manned-Unmanned Teaming with Super Hornet Flight Tests

Boeing and the U.S. Navy have completed a series of manned-unmanned teaming (MUM-T) flight tests in which a Block III F/A-18 Super Hornet successfully demonstrated command and control of three unmanned aerial vehicles (UAVs).

Boeing system engineers connected Block III's adjunct processor, known as the Distributed Targeting Processor – Networked (DTP-N), with a third-party tablet to team with the UAVs. Boeing developed new software loads for the DTP-N specific to running the third-party tablet and transmitting commands. The software development, tablet connection to the fighter and all flight tests were completed in less than six months.

Boeing partnered with the F/A-18 & EA-18G Program Office (PMA-265), Air Test and Evaluation Squadrons (VX) 23 and 31, Naval Air Warfare Center-Weapons Division at China Lake, Calif., and a third-party vendor on the demonstration. During the test flights, F/A-18 pilots entered commands into the tablet, which were processed and transmitted through Block III's hardware. The UAVs executed all commands given by F/A-18 pilots during tests over a two-week period.

"This successful MUM-T demonstration represents a significant step toward the Navy's vision for Distributed Maritime Operations. It highlights the potential of unmanned concepts to expand and extend the Navy's reach," said Scott Dickson, Boeing's director for Multi-Domain Integration. "As part of a Joint All-Domain Command and Control network, teams of UAV conducting ISR missions led by the latest Super Hornets equipped with network-enabled data fusion and advanced capabilities would provide warfighters across the Joint Force with significant information advantage."

Block III F/A-18 (Source: Boeing)

Advanced Missile Tracking Space Development Agency Program

L3Harris Technologies has been awarded a contract to build the Space Development Agency's (SDA) Tranche 1 Tracking Layer satellite program to serve as "eyes in the sky" detecting, identifying and tracking advanced missile threats. The contract has a potential total value of $700 million.

L3Harris will build a 14-vehicle satellite constellation that will include optical communications terminals, infrared mission payloads, Ka-Band communications payloads and multiple pointing modes—advanced technology specifically designed to identify and track the fastest missiles known to exist. The program also includes related ground, operations and sustainment support.

L3Harris developed four prototype satellites under the SDA's Tracking Layer Tranche 0 award in 2020. The four space vehicles produced under the $193 million firm fixed-price contract will launch in 2023.

"L3Harris is successfully executing SDA's foundational Tracking Layer Tranche 0 program, which set their strategic way forward for rapidly deploying relevant mission capabilities to our nation's warfighters," said Kelle Wendling, president, Space Systems, L3Harris. "This Tranche 1 win demonstrates our ability to nimbly scale from initial demonstration to proliferation with enhanced mission capability, resilience, global coverage and speed to deployment as threats continue to evolve."

USMC Successfully Tests Iron Dome Based Air Defense Prototype

A major breakthrough for the U.S. Marine Corps (USMC) is the integration of RAFAEL's Iron Dome ground launcher and Tamir interceptor missile into Marine Corps' Medium-Range Intercept Capability Prototype with the USMC G/ATOR Radar and the CAC2S Battle Management System.

A recent live-fire test at the White Sands Missile Range in New Mexico proved:

- USMC has Iron Dome defense capabilities
- Iron Dome was successfully integrated into USMC Architecture
- The system performed exactly as was predicted by a USMC simulation prior to the test itself.

"This demonstration proves that we now have a relevant capability," said Don Kelley, program manager for Ground-Based Air Defense at Program Executive Office Land Systems, immediately following the successful test.

Iron Dome Live Test (Source: Rafael Advanced Defense Systems Ltd.)

Brigadier General (Res.) Pinhas Yungman, executive vice president and head of RAFAEL's Air Defense Systems Directorate said, "Once again, RAFAEL's systems have proven that they are capable of seamless, optimized integration with other defense systems. The Marines live-fire test demon-

For More Information Visit mwjournal.com for more defense news.

strated a successful combination of an Iron Dome ground launcher and Tamir interceptor with the Marines' radar system and battle management system. This is an important and significant message for RAFAEL, for the Marines and the other customers in the United States and in the international market."

Second Successful Hypersonic Weapon Flight Test

Raytheon Missiles & Defense, in partnership with Northrop Grumman, successfully completed its second flight

HAWC (Source: Northrop Grumman)

test of the scramjet-powered hypersonic air-breathing weapon concept (HAWC) for the Defense Advanced Research Projects Agency and the U.S. Air Force.

The HAWC team completed a second flight test using Northrop Grumman's scramjet engine.

This flight test applied the data and lessons learned from the first flight to mature the operationally relevant weapon concept design. The test met all primary and secondary objectives, including demonstrating tactical range capabilities.

During the flight test, after releasing HAWC from an aircraft and accelerating to hypersonic speeds using the scramjet engine, the vehicle flew a trajectory that engineers designed to intentionally stress the weapon concept to explore its limits and further validate digital performance models. These models, grounded in real-world flight data, are being used to accurately predict and increase performance as the system matures.

Scramjet engines use high vehicle speed to forcibly compress incoming air before combustion to enable sustained flight at hypersonic speeds—Mach 5 or greater. The system was designed to use a widely available hydrocarbon fuel, and since it uses air for combustion, it does not have to carry the added weight of an onboard oxidizer. These key attributes enable a safe, efficient and tactically sized, long range hypersonic weapon. By traveling at these speeds, hypersonic weapons like HAWC can reach their targets more quickly than traditional missiles, allowing them to potentially evade defense systems.

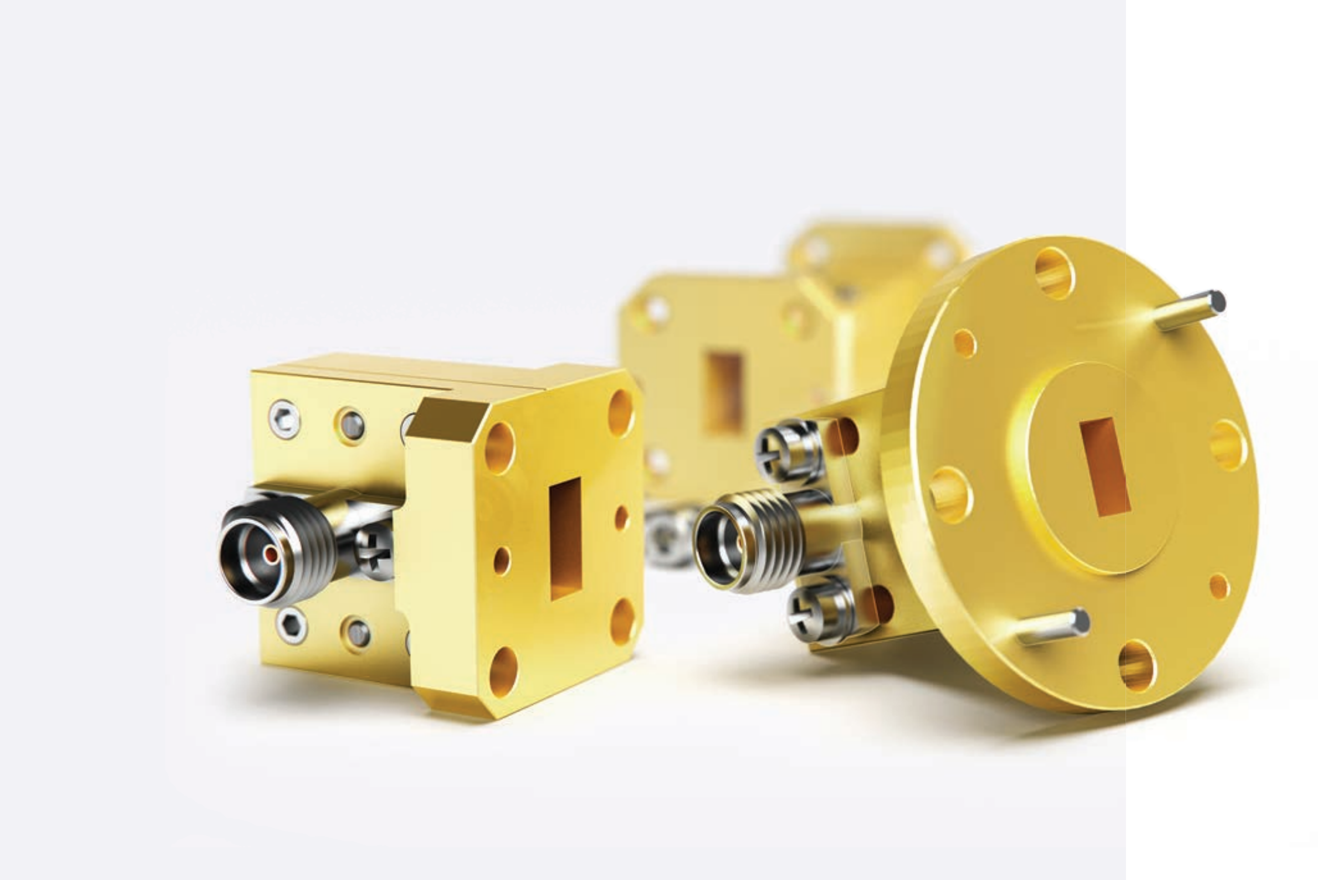

CommercialMarket

Cliff Drubin, Associate Technical Editor

Digital Twins, IoT and AI are Critical Enablers in the Journey to Net Zero in Cities

Cities account for more than 50 percent of the planet's population and are responsible for more than 70 percent of global carbon emissions. To combat this, decarbonization strategies are being employed by cities around the world. According to ABI Research, smart city technologies will be a critical asset for this transformation.

"The principles behind smart city technologies, such as increasing efficiency, better data management and better decision making are also essential for decarbonization and reaching net zero goals. Technologies such as digital twins, smart streetlights, micro-grids, computer vision, smart city management platforms and micro-mobility are all growing in popularity and can help with decarbonization," explained Dominique Bonte, vice president, End Markets at ABI Research. "The technologies can enhance decarbonization through more efficient energy use, better project planning, predictive maintenance, greener mobility options (such as e-bikes and e-scooters) and greater urban management through better data management."

There are many examples of cities deploying smart city technologies to enable decarbonization including London's recent expansion of the Ultra-Low Emission Zone, which uses a variety of technologies such as automatic number plate readers, CCTV cameras and environmental sensors to assess the impact of the new regulations. Another example is Tengah, Singapore. Tengah is Singapore's innovation district and uses a variety of technologies to support decarbonization including a centralized cooling system, smart streetlights, smart waste removal, a mobile app for citizens' smart meters and mass rapid transport with a car-free city center. These strategies not only have a direct impact on energy consumption by also encourage and enable citizens to make better choices to help the city decarbonize.

"Cities have a great opportunity to influence how we reach net zero goals through their ability to regulate, purchase and influence their services. By opting for smarter, more resilient solutions they can reach and maintain their decarbonization goals to increase the health of their citizens and the wider community," Bonte concluded.

3GPP Release 17 and UAV Applications

The Alliance for Telecommunications Industry Solutions (ATIS) recently published its free 3GPP Release 17 – Building Blocks for UAV Applications report, describing how mobile networks supporting 3GPP Release 17 specifications can enable uncrewed aerial vehicle (UAV) applications. It also shows how the 3GPP system can be used to enhance the safe use of UAVs for commercial and leisure applications.

UAVs are heavily dependent on wireless communications in areas such as command and control, location-finding, collision avoidance and remote identification. "Evolving technology, standards and regulations are increasing the market for UAV services," noted ATIS President and CEO Susan Miller. "Because UAV applications interact with several different parts of the 3GPP system, it can be difficult to fully appreciate how 3GPP addresses UAV requirements by direct reference to the specifications. In many cases, the capabilities in 3GPP specifications are intended to be integrated with other standards to build complete solutions. With this new report, ATIS makes a major contribution to help technical decision makers and system architects better understand the role of 3GPP's UAV specifications and how they fit with other initiatives."

As a leading technology and solutions development organization, ATIS brings together the top global information and communications technology companies to advance the industry's most pressing business priorities. ATIS' nearly 200-member companies are currently working to address the all-Internet Protocol transition, 5G, network functions virtualization, big data analytics, cloud services, device solutions, emergency services, M2M, cyber security, network evolution, quality of service, billing support, operations and more. These priorities follow a fast-track development lifecycle—from design and innovation through standards, specifications, requirements, business use cases, software toolkits, open-source solutions and interoperability testing.

ATIS is accredited by the American National Standards Institute. ATIS is the North American organizational partner for the 3rd Generation Partnership Project, a founding partner of the oneM2M global initiative, a member of the International Telecommunication Union, as well as a member of the Inter-American Telecommunication Commission.

5G-Advanced to Launch in 2025

The 3GPP approved the Release 18 package in December 2021, making the official start of 5G-Advanced with the planned freeze date in December 2023. ABI Research expects that 75 percent of 5G base stations will be upgraded to 5G-Advanced by 2030, five years after the estimated commercial launch. 5G-Advanced will bring continuous enhancements to mobile network capabilities and use case-based support to help mobile operators with 5G

For More Information Visit mwjournal.com for more commercial market news.

commercialization, long-term development of AI/machine learning (ML) and network energy savings for a fully automated network and a sustainable future.

"In 5G-Advanced, extended reality (XR) applications will promise monetary opportunities to both the consumer markets with use cases like gaming, video streaming, as well as enterprise opportunities such as remote working and virtual training. Therefore, XR applications are a major focus of 3GPP working groups to significantly improve XR-specific traffic performance and power consumption for mass market adoption," explained Gu Zhang, 5G & Mobile Network Infrastructure principal analyst at ABI Research. "Another noticeable feature is AI/ML which will become essential for future networks given the predictive rapid growth in 5G network usage and use case complexities which can't be managed by legacy optimization approaches with presumed models. System-level network energy saving is also a critical aspect as operators need to reduce the deployment cost but assure network performance for various use cases."

The upgrade of 5G network infrastructure is expected to be faster in the consumer market than in enterprises. ABI Research forecasts that 75 percent of 5G base stations will be upgraded to 5G-Advanced, while in the enterprise market the ratio is about half. 5G-Advanced devices per radio base station will quickly gain traction around 2024 to 2026 at the early stage of the commercial launch because devices will grow more aggressively than network deployments over the period.

> Expect 75 percent of 5G networks to upgrade by 2030.

"The commercial launch of 5G-Advanced will take two or three years, but the competition has already started," Zhang points out. "Taking AI/ML development as an example, industrial leaders such as Ericsson, Huawei, Nokia, ZTE and Qualcomm have trialed their solutions with mobile operators across the world. Ongoing development in this area will continue to bring improvements on traffic throughputs, network coverage, power saving, anomaly detection, etc."

Different from previous generations, 5G creates an ecosystem for vertical markets such as automotive, energy, food and agriculture, city management, government, healthcare, manufacturing and public transportation. "The influence on the domestic economy from the telco players will be more significant than before and that trend will continue for 5G-Advanced onward. Network operators and vendors should keep close to the regulators and make sure all parties involved grow together when the time-to-market arrives," Zhang concluded.

Around the **Circuit**

Barbara Walsh, Multimedia Staff Editor

MERGERS & ACQUISITIONS

After an exclusive negotiation process that began in December 2021, **Orolia,** a company recognized globally for its positioning, navigation and timing and related activities, technologies and equipment joins **Safran Electronics & Defense**, the European leader and world number three in inertial navigation systems. Orolia employs more than 435 people in Europe and North America and has revenues of around €100 million. Its solutions include atomic clocks, time servers, simulation and resilience equipment for GNSS signals, as well as emergency locator beacons for commercial aviation and military applications. These make Orolia a highly complementary and synergistic part of Safran Electronics & Defense's activities as it meets the challenges of positioning, navigation and synchronization in contested and vulnerable environments.

Signal Hound announced the sale of the company to **Harrison Osbourn**. This new era at Signal Hound comes after Bruce Devine's decision to retire. From a small shop in La Center, Wash., to the impressive facility it now occupies in Battle Ground, the company is poised for the next level of its development. With new expertise, the addition of resources and a focused leadership team, Signal Hound has substantial plans for new product development. The R&D pipeline is both noteworthy and timely.

Arcline Investment Management announced the acquisition of **Custom Interconnects LLC** and the formation of **Qnnect LLC**, a specialty interconnects platform aimed at solving critical connectivity challenges in high performance applications. Qnnect brings Custom Interconnects together with Meritec and Joy Signal Technology. Custom Interconnects designs and manufacturers Fuzz Buttons, a high performance, proprietary contact pin technology enabling critical applications within the aerospace, defense and semiconductor industries. Fuzz Buttons perform exceptionally well in small form factor electronics that require low signal distortion, high frequency, low insertion force and shock and vibration resistance.

Eutelsat Communications and **OneWeb** have signed a Memorandum of Understanding with the objective of creating a leading global player in satellite connectivity through the combination of both companies in an all-share transaction. Eutelsat will combine its 36-strong fleet of GEO satellites with OneWeb's constellation of 648 LEO satellites, of which 428 are currently in orbit. The potential transaction builds on the deepening collaboration between Eutelsat and OneWeb, which began with the equity stake acquired by Eutelsat in OneWeb in April 2021, the global distribution agreement between Eutelsat and OneWeb announced in March 2022 and the new exclusive commercial partnership.

COLLABORATIONS

Granite River Labs (GRL), a global leader in compliance test and certification of high speed digital designs, cables and connectors, and **Rohde & Schwarz** continue their partnership to build up GRL's new European test laboratory in Karlsruhe, Germany, opened in December 2021. GRL has added the R&S ZNB20 vector network analyzer (VNA) from Rohde & Schwarz to the test equipment resources of their test lab. With this step, the lab's range of industry services is being extended to VNA-based measurements for verification, debugging and compliance tests of cable assemblies and connectors for Automotive Ethernet, Automotive SerDes Alliance, USB, HDMI and many other standards.

Indium Corporation®, a leader in supplying products to global electronics, semiconductor, thin-film and thermal management markets, is partnering with **SAFI-Tech**, an Iowa-based startup that is creating no-heat and low-heat solder and metallic joining products. Metallic soldering represents a key manufacturing process across many industries, including aerospace, automotive and electronics. Current solder products trade off the reliability of joints formed with the very high processing temperatures needed to form those joints—a problem that has limited material selection and product design. SAFI-Tech's patented supercooling platform removes this tradeoff by creating capsules of molten solder that can remain liquid far below the normal freezing point of metal.

EdgeCortix® Inc., an innovative fabless semiconductor design company with a software first approach, focused on delivering class-leading compute efficiency and latency for edge artificial intelligence (AI) inference, announced a collaboration with **Renesas Electronics Corp**. Through this collaboration, EdgeCortix has taken its industry-leading heterogeneous platform-based compiler framework MERA and developed a new compiler, DRP-AI TVM for Renesas' DRP-AI accelerator. The new compiler is available with associated software and tools and works in combination with Renesas' DRP-AI tools.

Nokia announced it will lead 6G-ANNA, a German national-funded 6G lighthouse project. Nokia will collaborate with the 29 partners in 6G-ANNA to lead and drive 6G research and standardization. Funding for 6G-ANNA will come from the German Federal Ministry of Education and Research (Bundesministerium für Bildung und Forschung, BMBF), with an aim of strengthening and pushing German and European 6G agendas and driving global pre-standardization activities from a German and European perspective. 6G-ANNA is part of the larger "6G Platform German" national initiative and has a total volume of €38.4 million with a duration of three years.

For More Information For up-to-date news briefs, visit mwjournal.com

SPARK Microsystems, a Canadian fabless semiconductor company specializing in next-generation ultra-wideband (UWB), and **UWB Alliance**, an international non-profit organization dedicated to the promotion and growth of the UWB industry, have initiated a joint effort to test the coexistence and aggregation capabilities of UWB technology in environments where other UWB or other wireless protocols and radio devices are in use. This first phase includes testing the interoperability and compatibility of a pair of UWB technologies operating in a single environment simultaneously with UWB transceivers from SPARK Microsystems and other industry players.

3D Systems, a leader in delivering additive manufacturing solutions and expertise to advance applications and industries, has announced a new collaboration with **Fleet Space Technologies**, which has led to the production of innovative RF patch antennas for use on their Alpha satellite constellation. The combination of Fleet Space Technologies' unique design along with the expertise of 3D Systems' Application Innovation Group allowed them to architect a complete additive manufacturing solution—which includes process development and bridge production on its DMP Flex 350—enabling the companies to move from Fleet Space's existing RF patch design to small batch production in just three weeks.

CONTRACTS

L3Harris Technologies has been awarded a contract to build the **Space Development Agency's** Tranche 1 Tracking Layer satellite program to serve as "eyes in the sky" detecting, identifying and tracking advanced missile threats. The contract has a potential total value of $700 million. L3Harris will build a 14-vehicle satellite constellation that will include optical communications terminals, infrared mission payloads, Ka-Band communications payloads and multiple pointing modes—advanced technology specifically designed to identify and track the fastest missiles known to exist. The program also includes related ground, operations and sustainment support.

Stellant Systems Inc. was one of two companies recently awarded a $91M IDIQ contract from the **U.S. Navy**. The five-year contract is to repair crossed field amplifiers (CFAs) for the AEGIS Combat System. The multiple-award contract will involve reconditioning and overhauling three different types of CFA electron tubes. This work will be performed at Stellant's Williamsport, Pa., facility. Naval Supply Systems Command's weapon systems support organization carried out the solicitation for the "limited-competitive requirement," according to the award notice. The AEGIS Combat System, produced by Lockheed Martin, uses computer and radar technology to track and guide weapons to destroy enemy targets.

Mission Microwave Technologies LLC, a manufacturer of highly efficient solid-state power amplifiers, has confirmed an eight million dollar order for the continuation of a major upgrade program for a customer supporting a U.S. government requirement. Mission Microwave engineers worked with their customer to create an upgrade path for the U.S. Government to replace legacy TWTA based block up-converters (BUCs) with state-of-the-art solid-state BUCs, based on GaN technology, to upgrade a fleet of widely deployed transportable terminals. The initial upgrades started in late 2019 and prior to this recent award over one hundred sets of Ku- and Ka-Band BUCs have been delivered to Mission Microwave's customer on the program.

Gapwaves, a Swedish tech company, and **Bosch**, a leading global automotive supplier, have entered into an agreement regarding the development and large-scale production of high-resolution radar antennas for automotive vehicle applications

RICHARDSON RFPD

DESIGN ACCELERATORS

WE'RE ENGINEERS. WE GET IT.

Richardson RFPD understands the race to the finish line when it comes to new designs. Our Design Accelerators help design engineers get the job done faster and better, from prototype to production.

HARDWARE + SOFTWARE + SUPPORT + DESIGN PARTNERS

Design Accelerators speed time-to-market and decrease risk

- Off-the-shelf solutions with various levels of integration available
- Complete ecosystem of hardware, software, support and design partners
- Licensable and customizable designs
- Ideal for R&D, prototyping and proving concepts
- Versatile for communications, radar, electronic warfare and instrumentation

Accelerate your design.

Visit richardsonrfpd.com/design-accelerators

RichardsonRFPD
An Arrow Company

Your Global Source for RF, Wireless, IoT & Power Technologies

www.richardsonrfpd.com | 800.737.6937 | 630.262.6800 aiming at highly automated driving. The contract has an expected sales value of high double-digit million-euro range over the next decade. Corresponding contracts were signed on July 22, 2022, by the two companies. Due to the increased demand of advanced active safety systems and autonomous applications, the market for high-resolution radar antennas for the higher levels of automated driving (SAE level 4) is predicted to strongly increase within the coming years.

Sensor solutions specialist **HENSOLDT** will deliver its latest-technology identification-friend-or-foe (IFF) products to **ELTA Systems Ltd**, a subsidiary of Israel Aerospace Industries Ltd. HENSOLDT was awarded by ELTA several contracts worth approximately 10 million Euros to deliver a number of MSSR 2000 ID and MSR1000I secondary radars, including test equipment. The IFF systems working according to the latest Mode 5 NATO standard will be integrated into civil air traffic control radars as well as military air defence radars operated by several customer nations. Military IFF systems, like civil air traffic control radars called secondary surveillance radars, precisely identify aircraft by automatically sending interrogation signals which are answered by so-called transponders on-board friendly aircraft.

Kratos Defense & Security Solutions Inc. announced that it was awarded a contract from the **U.S. Army's Combat Capabilities Development Command** to demonstrate a virtualized satcom ground system. Based upon Kratos' Open Space Platform, the solution will enable the government to field satcom networks in line with modernization goals including streamlining gateway and remote terminal capabilities supported by multiple vendors, reducing life-cycle costs and supporting adaptive, dynamic space operations. Funding for this award was through the Network Command, Control, Communication and Intelligence Cross-Functional Team (N-CFT) established by the Army's Future Command.

PEOPLE

▲ *Kamran Cheema*

Akoustis Technologies Inc., an integrated device manufacturer of patented bulk acoustic wave (BAW) highband RF filters for mobile and other wireless applications, announced that **Kamran Cheema** has been appointed its new chief product officer. Cheema joined Akoustis in August 2021 as VP of Engineering, bringing a wealth of RF experience in product design, manufacturing, technology development, program management and quality management with over 30 years of experience in acoustic technology. He will be responsible for the device engineering and product design teams as well as the testing, characterization and mechanical design of all Akoustis products for all end markets including 5G mobile, 5G infrastructure, Wi-Fi and other markets.

▲ *Michael V. Carano*

Averatek announced that **Michael V. Carano** has joined their corporate leadership team as vice president of quality. Carano brings 40 years of electronics industry experience to Averatek, with special expertise in manufacturing, chemicals, metals, semiconductors, medical devices and printing. A recognized thought leader, subject matter expert and author, Carano holds seven U.S. and 20 foreign patents. He serves as a member of the Board of Directors, a committee chair and as an instructor for the IPC global industry association.

Mitsubishi Electric Automation Inc. announced the promotion of **Sunil "Sunny" Ainapure** to director of product marketing, **Deana Fu** to director of product management and the hiring of **Dean Norton** as strategic marketing director. Ainapure, who has been with Mitsubishi Electric Automation for 18 years, will lead the company's product marketing department. In her role as director of product management, Fu is taking on a strategic role focused on delivering products and solutions that are customer- and market-centric. Norton comes to Mitsubishi Electric Automation as a new hire and will assume the role of strategic marketing director.

▲ *Cesar "Rico" Rodriguez*

Marvin Test Solutions Inc. announced it has selected **Cesar "Rico" Rodriguez**, CEO of SPLASH 3 LLC, as its director of Military & Aerospace Business Development. A graduate of The Citadel and the U.S. Naval War College, Rodriguez is a U.S. Air Force (USAF) veteran who retired after a storied 25-year career of service in the USAF as a colonel, commander and fighter pilot. His private sector experience spans 16 years and includes business strategy and business development roles with various business units of Raytheon and Raytheon Technologies.

REP APPOINTMENTS

Peraso Inc., a leader in mmWave technology for 5G networks, announced a distribution agreement that enables **Richardson RFPD**, a global leader in the RF, wireless, IoT and power technologies markets, to sell Peraso's RF products on a global basis. Peraso's product offerings include the PERSPECTUS™ and PRO module product families, a new generation of integrated 60 GHz modules operating in the unlicensed 57 to 71 GHz V-Band spectrum and enabling rapid deployment in both private and public 5G applications. These module families allow for the ability to select multiple different performance levels that best meet the application's requirements and configuration.

Richardson Electronics Ltd. announced a global sales distribution agreement with **Altum RF**, a supplier of high performance RF to mmWave semiconductor solutions for next-generation markets and applications. With amplifiers, switches and other products working up to 100 GHz, Altum will further expand Richardson Electronics' portfolio to support continually rising frequencies in the market, including 5G/6G, satcom, test and defense applications. Inspired by leading experts in the RF/microwave industry, Altum RF transforms how partnerships work to develop high performance products with a focus on excellent technical support and customer service. Richardson Electronics provides solutions and adds value through design-in support, systems integration, prototype design and manufacturing, testing, logistics and aftermarket technical service and repair on a global basis.

Quantic Wenzel, an industry leader in crystal oscillators, fixed-frequency systems, integrated microwave assemblies and synthesizers, announced that they have partnered with **Deh-Ron, Ltd.** to support customers with mission-critical applications throughout Israel. Founded in 1982, Deh-Ron is headquartered in Tel Aviv-Yafo, Israel, and specializes in RF, microwave and mmWave solutions.

INVITED PAPER

Answering High Frequency Radome Needs with Fluoropolymer Fabrics

Alex Blenkinsop
Saint-Gobain, Merrimack, N.H.

The best radome is no radome. But when one is needed, it is required to protect the underlying electronic equipment from the outdoor environment while creating as little attenuation as possible to the transmitting signal. Radomes have historically been used in one of three applications: 1) aerospace, 2) large ground installations operating at high frequency and 3) simple shrouding used for low frequency telecommunications. With the onset of 5G mmWave applications, many IoT use cases, LEO Internet and increased backhaul applications, numerous communication technologies are poised to take over this market, all of which are operating at higher frequencies than their incumbent technologies.

Higher operating frequencies have several advantages over low frequency systems; but at the core of why they are synonymous with new use cases is that they allow the system to carry more data, at faster speeds, for a greater capacity of users. These benefits are critical to the viability of almost all use cases, but they do cause significant challenges that the new infrastructure must overcome.

RADOME OPTIONS

Historically, there have been two main construction options for telecommunication radomes: 1) single layer monolithic materials, such as glass reinforced thermosets or thermoplastics and 2) multilayer sandwich

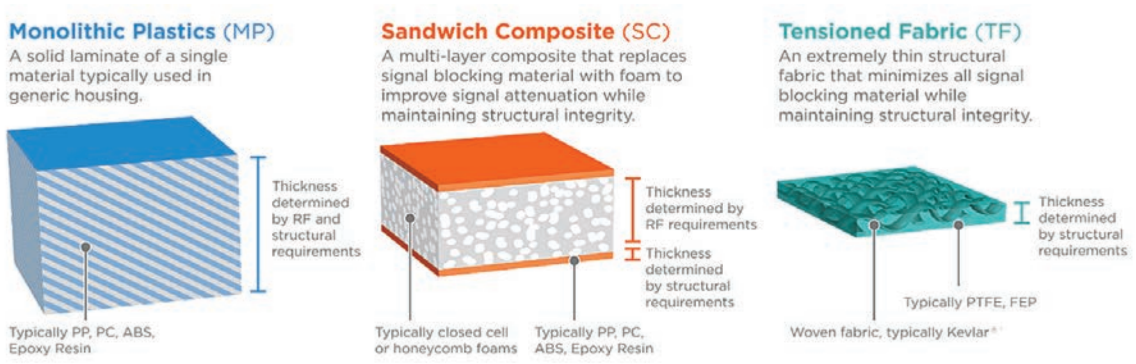

Fig. 1 Radome construction options for use in high frequency applications.


Portable Handheld Field Solutions
Expand your choice signal analysis setup
Direct-Connect or Remote Connect
24 to 110 GHz
Direct-Connect
Standard 1/4-20 Threaded Camera MountHole for Remote Connect
Remote Connect
Innovation in Millimeter Wave Solutions
www.omlinc.com
(408) 779-2698
OML

composites, which use structural skins on either side of an electrically invisible core to limit the amount of signal blocking material. These solutions are well suited to current low frequency technology; however, they experience significant electrical and thermal limitations at higher frequencies. Therefore, a third construction type has been developed and is introduced here: 3) structural fabrics tensioned by a supporting frame. All three options for high frequency radomes are shown in ***Figure 1***.

The primary function of a radome is to protect the underlying electronics while not impeding the transmitted signal; and the effectiveness of any radome is largely governed by understanding their impact on the transmitted and reflected waves. All radomes are comprised of dielectric materials that are defined predominantly by their dielectric constant (D_k), dissipation factor (D_f) and their associated thicknesses. For a signal passing from air through an isotropic, homogenous dielectric with negligible magnetic field properties, the impedance of free space and of the dielectric is defined as follows:

$$Z_0 = \frac{E}{H} = \sqrt{\frac{\mu_0}{\varepsilon_0}} = 377\Omega$$

and (1)

$$Z_1 = \sqrt{\frac{\mu_0}{\varepsilon_0 \cdot \varepsilon_1}} = \frac{Z_0}{\sqrt{\varepsilon_1}} = \frac{377\Omega}{\sqrt{\varepsilon_1}}$$

where Z_0 is the impedance of free space, Z_1 is the impedance of dielectric, E is the electric field strength, H is the magnetic field strength, μ_0 is the magnetic constant (permeability of free space) and ε_0 is the electric constant (permittivity of free space).

As an incident signal is transmitted through a monolithic dielectric, it experiences two changes in medium: the first at the free space/dielectric boundary as the wave enters the radome, the second at the dielectric/free space boundary as the wave exits the radome. Both interfaces create a reflected and transmitted wave; and both create loss through a combination of reflection and absorption. The ratio

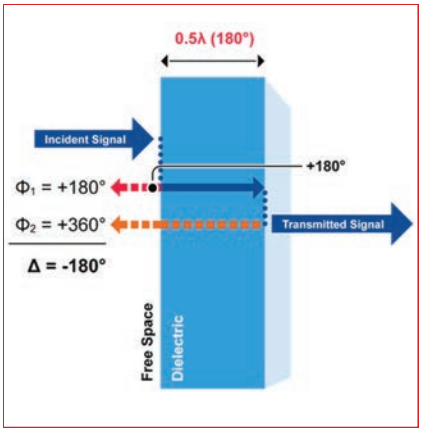

Fig. 2 **The reflected vs. transmitted wave relationship of an electrically thick radome.**

of losses created is governed by the reflection and transmission coefficients that are defined as follows:

$$\Gamma = \frac{Z_1 - Z_0}{Z_1 + Z_0}$$

and (2)

$$\Pi = \frac{2Z_1}{Z_1 + Z_0} (\text{or } \Pi = 1 + \Gamma)$$

where Γ is the reflection coefficient and Π is the transmission coefficient.

As radomes intentionally use low loss materials, it is the reflective loss rather than absorption that governs the overall performance; therefore, the purpose of a radome can be simplified to a device that uses its construction to cancel out the complex amplitude of the reflected waves so that virtually no energy is sent back to the transmitter. There are an infinite number of reflected and transmitted waves inside the dielectric, but if a first order approximation is assumed, this cancellation is achieved by matching the thickness to half the signal's free space wavelength, or a multiple thereof, as designated below:

$$\Delta\varphi = \varphi_1 - \varphi_2 = 180° \quad (3)$$

where φ_1 is the accumulated phase of first reflection, φ_2 is the accumulated phase of second reflection and $\Delta\varphi$ is the desired phase difference.

In calculating the accumulated phase shift of the first reflected wave, it is important to note that a reflected wave naturally experiences a +180-degree phase shift when crossing from a medium of a lower refraction index to one with a higher refraction index, i.e.: when trying to enter the radome. By designing the electrical thickness of the radome to exactly 0.5λ, the second reflected wave has naturally undergone +360 degrees of phase change via the two-legged journey through the radome and achieves the +180-degree difference required for cancellation. This behavior is graphically illustrated in ***Figure 2***.

To ascertain the correct physical thickness of the dielectric, the electrical length is assumed to equal the refraction index multiplied by the physical thickness; and as loss tangents for radome materials are low, this can be further simplified to equal physical thickness multiplied by the square root for the dielectric constant. Resolving the accumulated phase of the second reflected wave against the required phase change for cancellation equals the following:

$$(+180°) - \left(\frac{2\pi}{\lambda} \cdot \sqrt{D_k} \cdot 2t\right) = \pm 180°$$

$$\text{therefore } \sqrt{D_k} \cdot t = \frac{\lambda}{2} \quad (4)$$

where λ is the free space wavelength, D_k represents the dielectric constant of radome and t is the physical thickness.

When done correctly, and at a normal angle of incidence, this solution can provide extremely low losses with the required structural support for environmental protection. However, this construction type greatly suffers when either high angles of incidence are expected or wide bandwidth systems require multiple frequencies to pass through unimpeded.

A sandwich laminate operates in much the same way but with additional boundary interfaces. Griffiths[1] and others have cited that the ideal construction for cancellation is a core thickness of a quarter wavelength; however, this rule of thumb is only an approximation, and the interaction is more accurately described by Mazlumi.[2] With the approximation of an air core, the following condition emerges for maximum transmission (eq. 23 Mazlumi, 2018):


3H Communication Systems
YOUR CUSTOMER CAN'T WAIT.
WHY SHOULD YOU?
3H DELIVERS RF/MICROWAVE FILTERS AND TECH SUPPORT FASTER.
Miniature SMT, Cavity Filters, available from 5.0 to 25 GHz
Nano, SMT Filters, available from 40 MHz to 6.0 GHz, in LC and Ceramic Topologies
Pico, SMT Filters, available from 5.0 GHz to 27 GHz
Cavity Filter 10 MHz to 50 GHz. Bandwidths: 0.2 to 100%. Low or high PIM
Miniature Diplexers, available from 40 MHz to 27 GHz
The 3H quick-response team is ready to design and deliver DC to 50 GHz custom filter and diplexer solutions when you need them. Leadless surface mount options are available.
Custom designed and manufactured to your specific needs
Smallest possible package designs without performance loss
Delivered faster — compare delivery times first!
Better — in fact, the best customer service and engineering support!
High- and low-power applications available in the smallest packages
AS9100 and ISO9001:2015 Certified
3H Communication Systems
Learn more about how 3H can keep your project on track by talking to one of our engineers.
Call 949.529.1583 or visit 3HCommunicationSystems.com.

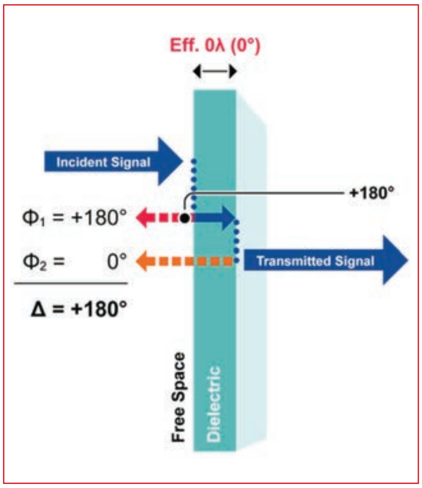

Fig. 3 The reflected vs. transmitted wave relationship of an electrically thin radome.

$$e^{2j\delta_2} = -e^{-2j\delta_1}\frac{1-e^{+2j\delta_1}\rho^2}{1-e^{-2j\delta_1}\rho^2} \qquad (5)$$

where $j=\sqrt{(-1)}$, δ_1 (resp. δ_2) the one-way phase accumulation $2\pi/\lambda\cdot t\cdot\sqrt{D_k}$ through the skin (resp. the core) and ρ is the transverse reflection coefficient at the air-skin interface.

If the skin is electrically negligible ($e^{\pm 2j\delta_1}$ = 1), the electrical thickness of the core has to be a quarter wavelength for maximum transmission. However, if the skin is not absolutely electrically thin or the core has a refractive index $n_{core}\neq 1$, the condition is no longer met and a numerical optimization of the thicknesses has to be used to get the best transmission.

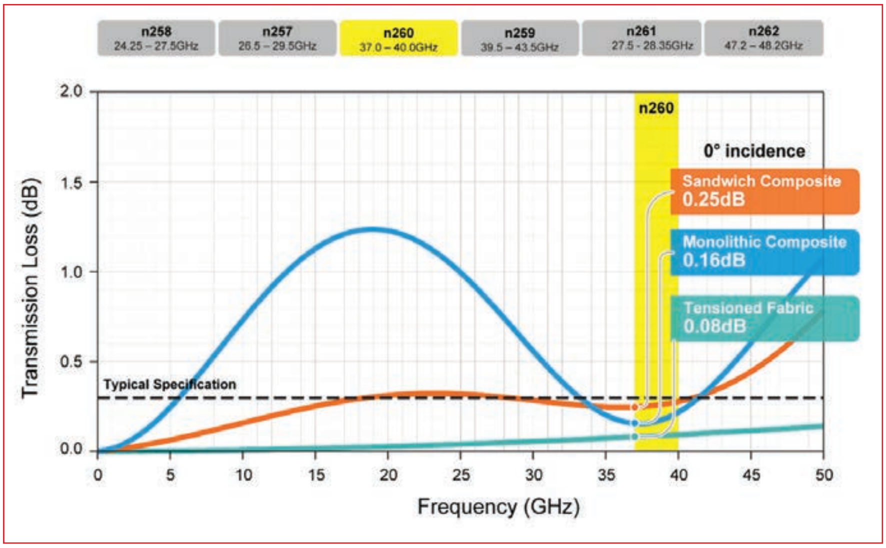

Fig. 4 Three radome constructions tuned for optimum performance at 37 GHz frequency at 0° angle of incidence.

FABRICS IN HIGH FREQUENCY RADOMES

Fabrics have been traditionally used in much larger air-inflated radomes that use positive pressure to retain structural integrity. For high frequency systems, they have been redesigned to optimize for the new application. The fabric composite is constructed from high strength aramid fibers (Kevlar®) with a blended fluoropolymer matrix. The aramid fibers are oriented in a flat, plain weave for enhanced flexural characteristics and high tear strength specifically for use in radome applications. The blended fluoropolymer matrix uses polytetrafluoroethylene (PTFE) and fluorinated ethylene-propylene (FEP) to provide optimum hydrophobicity preventing water accumulation and actively encouraging rain to slide off the exterior surface.

Much like other radome constructions, their behavior with an incident signal is governed by the same physical principles demonstrated with monolithic plastics in Figure 2; with the key difference being their extremely reduced thickness. A radome can be defined as being electrically thin if the thickness of the dielectric material is less than approximately one tenth the

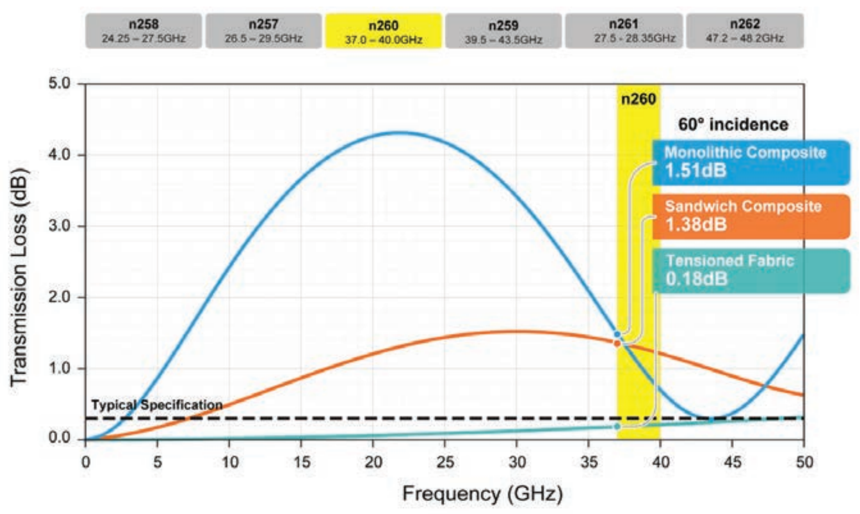

Fig. 5 Three radome constructions tuned for optimum performance at 37 GHz frequency at 60° angle of incidence.

signal's wavelength in free space ($t < 0.1\lambda$). Under these conditions, the radome works to achieve the required 180-degree phase difference by minimizing the distance traveled by the second reflected wave so that the subsequent accumulated phase shift is negligible. This is illustrated in ***Figure 3***.

The structural fabrics used in radome applications have a total nominal thickness of 0.008" [0.20 mm] compared to approximately 0.200" [5 mm] in monolithic plastics, where the additional thickness is necessary to provide the required structural performance. The importance of this thickness difference is correlated closely to the wavelength of the signal passing through and illustrates why high frequency applications require new radome solutions.

At 1 GHz (the approximate frequency of 4G telecommunications), the signal passing through the radome has a wavelength of 300 mm. This long wavelength makes both plastic- and fabric-based systems qualify as electrically thin ($t_{plastic} = 0.0167\lambda$ and $t_{fabric} = 0.0007\lambda$) and so the degree of phase change through either system is negligible. However, at 40 GHz (the high end of current 5G mmWave applications), the signal's wavelength is now only 7.5 mm and so only fabric-based systems continue to behave as an electrically thin dielectric ($t_{plastic} = 0.67\lambda$ and $t_{fabric} = 0.03\lambda$). The importance of this difference is seen when analyzing the total transmission loss of each radome type at a specific frequency. ***Figure 4*** shows an optimized design of each style of radome tuned to the bottom of n260 band within 5G mmWave frequencies.

The impact of thickness can be seen where the monolithic plastic (blue) has a designed electrical thickness equal to half wavelength to tune to the desired 37 GHz frequency versus the tensioned fabric (green) for which the loss remains low as maximum reflections occur at much higher frequencies. This fundamental difference of behaving like an electrically thin dielectric even at high frequencies allows fluoropolymer fabrics to be band agnostic and provide low loss across a wide frequency range. The sandwich composite (orange) plot shows how adding additional skins on either side of an electronically invisible core can provide additional wide bandwidth benefits at 0-degree angles of incidence.

Up until now, every electrical situation has analyzed the impact of a radome at normal incidence angles, but this is rarely true in real world applications. The angle of the incident signal can create additional transmission losses if deviating too far from normal. Although the proximity to the emitting signal adds complexity in understanding the im-

pact of these angles, its effect can be simplified by equating it to the changing geometry the transmitting wave experiences.

For tuned radome systems, such as the existing sandwich and monolithic technologies, this change in geometry increases the amount of material the wave must travel through and so increases the accumulative phase of the second reflection. If this incidence angle is significant, it will cause the second reflected wave to no longer cancel the amplitude of the first wave and create significant signal attenuation. The effect a 60-degree incidence angle has on each technology is shown in ***Figure 5***.

The final electrical parameter important to radome performance is its ability to minimize water accumulation on the surface in the form of rain, snow or ice. This is arguably the most critical function of a high performing radome as water has such high attenuation properties compared to typical radome materials, that even a small amount can create tremendous signal degradation. The high dielectric constant (approximately 25× higher than typical radome materials) will create additional reflective losses; while the increased loss tangent (approximately 30×) will create absorption losses typically made negligible using low loss materials. At frequencies in the mmWave band, these losses can easily exceed 1 dB rendering even a well-designed radome unusable.

Fluoropolymer fabrics are inherently hydrophobic and are specifically designed to prevent water accumulation by maximizing the mobility of water on their surfaces. Hydrophobicity is typically defined as a surface that creates a > 90-degree static contact angle with a polar molecule, with any angle < 90-degrees defined as hydrophilic. While this definition has served many industries well in the past, the static contact angles of hydrophobic materials do not always correlate well with signal attenuation in wet conditions because those measurements fail to account for the impacts of surface texture and micro features on water droplet mobility. The fabrics presented here combine a uniquely

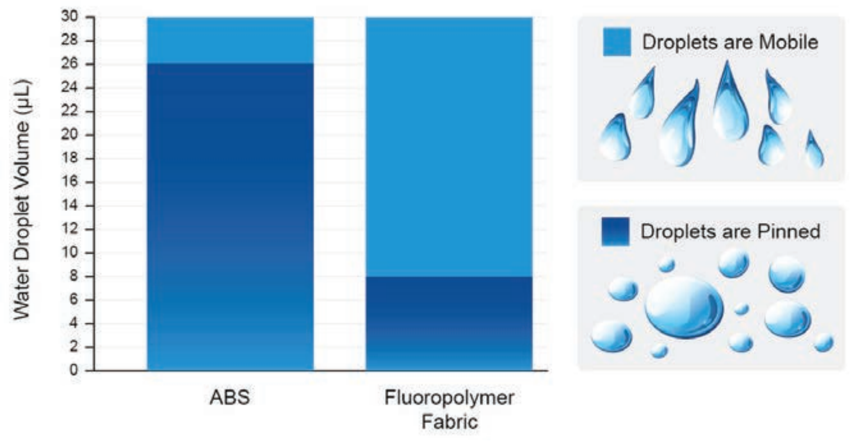

Fig. 6 **Water mobility as a function of droplet volume on an ABS surface and on a fluoropolymer fabric surface.**

effective blend of fluoropolymer compounds, woven fabrics and engineered surfaces to provide not only conventionally defined hydrophobic surfaces, but surfaces that have been proven to increase the likelihood of water runoff.

Drop mobility can be quantified by choosing a fixed surface angle and assessing the mobility of water droplets of different volumes to determine which stay pinned and which are mobile. ***Figure 6*** compares ABS (a typical monolithic plastic radome material) to a fluoropolymer fabric in the case of a completely vertical (90-degree incline) surface. In this study, it was seen that water droplets up to 26 µL in volume stay pinned to an ABS surface, while any water droplet > 8 µL is mobile on a fluoropolymer fabric surface. This increased drop mobility promotes enhanced water shedding and minimizes subsequent signal degradation.

SECONDARY BENEFITS OF FABRIC RADOMES

Fluoropolymer fabrics have two additional benefits over the incumbent technology that do not relate to their electrical performance. First, they are naturally UV stable compounds to offer enhanced performance over a given lifespan and second, they are less thermally conductive than their incumbent counterparts and so dissipate heat at a faster rate.

Fluoropolymer fabrics, in some capacity, have been used in radome applications for decades as a naturally inert PTFE compound that can resist environmental weathering without the need for repair or replacement. For high frequency fabric radomes, this technology has been compounded with highly effective UV blockers that enable the strong aramid weave to remain fully protected, ensuring lasting structural integrity while retaining its hydrophobic properties for the full life of the radome.

Their thermal advantage is a function of a greater stiffness combined with lower thermal conductivity. Fluoropolymer fabrics subjected to ASTM D5470 testing yield a thermal conductivity of 0.18 W/mK, which combined with a nominal thickness of 0.20 mm gives an R-value of 0.011 m^2K/W. For a well-designed monolithic plastic or sandwich composite radome, the comparative R-values will be approximately 3× and 6× higher, respectively, than any fabric solution. By dissipating heat at a faster rate, fluoropolymer fabrics can minimize the need for complex cooling systems, extend the life span of underlying electronic equipment by reducing the ambient operating temperature and help melt snow and ice from the surface during inclement weather. ■

References

1. L. Griffiths, "A Fundamental and Technical Review of Radomes," *MP Digest*, 2008.
2. F. Mazlumi, "Analysis and Design of Flat Asymmetrical A-Sandwich Radomes," *Journal of Telecommunication, Electronic and Computer Engineering*, Vol. 10, July 2018, pp. 9-13.

Ultra Low Phase Noise Phase Locked Clock Translators

Up to 27.5 GHz

Features
- Cost Effective
- Eliminates Noisy Multipliers
- Patented Technology

Applications
- Scanning & Radar Systems
- High Frequency Network Clocking (A/D & D/A)
- Test & Measurement Equipment
- High Performance Frequency Converters
- Base Station Applications
- Agile LO Frequency Synthesis

New!

Model	Frequency (Mhz)	Typical Phase Noise		Package
		@10 kHz	@100 kHz	
VFCTS100-10	100	-156	-165	
VFCTS105-10	105	-156	-165	
VFCTS120-10	120	-156	-165	
VFCTS125-10	125	-156	-165	
VFCTS128-10	128	-155	-160	
FCTS800-10-5	800	-144	-158	
FCTS1000-10-5	1000	-141	-158	
FCTS1000-100-5	1000	-141	-158	
FSA1000-100	1000	-145	-160	
FXLNS-1000	1000	-149	-154	
KFCTS1000-10-5	1000	-141	-158	
KFCTS1000-100-5	1000	-141	-158	
KFSA1000-100	1000	-145	-160	
KFXLNS-1000	1000	-149	-154	
FCTS2000-10-5	2000	-135	-158	
FCTS2000-100-5	2000	-135	-158	
KFCTS2000-100-5	2000	-135	-158	
KSFLOD12800-12-1280	12800	-122	-123	
KSFLOD25600-12-1280	25600	-118	-118	
KSFLO27R5-100-12	27500	-88	-98	

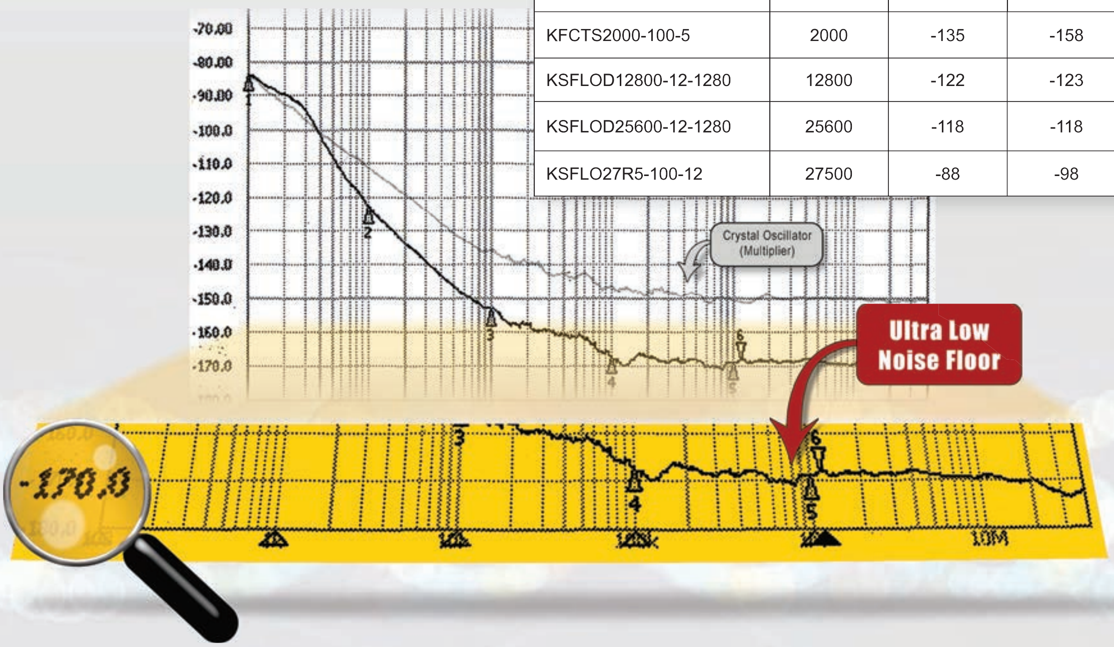

Talk To Us About Your Custom Requirements.

SYNERGY® MICROWAVE CORPORATION
Phone: (973) 881-8800 | Fax: (973) 881-8361
E-mail: sales@synergymwave.com | Web: www.synergymwave.com
Mail: 201 McLean Boulevard, Paterson, NJ 07504

INVITED PAPER

Open RAN Radio Unit Architecture for mMIMO

Volker Aue
AMD-Xilinx, Dresden, Germany

The article "The Open RAN System Architecture and mMIMO," published in the November 2021 issue of *Microwave Journal*,[1] described the open RAN (O-RAN) architecture and the split between the distributed unit (DU) and radio unit (RU) chosen by the O-RAN Alliance.[2] This article expands the discussion of the RU, focusing on the architecture and key requirements of the RU used for mMIMO. The article concludes with the design and initial measurement results of an RU for 5G band 77 using the AMD-Xilinx digital front-end (DFE) and Versal processor.

MMIMO RADIO UNIT

The principal elements that determine the performance of a mMIMO RU are the

- Antenna — all parameters related to the radiation layer
- RF signal chain — parameters primarily related to the RF transceiver
- Product — Additional elements contributing to the performance of the RU
- Mechanical and thermal design and the external operating environment

Each will be described in this section.

Antenna

The performance of an antenna in the RU is characterized by its gain and equivalent isotropic radiated power (EIRP), sidelobe levels, steering angle and elevation tilt.

Gain and EIRP — The maximum achievable gain of the mMIMO panel determines the maximum transmit power that can be directed to a specific user, where the EIRP is directly related to the gain of the antenna array. When receiving a signal from the user, the corresponding measure is equivalent isotropic sensitivity.

Gain comes at a price. To achieve higher gain, the antenna must have a larger active area, i.e., the size of the panel increases with gain. As the gain increases, the beamwidth decreases, which is intuitively expected as the antenna focus increases. With a limited number of transceivers, the steering—the azimuth or elevation range a beam can steer from boresight—decreases for a given maximum sidelobe level. The antenna design depends on the deployment environment and desired steering range. For a typical macro base station, a horizontal steering range up to ±60 degrees is desirable, depending on the minimum beam-

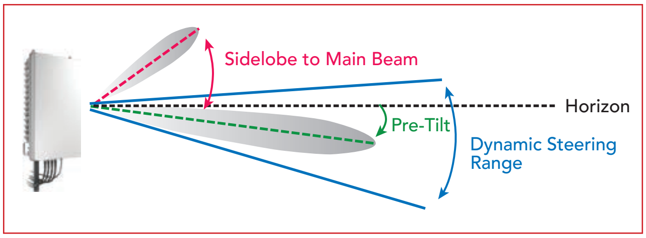

Fig. 1 Antenna beam vertical steering and pre-tilting.

width. A vertical steering range of ±10 degrees or less from boresight is typically sufficient.

Sidelobe levels (SLL) — mMIMO and RU performance depend on the sidelobes generated by the antenna radiation layer. Today's O-RAN mMIMO systems aim to limit sidelobe levels to below -10 dB across the whole sphere, particularly the horizontal and vertical steering ranges. A sidelobe that is not actively suppressed means power is also transmitted in the directions of the sidelobe, taking power from the desired direction. While active suppression techniques can reduce sidelobe levels, they also reduce the power in the main lobe.

Signals radiated from the sidelobes can cause interference in the unintended directions, with horizontal sidelobes interfering with adjacent sectors and vertical sidelobes interfering with adjacent cells. Both the upper and lower sidelobes should be considered. Upper sidelobes can reach into another cell when the main beam is steered downward, and the ground reflection of a lower vertical sidelobe can have a similar effect.

When receiving, power may come through a sidelobe from unwanted directions. Even though the DU can compensate for this, compensation typically increases the noise level of the remaining signal.

Steering — The ability of the RU to direct a beam away from boresight while keeping the SLLs low defines the steering range. Sidelobes tend to increase as the beam is directed away from boresight. Vertically, the steering range is often limited by a grating lobe, which causes the SLL to exceed the specified limit.

Typical values for the dynamic steering ranges for an RU with 64 transmit and 64 receive elements (64T64R) with SLLs ≤ -10 dB are ±45 degrees horizontal and ±5 degrees vertical. For 32T32R RUs with only two-element subarrays per column, the vertical steering range is less. For most macro base stations, ±2 degrees is sufficient.

Electrical pre-tilt — Macro base station RUs are often installed at elevated sites. From the viewpoint of the antenna, the user traffic is coming mostly from below the horizon. Since the vertical steering range is limited, antennas are often installed with a pre-tilt, implemented either mechanically or with a linearly progressing phase difference between the elements in the subarray (see ***Figure 1***). Pre-tilt is commonly used with RUs with 32 transceivers or less.

Remote electrical tilt (RET) — RET enables the pre-tilt of the RU to be adjusted remotely. This is easily done by remotely adjusting phase shifters built into the subarrays or by using a motorized bracket that tilts the antenna. Like pre-tilting, RET is typically used only for RUs with 32 or fewer transceivers because they have limited vertical steering compared to RUs with a larger number of transceivers.

RF Signal Chain

Connecting to the antenna, the RF signal chain influences the performance of the RU through its transmit power, bandwidth and error vector magnitude (EVM).

Conducted RF power — The transmit power supplied by the power amplifier (PA) to the antenna, known as the conducted RF power, determines the limits of coverage and cell capacity. The transmit power and antenna gain determine the maximum propagation loss the link can accommodate. In a mMIMO RU, the RF power is distributed over several spatial streams as well as resource blocks (RB). For larger cells, higher PA power increases the downlink capacity of the cell.

Bandwidth — Three bandwidths are associated with RUs. First, the occupied bandwidth (OBW) is the aggregate bandwidth over which the RU actively transmits and receives. Synonymous with the utilized spectrum, the OBW is the sum of all the active carrier bandwidths and the upper limit the RU can handle. Second, the instantaneous bandwidth (IBW) of the RU is defined from the left edge of the lowest frequency carrier to the right edge of the highest frequency carrier. Last, the operating bandwidth is the bandwidth supported by the RU, typically referred to as the operating band. For spectrum agility, operators desire the RU's IBW to support the entire band, i.e., the IBW should equal the OBW.

EVM — EVM is a measure of the distortion within a modulated signal and indicates the linearity of a transmit chain. In more efficient modulation schemes, such as 256- or 1024-QAM, more bits are mapped to a subcarrier, which requires increasingly cleaner transmit signals compared to lower-order modulation. Nonlinearities in the transmit chain add noise to the transmit signal, causing the constellation points to deviate from their ideal values, which makes demodulating the transmitted information in the receiver more challenging.

Product

In addition to the antenna and RF signal chain, these aspects of the design contribute to the performance of a mMIMO RU system: the number of data streams, phase and amplitude control and calibration, fronthaul, programmability, security and power consumption.

Number of data streams — The objective of the mMIMO architecture is to increase data capacity by tapping the spatial domain. If propagation conditions enable users to be separated, the number of spatial streams the RU can handle becomes the limitation. For a 64T64R RU, being able to handle 16 layers downlink and eight layers uplink is typically considered enough. For a 32T32R RU, the number of spatially resolvable signals will be less. To reduce fronthaul data rates, 32T32R RUs often use eight downlink and four uplink streams.

Phase and amplitude control and calibration — The 3GPP standard stipulates the structure of 5G signals.[3] While specifying the methodology used to generate channels and signals, 3GPP does not dictate how to process the signals at the receiver. Those algorithms are left to the equipment designer. Likewise, 3GPP does not prescribe the algorithms used in the radio resource manager (RRM). The RRM is the entity in the base station that allocates radio resources to users to maximize cell capacity, coverage and user experience, by assigning RBs to users and controlling parameters such as modulation and error coding.

In mMIMO, the RRM also controls parameters such as the beamforming vectors. Some of the algorithms may assume specific beam shapes, including sidelobe levels to be produced after downloading the corresponding beamforming patterns to the RU. For this to be accurate, the actual amplitudes and phases of the radiating elements must not deviate significantly from the values defined by the beamforming vectors. The main lobes are relatively robust to amplitude and phase errors; simulations have shown deviations up to 5 degrees and 0.5 dB do not have a "visible" impact on the overall shape of a beam.

In a time-division duplex system, where the uplink and downlink time share the same band, the DU may use the reciprocal characteristics of the propagation channel. For example, the DU may use uplink channel estimates to derive downlink beam weight vectors. So the RU should ensure that channel reciprocity is not degraded in the transmitters and receivers. To keep a user free from interference from other users' signals, the DU must be able to place notches in the direction of these signals, reducing them to 35 to 40 dB below the desired signal. If the notches are calculated assuming reciprocity, the phase and amplitude differences between transceivers must be less than 1 degree and a fraction of a dB, respectively.

As component parameters tend to change with temperature, voltage and age, precise closed loop calibration is necessary to maintain the required precision. The required calibration update speeds will vary with the deployment scenarios and geographies, so the mMIMO design should enable selecting among various accuracies and update rates.

Fronthaul — The fronthaul (FH) connects the DU to the RU. Generally, the RU and DU should use techniques to reduce FH bandwidth, as the bandwidth will drive the cost of the interconnect solution, i.e., the cost for cables, switches and transceivers increases with bandwidth. The O-RAN "Control, User and Synchronization Plane Specification" defines several compression techniques to reduce the FH traffic.[4] For the user plane, various bit widths are specified, with modulation compression the most prominent technique, where the modulation function is shifted to the RU. The DU sends the raw unmodulated bits to the RU instead of the frequency domain symbols to be transmitted. The introduction of different sections in the U-plane enable sending only the symbols that are used over the FH interface.

The C-plane traffic includes updating the beamforming vectors. In 5G, these vectors can be updated as often as every orthogonal frequency division multiplexing (OFDM) symbol. For vector updates with every time slot, this can represent more than 30 percent of the FH traffic. Therefore, the O-RAN Alliance has introduced techniques for reducing C-plane traffic. The O-RAN standard enables storing the beamforming vectors in a database at the O-RAN RU using an index, where the stored beamforming vectors are retrieved from the database by referring to the corresponding index. Updating the beamforming vectors is also possible. The O-RAN standard also supports calculating the beamforming vectors in the RU. However, the technique is not well standardized, such that the DU may not know the actual result of the calculation—making this technique of limited use.

The O-RAN Alliance is defining interoperability profiles to enable RUs to be used with DUs from various vendors. It is important for an RU to comply with the selected interoperability testing profile to guarantee interoperability.

Programmability — mMIMO in 5G O-RAN systems is still relatively new and needs to mature in the field. Field experience after deployment will likely lead to adding functionality for the RU to improve system performance. As the cost of exchanging equipment in a cellular network is considerable, the equipment should be designed to support long lifetimes once deployed, i.e., a minimum of seven years. To achieve this, the RU must have inherent flexibility to be updated with new functionality, whether the software on the main RU controller or features in the data paths.

The O-RAN Alliance will continue improving FH performance by adding compression techniques that more efficiently use available FH bandwidth. One candidate is supporting semi-persistent scheduling (SPS) in the RU. By conveying

SPS information to the RU, the scheduling information only needs to be signaled once. If the available FH bandwidth without this feature limits the update rate for the beamforming vectors, enabling SPS in the RU will free bandwidth and improve system performance. Other examples where updates will likely occur are improving the linearization in the DFE, reducing power consumption and improving temperature control.

Designing flexibility in the RU architecture enables manufacturers to introduce new technology as it becomes available and create derivatives tailored to various market needs. To update units already deployed in the field, the O-RAN Alliance has standardized field upgrades through the M-plane.

Security — To protect the infrastructure from attack, the RU must have security mechanisms, including authentication and integrity checks for software updates.

Power consumption — The power consumed by the RU adds to the operating expense of the network—with thousands of units consuming about 1 kW, the cost of energy is considerable. The power consumption of a mMIMO base station depends on the load, the instantaneous RF output power and the efficiency of the system. At full capacity, the power consumption is dominated by the PA and the efficiency of the transmit chains. While the efficiency of the PA is important, the losses between the PA and antenna must also be minimized, as well as the power consumption of the receive chains, the digital circuitry and the power regulators.

In most cases, the maximum load on the RU represents an extreme situation during peak hours of the day. The power consumption must also be optimized for typical and low load conditions. This is typically accomplished using RU power saving techniques like shutting off PAs, even shutting off complete carriers. Other than the RF power that gets radiated, the power consumed by the RU is converted into heat and needs to be efficiently transferred to the ambient environment while minimizing the temperature of the electronics. The power consumption drives the thermal design of the system, which adds to the size and weight of the RU.

Mechanical and Environmental

The size of an RU is a key requirement because the available real estate on the tower or at a pole is limited. In some cases, there is just enough space above the existing multi-band passive antenna to mount a 5G panel, provided it is not too tall.

Wind load is important because poles and tower structures are built and certified for a maximum wind load. Base stations are typically expected to remain operational in winds up to 150 km/h and to survive wind speeds of 200 km/h. The wind load of the RU is proportional to its surface area, i.e., panel size, and the form factor. Rounding the edges and using dedicated fins can reduce the wind load without changing the outer dimensions.

The weight of the RU determines the installation cost — how many technicians are needed to mount the equipment, possibly assisted with equipment like cherry pickers. In some cases, tower companies factor the wind load and weight into the rent, which contribute to an operator's monthly expenses.

Other requirements common to all radio designs include the

- Operating temperature range, typically -40°C to +55°C, with the output power reduced at higher temperatures to keep the unit operating reliably
- MTBF, typically greater than 200,000 hours, which is a challenge because of the large number of components in the RU
- Surge protection, to protect the RU from lightning strikes
- Ingress protection, typically rated at IP65
- Aesthetics.

O-RAN SPLIT 7.X MMIMO

To facilitate the deployment of mMIMO RUs for O-RAN, AMD-Xilinx has created reference designs and prototypes based on AMD-Xilinx IC technology (see ***Figure 2***). As an example, ***Table 1*** shows the design requirements for a 64T64R mMIMO RU covering 5G band n77 that has been implemented with the AMD-Xilinx architecture and chipset.

The O-RAN FH interface, beamformer, physical random-access channel and sounding reference signal extraction are all mapped onto a single Versal™ VC1902 SoC. Versal ACAP is a fully software-programmable,

heterogeneous computing platform that combines scalar adaptable and intelligent engines to achieve performance improvements up to 20x over the fastest FPGA implementations and > 100x over the fastest CPU implementations.[6] The Versal device contains a powerful ARM® processor subsystem, programmable logic (PL), and AI engines. The AI engines are very long instruction word, single instruction multiple data vector processing engines, well suited for efficiently computing beamformer operations like matrix multiplication, singular value decompensation and, if needed, matrix inversion.[7]

The Zynq UltraScale+ RFSoC was designed primarily for RF applications. It integrates the key subsystems required to implement direct RF sampling transceivers. Significant investments have been made in high performance data converters using 16 nm FinFET CMOS technology. Each Zynq UltraScale+ RFSoC contains multiple GSPS analog-to-digital and digital-to-analog data converters. The converters are high precision, high speed and power efficient as well as highly configurable.

The latest version of the Zynq UltraScale+ RFSoC—called the Zynq UltraScale+ RFSoC DFE—

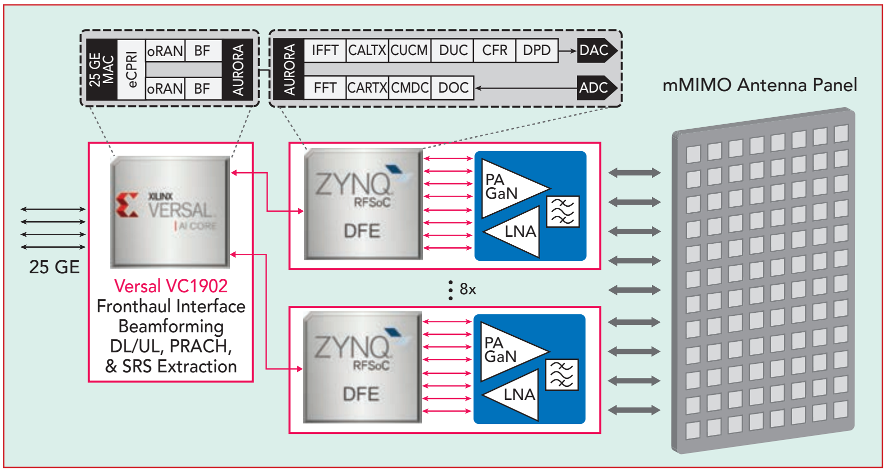

Fig. 2 AMD-Xilinx 64T64R RU hardware architecture.

TABLE 1

MMIMO RU DESIGN REQUIREMENTS

Parameter	Specification
MIMO Configuration	64T64R
5G Band	n77
Operating Bandwidth (MHz)	3700 – 3980 (U.S.) 3400 – 3800 (Europe and Other Regions) 3300 – 3700 (India and Latin America)
Instantaneous Bandwidth (MHz)	280 (U.S.) 300 or 400 (Europe, India and Latin America)
Occupied Bandwidth (MHz)	200
Maximum EIRP (dBm)	80
Conducted Power (W)	≤ 320
Number of Layers	16 Downlink, 8 Uplink
Operating Temperature	-40°C – +55°C
Fronthaul interface	ORAN Split 7.2x 4 x 25 Gbps Optical Ethernet
Antenna Array	12 x 8 x 2 Elements, 25 dBi Gain
Beam Steering	Horizontal: ±45° Vertical: ±5° @10 dB SLS, Pre-Tilt Supported
Minimum Beamwidth	Horizontal: 12° Vertical: 6°

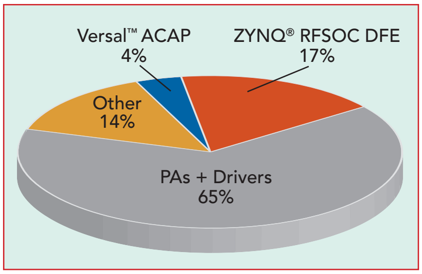

Fig. 3 Component energy use in a 320 W 64T64R mMIMO radio using Xilinx SoCs and GaN PAs.

uses dedicated logic for the digital functions often used in communications. They support the range of cellular applications, including indoor base stations for sub-6 GHz (FR1) and mmWave (FR2) bands, macro base stations and FR1 mMIMO RUs. The DFE's dedicated logic functions are optimized, scalable and parametrizable using standard cell hard-blocks for computing, combined with PL to adapt the functions to different application requirements. The standard cell hard-blocks deliver performance typically only found with ASICs, while the PL offers the flexibility of an FPGA. With both functions, the Zynq UltraScale+ RFSoC DFE provides twice the performance of the previous RFSoC generation while consuming half the power.

The logic blocks are used for the filtering, digital up- and down-conversion (DUC and DDC), interpolation and decimation, crest factor reduction (CFR) and digital predistortion (DPD). Other logic blocks include the fast Fourier transformation often used for OFDM modulation, which is part of the RU because of the 7.2 functional split chosen by the O-RAN Alliance. Unused FPGA capacity is available on the RFSoC to add functionality, enabling new functions to be added to RUs deployed in the field.

Figure 3 shows the relative energy consumption of the components of a 320 W 64T64R mMIMO radio using AMD's SoCs and GaN PAs. 65 percent of the power is consumed by the analog components such as the PAs and drivers. 17 percent is consumed by the RFSoC DFEs, of which a significant portion is used for the analog-to-digital conversion and DFE functions. These are also found in ASIC implementations.

RU PERFORMANCE

AMD built and tested a prototype of this RU for the North American n77 band. The transmit, receive and beamforming performance were measured and compared to the 3GPP specifications. A DU emulator from Keysight Technologies was used to stimulate the RU using the O-RAN FH interface.

Figure 4 shows the measured performance of the RU with a 256-QAM, 100 MHz wide signal and 8.8 dB CFR. The measured RF output power met the requirement of 37 dBm (5 W) per port with good EVM quality, i.e., 2.6 percent for the physical downlink shared channel. The adjacent channel leakage ratio measured -49 dBc, confirming the digital predistortion algorithm linearizes the GaN PA sufficiently to meet the leakage requirements. Frequency and time alignment errors met 3GPP requirements, and the defined signal bandwidth was 97.3 MHz, the exact requirement.

Beamforming performance was measured over the air in an anechoic chamber using all 64 transceivers of the RU, and the results were compared with a measurement of the antenna layer (see *Figure 5*). The antenna was set to boresight, i.e., 0 degrees both horizontal and vertical, using a beamforming vector with uniform coefficients. Specified for a steering range of ±45 degrees, the two plots overlap from

Fig. 4 EVM measurement of a 100 MHz bandwidth 256-QAM signal.

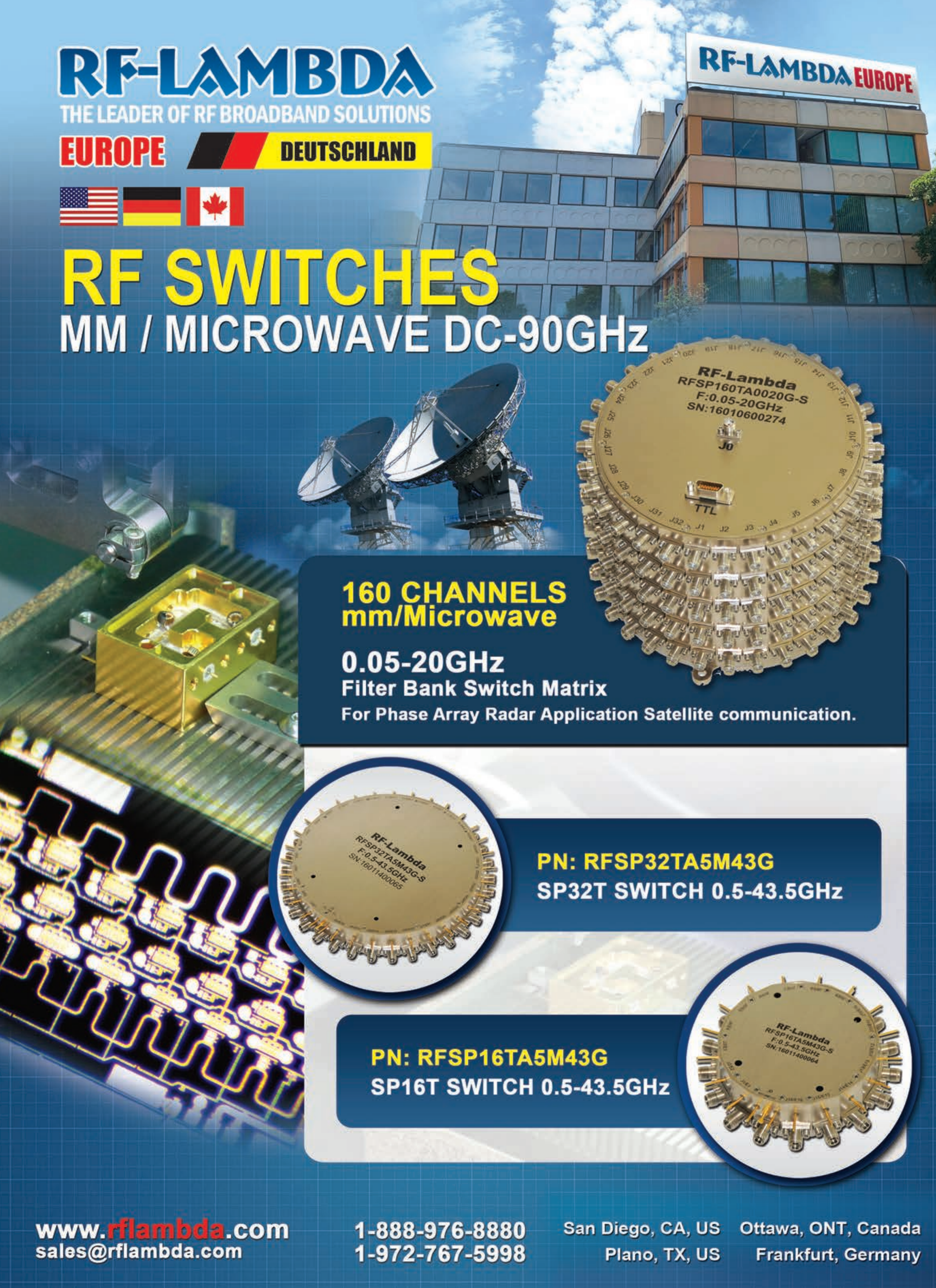
RF-LAMBDA
THE LEADER OF RF BROADBAND SOLUTIONS
EUROPE
DEUTSCHLAND
RF-LAMBDA EUROPE
RF SWITCHES
MM / MICROWAVE DC-90GHz
RF-Lambda
RFSP160TA0020G-S
F:0.05-20GHz
SN:16010600274
TTL
160 CHANNELS
mm/Microwave
0.05-20GHz
Filter Bank Switch Matrix
For Phase Array Radar Application Satellite communication.
PN: RFSP32TA5M43G
SP32T SWITCH 0.5-43.5GHz
PN: RFSP16TA5M43G
SP16T SWITCH 0.5-43.5GHz
www.rflambda.com
sales@rflambda.com
1-888-976-8880
1-972-767-5998
San Diego, CA, US
Plano, TX, US
Ottawa, ONT, Canada
Frankfurt, Germany

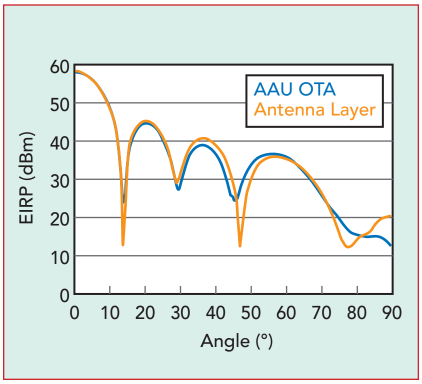

Fig. 5 OTA beamforming measurements of the antenna layer and RU.

0 to 30 degrees and show some divergence from 30 to 45 degrees.

SUMMARY

The O-RAN ecosystem is young. O-RAN systems are competing with the end-to-end options offered by the incumbent network equipment manufacturers. To achieve market acceptance, O-RAN solutions need to deliver equal or better performance at a cost advantage than the solutions offered by the established players.

The mMIMO RU adds uncertainty because it's a new architecture with limited history. The installation cost for a mMIMO panel can only be justified if it is reliable and will stay on the mast for several years without coming down for updates or maintenance. Ironically, mMIMO performance will certainly improve with time, coming largely from software and algorithm improvements, so the current generation of hardware that is fielded must have the flexibility to adopt these new capabilities that will improve system performance.

The Xilinx UltraScale+ RFSoC DFE provides a direct RF sampling transceiver platform for mMIMO applications. It delivers ASIC-like performance with the flexibility of an FPGA and moderate power consumption. Measurements confirm 3GPP and O-RAN Alliance performance targets can be met with this SoC solution. By bringing this high performance and flexible capability to O-RAN, AMD-Xilinx hopes to accelerate market adoption of O-RAN and mMIMO RUs. ■

References

1. V. Aue, "The Open RAN System Architecture," *Microwave Journal*, Vol. 64, No. 11, November 2021, pp. 70–82.
2. O-RAN Alliance, Web: www.o-ran.org/.
3. 3GPP RAN3 Technical Report TR38.803v1.1.0, Section 11, Figure 11.1.1-1, Web: www.3gpp.org/ftp//Specs/archive/38_series/38.801/38801-100.zip.
4. O-RAN Fronthaul Working Group, "Control, User and Synchronization Plane Specification," O-RAN.WG4.CUS.0-v04.00
5. 3GPP TS 37.145-1 V16.5.0 (2020-12), "3rd Generation Partnership Project; Technical Specification Group Radio Access Network; Active Antenna System (AAS) Base Station (BS) conformance testing; Part 1: Conducted conformance testing (Release 16)," 3GPP, Chapter 4, December 2020.
6. Xilinx, "Versal: The First Adaptive Compute Acceleration Platform (ACAP)," WP505 (V1.1.1), September 29, 2020, Web: docs.xilinx.com/v/u/en-US/wp505-versal-acap.
7. Xilinx, "Xilinx AI Engines and Their Applications," WP506 (V1.1) July 10, 2020, Web: docs.xilinx.com/v/u/en-US/wp506-ai-engine.

INVITED PAPER

A mmWave Power Booster for Long-Reach 5G Wireless Transport

M. Oldoni, S. Moscato, G. Biscevic, G.L. Solazzi and G. Skiadas
SIAE MICROELETTRONICA, Milan, Italy

A mmWave power booster enables increased output power by more than 10 dB without appreciably deteriorating signal integrity. It enables high-power 71 to 86 GHz communications up to 10 Gbps in a 2 GHz channel and paves the way for commercial mmWave links up to 5x current link lengths at E-Band.

As mobile communications evolve into their fifth generation, the offer of higher data speed and reduced latency puts a strain on the radio access sites and on the whole network, including its transport segment.[1] For wireless backhauling connections, as well as fronthauling and midhauling links as envisaged by the open-RAN paradigm,[2] this entails capacities larger than 10 Gbps and advanced fast processing capabilities.

To deal with similar needs, existing spectrum regulations traditionally offer channels in the microwave range (6 to 42 GHz), but these are too narrow to support more than 1 Gbps in each; while 2 GHz channels are available in the mmWave domain, specifically in the commercial E-Band (71 to 86 GHz) where a 128-QAM modulation can easily sustain 10 Gbps. Network operators are thus planning and deploying equipment for E-Band communications, and equipment manufacturers spend substantial effort in researching and developing such products.

The shift to E-Band, however, comes with some steep costs: 1) difficulty to obtain high power from available components, 2) larger propagation attenuation and 3) higher sensitivity to precipitation (i.e. rain, hail and snow). All of these concur to limit the achievable link distance, hence the modern wireless tradeoff of capacity versus distance.

While the latter two costs express physical phenomena, the former represents a technological limitation, which can be tackled. Part of the answer is provided by the use of large, more directive antennas, in turn requiring precise compensation of misalignments.[3] Instead, this paper outlines a complementary answer: a novel E-Band power booster to enable high capacity backhauling, fronthauling or midhauling in the mmWave region, which has been developed and tested in the field.

POWER BOOSTER ARCHITECTURE

The typical architecture of commercial backhauling equipment is based on a digital modem, some analog baseband or intermediate frequency circuitry and upconversion to 71 to 86 GHz followed by a power amplifier (PA). Current commercial

as low as
$70.00
Qty 500

ERAVANT
FORMERLY **SAGE MILLIMETER**

WR-28 | WR-22 | WR-19
UNI-GUIDE™
WAVEGUIDE CONNECTOR

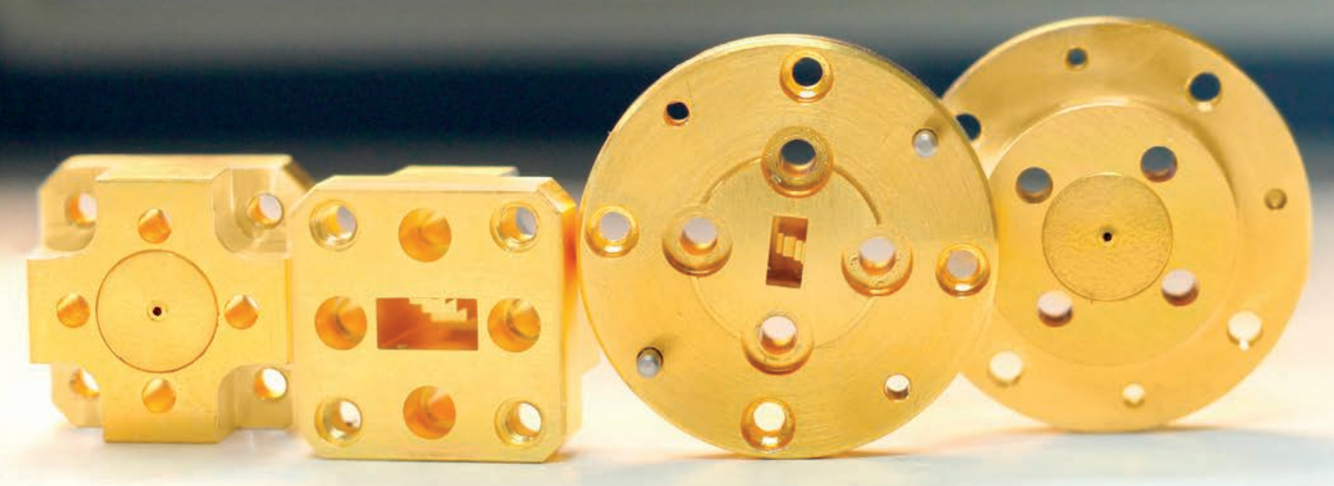

WAVEGUIDE INTERFACE WITHOUT DESIGN!

HERMETIC WAVEGUIDE SOLUTION

If the package is designed and manufactured to be hermetically sealed for coaxial connectors using a glass bead, it retains its integrity when using a **Uni-Guide™** to form the waveguide interface.

SAVE TIME & MONEY

Using the **Uni-Guide™** with a standard coaxial housing can provide any waveguide port needed instantaneously, without custom design or prototyping.

PORT TYPE & ORIENTATION FLEXIBILITY

Select any port configuration by using the proper coaxial connector or **Uni-Guide™**, simply rotating the waveguide connector yields a 90-degree or 180-degree change in port orientation to form various sub-assembly options.

WWW.ERAVANT.COM

www.eravant.com 501 Amapola Avenue Torrance, CA 90501
T: 424-757-0168 F: 424-757-0188 support@eravant.com

Adapters • Amplifiers • Antenna Feeds • Antennas • Attenuators • Bias Tees • Cable Assemblies • Corner Reflectors • Couplers • DC Blocks • Detectors • Ferrite Devices • Filters • Frequency Converters • Frequency Multipliers • Limiters • Magic Tees • Mixers • Noise Sources • Oscillators • Phase Shifters • Power Dividers • Radar Sensors • Subassemblies • Switches • Termination Loads • Test Equipment • Test Hardware & Accessories • TX/RX Modules • Uni-Guide™ • Waveguide Sections

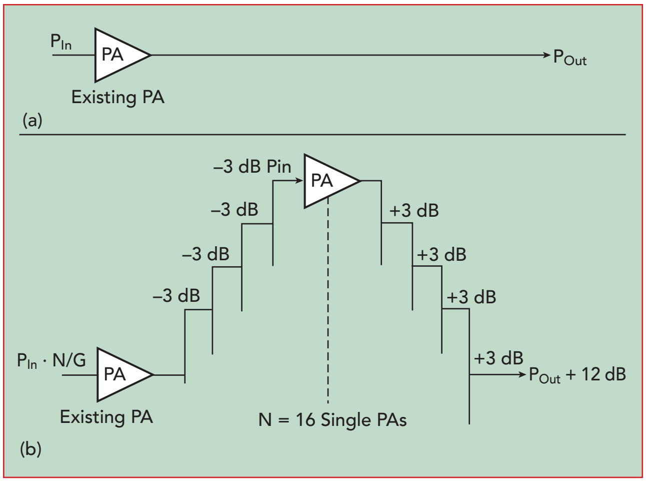

Fig. 1 Current single PA architecture with gain G (a) and parallel architecture with N identical PAs fed by a driver power amplifier (b).

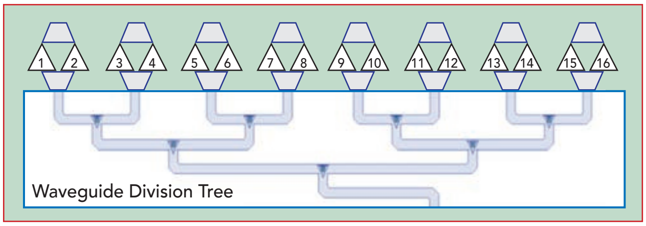

Fig. 2 16-way binary division with one to eight splits in waveguide, the last using an alumina splitters.

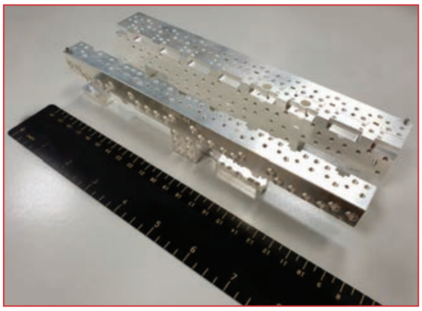

Fig. 3 Waveguide divider network shown at the top right, with the lid detached from body. The recombination network shown at the bottom left, with the lid and body assembled.

equipment dedicated to E-Band backhauling offers a transmitted power between 10 and 20 dBm at the various modulations.

Increasing the output power through the same components would cause severe distortion of the transmitted signal. Regardless of the traveled distance, it would reach the receiver with excessive distortion for error-free communication even after standard forward error-correcting schemes are applied.

Integrated PAs can leverage different semiconductors, chiefly GaAs, SiGe and GaN. Most of today's RF circuitry is GaAs based. Cost and power-handling capabilities, however, are directly related when switching to low-power cheap (in volume) SiGe and high power, but expensive, GaN. A reasonable tradeoff can instead be realized with an architectural change, by employing parallelization, while still using GaAs components.

As shown in ***Figure 1***, a driver amplifier provides, via an ideal division network, the same input power to each of the N PAs as in the single amplifier case. In the simple third order model of non-linearity, each amplifier

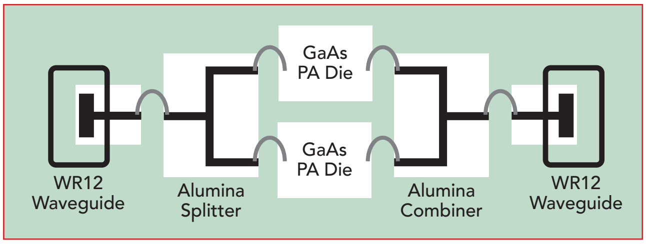

Fig. 4 PA structure, including the WR12 waveguide launchers, alumina splitters and PA die.

TABLE 1

POWER BOOSTER MEASUREMENTS

Measured Performance	Version with 8 PAs	Version with 16 PAs
Input Return Loss (dB)	> 10	> 10
Gain (dB)	> 14	> 13
OP_{1dB} (dBm)	> 29	> 31

produces a distortion component proportional to the cube of the input power. After proper in-phase recombination, the same signal-to-distortion ratio is obtained as with the single amplifier but with a much higher level of transmitted power; $10\log_{10}(N)$ = 12 dB is the theoretical output power increase achievable with this architecture when N=16 identical parallel PAs are used.

COMPONENTS

For a paralleled architecture to be of practical interest, the division and recombination network must avoid power loss along the path. To this purpose, the structure shown in ***Figure 2*** includes a one to eight waveguide binary tree,[4] providing low loss due to the fine surface finish of the inner metal walls. The binary tree guarantees uniformity in amplitude and phase. To minimize reflections at the interfaces and maintain isolation between the connected amplifiers, the basic node is designed as a so-called "magic tee."[5] The final further division by 2 is implemented in planar technology on alumina. The same binary tree is mirrored to serve as recombination network.

The waveguide networks are machined in two aluminum lids in which the waveguide trees and the internal loads are milled (see ***Figure 3***). The lids close as a sandwich to the inner aluminum body, which feature small pyramids to minimize impedance mismatches and seal the carved waveguide paths. The common input and output ports, in WR12, are located on the bottom side, where the 8+8 ports toward the amplification chains are visible on the top. Each tree exhibits a net 0.7 dB loss (beyond the theoretical 9 dB) and a total phase imbalance less than 15 degrees between all ports.

The 3 dB alumina splitters used as the topmost stages introduce a further 0.5 dB of loss each along with the various bonded interconnections shown in ***Figure 4***. All chains are fed with good in-phase and equal-amplitude signals and their recombination follows the same rule; considering recombination losses, an expected practical increase of output power of +10 dB with respect to the single amplifier case is the expected outcome.

TABLE 2 POWER BOOSTER PERFORMANCE COMPARISON			
Modulated Signal Bandwidth: 2 GHz	**ALFOplus 80HDX Standalone**	**ALFOplus80HDX + Power Booster (Factory Predistortion)**	**ALFOplus80HDX + Power Booster (Recalibrated Predistortion)**
PTx @ 128-QAM	13 dBm	24 dBm	23.5 dBm
S/D @ 128-QAM	> 30 dB	26.5 dB	> 29 dB
PTx @ 4-QAM	20 dBm	31 dBm	31 dBm
S/D @ 4-QAM	> 22 dB	> 20 dB	> 21 dB

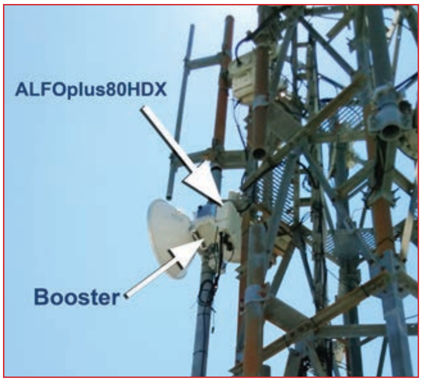

Fig. 5 Athens link with power booster.

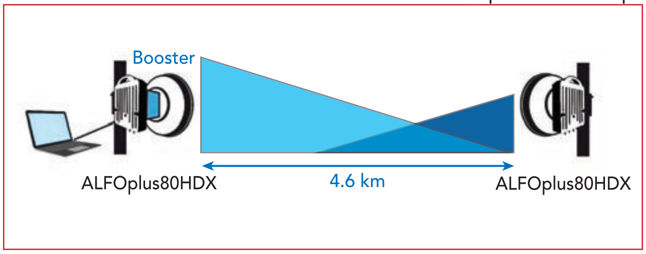

Fig. 6 Athens field trial using a site equipped with the power booster (left), transmitting at 74 GHz and receiving at 84 GHz, and a site without the booster (right), transmitting at 84 GHz and receiving at 74 GHz.

LABORATORY VALIDATION

The entire power booster is assembled in a first version with eight PAs without the alumina splitters, and then later in its full-fledged version with 16 PAs. ***Table 1*** summarizes the results from a 2-port characterization between 71 and 86 GHz.

These measurements show an increased variability versus frequency in the performance of the 16-PA version, due to the alumina splitting stage and the additional manual bonding introducing further uncertainty. The 16-PA version, however, exhibits an output power at 1 dB of compression (OP1dB) that is as much as 3 dB higher than the 8-PA version, thus enabling higher sustained output power.

The power booster is tested on actual modulated signals to assess whether the currently required signal-to-distortion ratio (S/D) is achievable at a +10 dBm output power level with respect to a state-of-the-art commercial unit based on a single PA (ALFOplus80HDX by SIAE MICROELETTRONICA). The ALFOplus80HDX full-outdoor unit is capable of 20 dBm in 4-QAM (2 Gbps throughput over 2 GHz bandwidth) and 13 dBm in 128- and 256-QAM (up to 10 Gbps), with a guaranteed overall S/D at the receiver of 29.5 dB in nominal conditions of received power and with a factory-calibrated transmitter.

By adding the power booster to an ALFOplus80HDX configured as transmitter-only and using a power meter and another ALFOplus80HDX as a receiving terminal, the performance summarized in ***Table 2*** is measured. The columns compare the transmitted power (PTx) and S/D ratio (as reported by the receiving equipment), which measures the quality of the received signal at a prescribed received power (dominated by distortion from the transmitter) in three configurations:

1. A standard ALFOplus80HDX equipment (without any power booster)
2. An ALFOplus80HDX with power booster but without any specific recalibration of predistortion coefficients
3. The same equipment with the power booster after recalibrating the predistortion coefficients of the transmitter.

Predistortion is a numerical process which allows compensation of nonlinearities introduced by the analog stages and should thus be fine-tuned for a specific transmitting chain, which justifies the large improvement of signal-to-noise ratio after recalibration. The results show that the power booster enables increased output power by more than 10 dB without appreciably deteriorating signal integrity after recalibration of the transmitter predistortion. It enables high-power 71 to 86 GHz communications up to 10 Gbps in a 2 GHz channel.

FIELD TRIAL

In the wake of successful laboratory tests, a field trial in cooperation with Deutsche Telekom/COSMOTE Greece uses an outdoor booster connected to existing ALFOplus80HDX equipment. However, since the booster acts only in transmission, while the equipment uses frequency-division duplexing to transmit and receive simultaneously through the same physical antenna port, the prototype includes:

1. A duplexer (to separate transmitted and received bands from the equipment)
2. The power booster on the transmit path
3. A straight waveguide on the receive path
4. Another duplexer (to expose a unique antenna port).

This waveguide structure, required only for the field prototype, is enclosed in a metal container providing heat sinks and mechanical interfaces with the equipment and the 60 cm antenna.

To compare in real time the advantages of the power booster, only one end of the trial link is equipped with the booster prototype, whereas the other end includes only an ALFOplus80HDX and a 60 cm parabolic antenna (see ***Figure 5***). The direction from the terminal with the power booster transmits at 74 GHz, where the direction from the terminal without the booster transmits at 84 GHz, both over 2 GHz channels.

Two suitable line-of-sight sites in the Athens region were identified with a separation of 4.6 km

AMCOM COMMUNICATIONS
The RF Power House

GaAs FETs pHEMTs

ISO 9001

AMCOM's AM030MH4-BI-R is part of the BI series of GaAsHiFETs. The HiFET is a partially matched patented device configuration for high voltage, high power, high linearity, and broadband applications. This part has a total device periphery of 12mm. The AM030MH4-BI-R is designed for high power microwave applications, operating up to 3GHz. The flange at the bottom of the package serves simultaneously as DC ground, RF ground and thermal path. This HiFET is RoHS compliant.

AMCOM's AM005MH2-BI-R is a part of the BI series ofGaAs HiFETs. The HiFET is a partially matched patented device configuration for high voltage, high power and broadband applications. This part has a total device periphery of 1mm. The AM005MH2-BI-R is designed for high power microwave applications, operating up to 6 Ghz. It is also an ideal driver for larger power devices. The flange at the bottom of the package serves simultaneously as DC ground, RF ground, and thermal path. This part is RoHS compliant.

AMCOM's AM032MH4-BI-R is part of the BI series of GaAs HiFETs. The HiFET is a partially matched patented device configuration for high voltage, high power and broadband applications. This part has a total device periphery of 12.8mm. The AM032MH4-BI-R is designed for high power microwave applications, operating up to 6GHz. The flange at the bottom of the package serves simultaneously as DC ground, RF ground and thermal path. This HiFET is RoHS compliant.

AMCOM's AM030WX-BI-R is a discrete GaAs pHEMT that has a total gate width of 3.0mm. It is in a ceramic BI package for operating up to 10 GHz.The BI package uses a specially designed ceramic package with bent (BI-G) or straight (BI) leads in a drop-in mounting style. The flange at the bottom of the package serves simultaneously as DC ground, RF ground, and thermal path. This part is RoHS compliant. For more information on this product or any other AMCOM product visit our website at www.amcomusa.com.

GaN MMIC Amplifiers

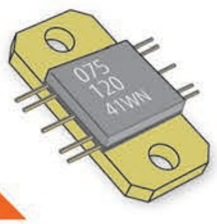

The AM07512041WN-SN-R is in a ceramic package with a flange and straight RF and DC leads for drop-in assembly. It has 27dB gain, and 41dBm output power over the 8.25 to 11.75 GHz band. Because of high DC power dissipation, good heat sinking is required.

Model	Freq(GHz)	Freq(GHz)	Gain(db)	Psat(dBm)	Eff(%)	Vd(V)	ECCN
AM003042WN-XX-R	0.05	3	23	42	33	40 / -2	EAR99
AM003042WN-00-R	0.05	3	24	42	35	40 / -2	EAR99
AM206041WN-SN-R	1.8	6.5	30	41	23	+28 / -1.8	EAR99
AM206041WN-00-R	1.8	6.5	32	42	27	+28 / -1.8	EAR99
AM408041WN-SN-R	3.75	8.25	31	41	23	+28 / -1.8	3A001.b.2.b
AM408041WN-00-R	3.75	8.25	33	42	27	+28 / -1.8	3A001.b.2.b
AM00010037WN-SN-R	DC	10	13	37	23	+28 / -1.8	EAR99
AM00010037WN-00-R	DC	10	13	37	25	+28 / -1.8	EAR99
AM00010037WN-QN6-R NEW	DC	10	13	36	25	+28 / -2.0	EAR99
AM08012041WN-SN-R	7.5	12	21	41	20	+28 / -1.9	3A001.b.2.b
AM08012041WN-00-R	7.5	12	22	42	20	+28 / -1.9	3A001.b.2.b
AM07512041WN-SN-R	7.75	12.25	27	41	22	+28 / -1.8	3A001.b.2.b
AM07512041WN-00-R	7.75	12.25	28	42	27	+28 / -1.8	3A001.b.2.b

MMIC in a Box

www.amcomusa.com

Phone 301.353.8400 - www.amcomusa.com - info@amcomusa.com

TABLE 3 FIELD TRIAL POWER MEASUREMENTS				
Received Power Levels (dBm)	***Direction Without Booster***		***Direction With Booster***	
	Expected	***Measured***	***Expected***	***Measured***
4-QAM	-27	-28	-16	-15
128-QAM	-33	-34	-22	-21

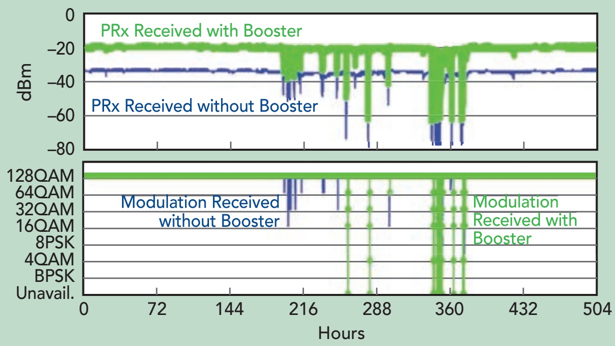

Fig. 7 Received power and modulation vs. time. The green traces show the power and modulation received from the transmitter with the power booster; the blue traces show the power and modulation received from the transmitter without the booster.

TABLE 4 EXTENDED PERFORMANCE DATA		
Statistics Over 8 Months	***Direction Without Booster***	***Direction With Booster***
Average Uptime (%)	99.911	99.992
Average Availability of Maximum Modulation (%)	98.911	99.655

(see ***Figure 6***). Monitoring equipment was also installed to record received power levels and modulation in both directions by querying the local and remote equipment every 2 seconds. After aligning the antennas on a clear day, received measured power levels are shown in ***Table 3***. The values highlight an improvement of more than 10 dB in received power because of the power booster. This considers the accuracy of the internal power meter of about ±1 dB and the inherent differences between the two directions due to the slightly different transmit frequencies.

Both ends were configured to use automatic modulation, so that the two ends automatically maintain the highest modulation compatible with error-free communication in the instantaneous link conditions (i.e. rain fading). Both equipment switched automatically to the maximum capacity of 10 Gbps.

Over the monitoring period, the link transported more than 2,000 Pbit (1 Pbit = 10^{15} bit) in each direction, as the maximum 10 Gbps (128-QAM modulation) could be maintained for the vast majority of time, where rain events occurred only in a few days. A sample of the monitored received power and modulation is shown in ***Figure 7***.

An exceptional rain event with torrential precipitations in the Athens area was recorded, with rain intensity greater than 100 mm/h, causing numerous power outages and unreachability of the network elements. Several tens of minutes of unavailability were gathered in both directions during this severe thunderstorm. Discarding this data, the rest of several seasons included light as well as medium rain events, obtaining the aggregated performance in ***Table 4***.

The direction that leverages the power booster reduced downtime by 91 percent and the non-maximum modulation (corresponding to less than 10 Gbps per direction) time by 70 percent with respect to the same link without the booster in transmission.

CONCLUSION

The modern needs for very-high capacity demanded by modern 5G networks is hampered by physical and technological constraints that limit the reachable hop length in wireless mmWave transport. The adoption of a parallelized PA architecture, however, circumvents some of the hurdles and so enables long-reach connections in the commercial E-Band.

The power booster prototype relies on a one-to-eight waveguide distribution and recombination structure feeding double PAs that yields a 10 dB increase in transmitted power. A 4.6 km field trial monitored through a multi-seasonal period validates the approach, thus paving the way for commercial mmWave links up to 5x current link lengths at E-Band.

Future activities will be dedicated to integrating the power booster in next-generation wireless transport equipment and industrializing the product, while also investigating alternative technologies such as GaN. ■

References

1. A. Nordrum and K. Clark, "5G Bytes: Millimeter Waves Explained," *IEEE Spectrum*, May 2017. Web. https://spectrum.ieee.org/video/telecom/wireless/5g-bytes-millimeter-waves-explained.
2. "O-RAN Architecture Overview," *O-RAN Alliance*. Web. https://docs.o-ran-sc.org/en/latest/architecture/architecture.html.
3. M. Oldoni, S. Moscato, G. Biscevic and G. Solazzi "A Steering Antenna for Long-Reach mmWave X-Haul Links," *Microwave Journal*, Vol. 21, No. 10, October 2021.
4. S. Moscato, M. Oldoni, G. Cannone, D. Tresoldi, A. Pini and A. Colzani "8-way Paralleled Power Amplifier for mm-Wave 5G Backhauling Networks," *European Conference on Antennas and Propagation*, March 2021.
5. "TEE Junction | E-Plane Tee, H-plane Tee, Magic Tee," *Electronics Club*. Web. https://electronics-club.com/tee-junction-e-plane-tee-h-plane-tee-magic-tee.

Wideband
High Accuracy
Butler Matrices

Excellent Phase Accuracy, Amplitude Unbalance

Low VSWR / Low Insertion Loss / High Isolation

P / N	Structure	Freq. Range (GHz)	VSWR Max. (:1)	Insertion Loss* Max. (dB)	Amplitude Unbal. Max. (dB)	Amplitude Flatness Max. (dB)	Phase Accuracy Max. (Deg.)	Isolation Min. (dB)
SA-07-4B006050	4x4	0.617~0.821	1.4	8.2	±1.1	±0.8	±10	16
		0.832~0.96	1.4	8.2	±1.1	±0.7	±9	16
		1.427~1.71	1.5	8.3	±0.9	±0.7	±9	15
		1.71~2.2	1.5	8.5	±0.9	±0.8	±10	14
		2.496~2.69	1.5	8.7	±0.9	±0.7	±9	13
		3.3~4.2	1.6	8.9	±1	±0.7	±12	13
		4.4~5	1.6	9.2	±1	±0.8	±12	13
SA-07-4B020080	4x4	2.4~2.5	1.4	7.3	±0.5	±0.3	±4	14
		5.18~5.83	1.5	7.7	±0.6	±0.4	±5	13
		5.9~7.25	1.5	7.8	±0.7	±0.5	±6	13
SA-07-8B020080	8x8	2.4~2.5	1.5	11.2	±0.6	±0.4	±8	13
		5.18~5.83	1.5	11.6	±0.8	±0.5	±10	12
		5.9~7.25	1.55	11.8	±0.9	±0.7	±12	12
SA-07-4B240430	4x4	24~43	2.0	12.4	±1.2	±2.0	±15	10

*Theoretical 6dB Included

Note: The connected components are available from MIcable which include the phase matched assemblies & low loss high isolation phase matched switches.

Typical Test Curve**

SA-07-4B006050

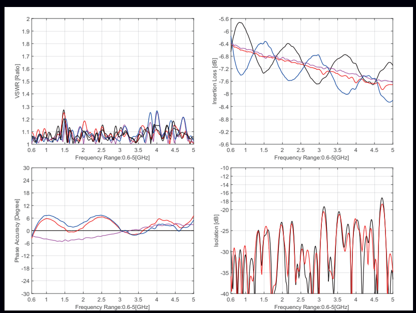

SA-07-4B020080

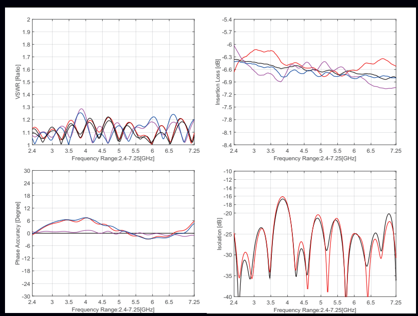

SA-07-4B240430

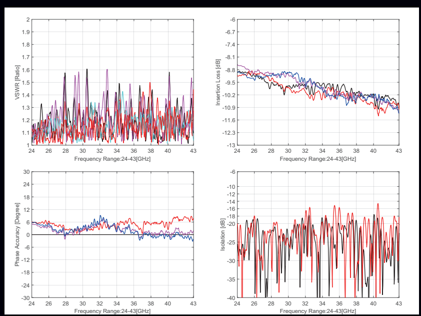

**Corresponding Channels：A1B1、A1B2、A1B3、A1B4

More Information-
Scan the QR Code

Fujian MIcable Electronic Technology Group Co.,Ltd

Tel: +86-591-87382856 Email: sales@micable.cn Website: www.micable.cn

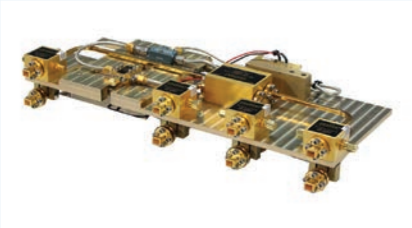

Design Library Taps COTS Components for mmWave System

New applications for mmWave technology often begin when fundamental design concepts are applied to solve real-world problems in novel ways. Examples include passive imaging systems to detect hidden materials, using their radiation signatures, or high bandwidth communication links difficult to detect or jam. To create a working prototype, the design process typically involves sketching a block diagram including the mmWave components, performing a system analysis to determine system and component performance, then selecting components that can be easily integrated to create the subsystem.

Eravant helps this development process with a wide range of commercial off-the-shelf (COTS) components, supported by block diagrams on the company's website. The block diagrams reference the product families of the various components used in mmWave systems, and many suggest part numbers from Eravant's COTS catalog. Design examples are provided, with technical notes that describe a subsystem's operating principles. The block diagrams offer designers a starting point to conceptualize the form and function of a prototype system, and the design examples provide references for exploring options with Eravant's technical staff.

In most cases, Eravant has components immediately available for prototyping, and the company can construct and test integrated subassemblies to shorten the time between concept and a working prototype. Eravant can also provide ancillary components such as power supplies, voltage regulators and control devices. One example is an eight-channel FMCW radar transceiver with antennas, which can be used for scanning objects. Eravant offers a fully assembled subsystem operating from 70 to 75 GHz (model SSC-7337331202-1212-B1). Documents describing this and other subsystems are available on Eravant's website.

VENDORVIEW

Eravant, Torrance, Calif.
www.eravant.com/science-academia

High Performance, Versatile and Cost-Effective RF Test Cables

As the technology needs of test and measurement (T&M) require more advanced broadband connectivity, Swift Bridge Technologies, an established global designer and manufacturer of RF cable assemblies, developed the FastEdge™ RF product line. It addresses the T&M challenge with a high quality, versatile and cost-effective RF cable assembly. FastEdge cable assemblies are flexible and low loss, built with precision RF connectors, custom molded flex reliefs and an abrasion resistant polyurethane jacket. The cable assemblies provide the adaptability needed for T&M, well-suited for connecting to spectrum analyzers, network analyzers, signal generators, oscilloscopes and multi-function production test sets. Their versatility is suitable for applications such as compliance testing, clock timing, probing and multiplexing — any operating environment to 125°C.

The FastEdge 40 series is optimized for low loss performance through 40 GHz, with transmission losses typically 2.8 dB for a 1 m cable assembly at 40 GHz. Low signal loss is achieved using air-enhanced PTFE in the cable construction. Return loss is guaranteed to be better than 18 dB through 40 GHz. Important for T&M, performance is stable with cable movement, typically ±0.05 dB in amplitude and ±9 degrees in phase.

To meet the broadest range of customer demands, the FastEdge RF product line can be ordered on the Digi-Key marketplace. FastEdge RF products are available with various connector types and multiple upper frequency ranges. The newest line, FastEdge 70, a 70 GHz solution, will be available soon. Phase-matched cable pairs up to 1.5 ps skew are available for all frequency ranges.

Swift Bridge Technologies, Tigard, Ore.
www.swiftbridgetechnologies.com

IMS

2023 IEEE MTT-S INTERNATIONAL MICROWAVE SYMPOSIUM

11–16 JUNE
CONVENTION CENTER
San Diego, California

IEEE

MTT-S
IEEE MICROWAVE THEORY & TECHNOLOGY SOCIETY

The Coolest Ideas Under the Sun
SAN DIEGO 2023

CALL FOR PAPERS

IMS2023 is the centerpiece of Microwave Week 2023, which includes the RFIC Symposium (www.rfic-ieee.org) and the ARFTG Microwave Measurement Conference (www.arftg.org).

Microwave Week is the world's largest gathering and industry exhibition for **MHz through THz** professionals. IMS2023 will feature an exciting Technical Program with the **Coolest Ideas Under the Sun** — think high efficiency, thermal management, model-based design, space and aerospace systems, and so much more. Microwave Week provides a wide variety of technical and social activities for attendees and exhibitors. Besides the diverse choice in technical sessions, explore interactive forums, plenary and panel sessions, workshops and technical lectures, application seminars, and also participate in paper contests for Students, Industry, and Young Professionals. The best Industry papers will be presented in a showcase as well as awarded "Best Industry Paper" prizes. Enjoy networking events such as Young Professionals, Women in Microwaves (WiM), Amateur Radio (HAM) enthusiasts, and Industry centric functions.

The location of IMS2023 is San Diego: very cool. The Convention Center is on the bayfront, adjacent to the Gaslamp Quarter, which is the lively social center of San Diego, with plenty of restaurants for all tastes. San Diego is also home to famous landmarks such as the USS Midway, Balboa Park containing many museums, the San Diego Zoo, and SeaWorld. And cool beaches.

San Diego is the bridge between North America and Latin America. One of our conference themes is to highlight advances in RF and Microwave research in Latin America, and we will have a Latin American flavor to social events throughout the week.

Important Dates

- 16 September 2022 (Friday)
  PROPOSAL SUBMISSION DEADLINE
  (workshops, technical lectures, focus and special sessions, panel and rump sessions)
- 6 December 2022 (Tuesday)
  PAPER SUBMISSION DEADLINE
  All submissions must be made electronically.
- 1 February 2023 (Wednesday)
  PAPER DISPOSITION
  Authors will be notified by email.
- 8 March 2023 (Wednesday)
  FINAL MANUSCRIPT SUBMISSION DEADLINE
  Manuscript and copyright of accepted papers
- 11-16 June 2023
  MICROWAVE WEEK
  IMS2023, RFIC 2023, ARFTG, and Exhibition

IMS2023 Conference Themes

At IMS2023 we will have several focus themes to highlight a number of areas of RF and microwave engineering that are of topical interest or impact. These themes are:

Systems & Applications

The development of RF, microwave, mm-wave and THz systems continues to expand in several areas, with many application examples. This broad topic can encompass design from semiconductor through device and module through to the overall system and applications. We are giving particular focus to:

Wireless Communications, including 6G developments, Wi-Fi, RF and microwave system-on-chip integration, massive MIMO systems and subsystems

Wireless Power Transfer;
Automotive Systems;
Model-Based Systems Engineering.

Space

In this area of Aerospace we are specifically calling out 'Space' as a focus theme. This can include such topics as: satellite communications, design for reliability, radiation hardness, internet of space systems, CubeSats.

Biomedical Applications

Illustrating the use of RF and microwave techniques and technology in biomedical applications.

These technical themes will be identified with different days of the conference, and will comprise special Focused Technical Paper Sessions, Panel Sessions, Invited Speakers, and Workshops. The Exhibition will feature a **Systems Pavilion** illustrating several practical examples of RF through THz systems and applications.

Authors are encouraged to submit technical papers in these themed topics.

In addition to this Call for Technical Papers, there will also be Calls for Focus and Special Sessions Proposals, Panel Session Proposals, and Workshop Proposals. Prospective organizers of these events are encouraged to target the conference themes. The submission date for these proposal is 16 September 2022.

RF & Microwaves in Latin America

In addition to the above technical themes, IMS2023 will feature a Focus Technical Paper Session to celebrate "RF and Microwaves in Latin America." This session is being championed by Professor Jose Rayas-Sanchez and Professor Apolinar Reynoso-Hernandez. There will also be a **Latin America Pavilion** in the Exhibition, and the Latin America flavor will run through the whole of IMS2023.

IMS2023 Conference and Technical Program Committee

Executive Committee

John Wood, *General Chair*
Gayle Collins, *Co-Chair*
Dominique Schreurs, *TPC Co-Chair*
Peter Zampardi, *TPC Co-Chair*
Kevin Chuang, *Finance Co-Chair*
Jean Rautio, *Finance Co-Chair*
Janet O'Neill, *Local Arrangements Co-Chair*
Sherry Hess, *Local Arrangements Co-Chair*
Judy Warner, *Marketing & Publicity Co-Chair*
Ryan Baker, *Marketing & Publicity Co-Chair*
Robert Caverly, *Student Events Co-Chair*
Rashaunda Henderson, *Student Events Co-Chair*
Damon Holmes, *Industry Participation Chair*
Donald Lie, *RFIC General Chair*
Basim Noori, *ARFTG General Chair*

IEEE Professional Conference Staff

Elsie Vega, *Conference Manager*
Erin Dolan, *Conference Planner*
Dillian Waldron, *Conference Planner*
Bob Alongi, Treasurer
Amanda Scacchitti, *Marketing Manager*

Exhibition Management

Carl Sheffres, *Exhibition Manager*
Janine Love, *Exhibition Co-ordinator*
Alisa Ufland, *Marketing*
Jim Rautio, *Exhibitor Outreach*

Technical Program Committee

Dominique Schreurs, *TPC Co-Chair*
Peter Zampardi, *TPC Co-Chair*
Danilo Manstretta, RFIC TPC Chair
Pere Gilabert, *Workshops Co-Chair*
Ethan Wang, *Workshops Co-Chair*
Andrej Rumiantsev, *Workshops*
Jose Carlos Pedro, Workshops
Roberto Gomez-Garcia, *Workshops*
Kamran Ghorbani, *Workshops*
Anding Zhu, *Focus/Special Sessions Co-Chair*
Alessandra Costanzo, *Focus/Special Sessions Co-Chair*
Holger Maune, *Space Theme Focus Sessions*
Markus Gardill, *Space Theme Focus Sessions*
Ian Gresham, *Systems/Apps Focus Sessions*
Ramon Beltran, *Systems/Apps Focus Sessions*
Jim Carroll, *Interactive Forum*
Gianpiero Gibiino, *Interactive Forum*
Nuno Carvalho, *Panel Sessions*
Ke Wu, *Panel Sessions*
Tomislav Markovic, *Technical Lectures*
Joseph Staudinger, *MicroApps*
David Runton, *MicroApps*

Electronic Paper Management

Sandy Owens

Student Paper Competition

Holger Maune
Mike Roberg

Student Design Competitions

Pawel Barmuta
Koen Buisman

Industry & Advanced Practice Paper Competitions

Freek van Straten
Neil Braithwaite

Early Career Paper Competition

Jonas Urbonas
Paolo deFalco

Industry Workshops

Venkata Vanukuru
Gustavo Avolio

Tutorials

Matt Ozalas

RF Bootcamp

Ulf Johannsen
JoAnne Mistler
Larry Dunleavy

Connected Futures Summit

Debabani Choudhury
Ashutosh Dutta
Peiying Zhu

Senior Advisors

John Barr
Fred Schindler

Technical Paper Submission

Authors are invited to submit technical papers describing original work and/or advanced practices on MHz through THz theory and technology. A double-blind review process will be used ensuring anonymity for both authors and reviewers. The Symposium proceedings will be archived electronically and submitted to IEEE Xplore.

Submission Instructions

- All submissions must be in English.
- Submissions must be 3-4 pages long, be compliant with the IEEE conference template, which can be downloaded from the IMS2023 website, and be compliant with double-blind requirements.
- The submission must be in PDF format and cannot exceed 4 MB in size.
- Authors must upload their paper submission by midnight Hawaii time on 6 December 2022. Late submissions will not be considered.

Paper Selection Criteria

- All papers are reviewed by subject-matter expert sub-committees of the IMS2023 Technical Program Review Committee (TPRC). The selection ciriteria will be:
- **Originality:** Is the contribution unique and significant? Does it advance the state of the art of the technology and / or practices? Are proper references to previous work by the authors and others provided?
- **Quantitative content:** Does the paper give a comprehensive description of the work with adequate independent verification (measurements, if applicable, or otherwise independent simulated data) ?
- **Clarity:** Is the paper contribution and technical content presented clearly and in a logical manner? Are the English writing and accompanying figures clear and understandable?
- **Interest to MTT-S membership:** Will this paper interest the IMS audience and encourage discussion?

Technical areas: During the paper submission process, authors will choose a primary and two alternative technical areas (see the Technical Areas). The paper abstract should contain information that clearly reflects the choice of the area(s). Author-selected technical areas will be used to determine an appropriate committee for reviewing the paper, whereby the TPC co-chairs reserve the right to place papers in the most appropriate technical area. The technical areas are divided into five different categories that are used to organize the paper presentation schedule. It is permissible to choose primary and alternative technical areas that are in different categories.

Presentation Format: IMS offers three types of presentation formats. The authors' preference will be honored where possible, but the final decision on the presentation format is with the IMS2023 TPRC

1. Full-length papers report significant contributions, advancements, or applications in a formal (20 minute) presentation format with questions and answers (Q&A) at the end.
2. Short papers typically report specific refinements or improvements in the state of the art in a formal (10 minute) presentation format with Q&A at the end.
3. Interactive forum papers provide an opportunity for authors to present their theoretical and/or experimental developments and results in greater detail and in a more informal and conversational setting. An IMS2023 template will be provided.

Notification

Authors will be notified of the decision by 1 February 2023. For accepted papers, an electronic version of the final 3-4 page manuscript along with copyright assignment to the IEEE must be submitted by 8 March 2023.

The submission instructions will also be provided through emails and can be accessed through the IMS2023 website.

Clearances

It is the responsibility of the authors to acquire all required company and government clearances, prior to submission of their manuscript

Paper Competitions

Competitions for the best Industry Paper, Advanced Practices Paper, Student Paper, and Early Career Paper will be held at the conference. Student and Early Career Awards will be presented at the Conference Closing Ceremony. The Industry Paper and Advanced Practice Paper Awards will be presented at the Opening Plenary Session/Industry Showcase Only papers submitted as 20-minute presentation format will be considered for these competitions.

Student Paper Competition: Eligible students are encouraged to submit papers for the Student Paper Competition. These papers will be reviewed in the same manner as all other contributed papers. First, second, and third prizes will be awarded based on content and presentation. To be considered for an award, the student must be a full-time student during the time the work was performed and still be a student on the submission deadline, be the lead author, and personally present the paper at IMS. Eligibility details can be found on the IMS2023 webpage.

Industry Paper Competition: Authors from industry are encouraged to submit papers for the Industry Paper Competition. Papers will be evaluated using the same standards as all contributed papers, the work should highlight technical innovation or state-of-the-art performance. The prize will be awarded based on content. and the prize includes a free advertisement in Microwave Journal or IEEE Microwave Magazine, for the author's company.

Advanced Practice Paper: Any author who submits a paper on advanced practices may be entered into the Advanced Practice Paper Competition. A paper on advanced practices describes an innovative RF/microwave design integration technique, process enhancement, and/or combination thereof that results in significant improvements in performance and/or in time to production for RF/microwave components, subsystems, or systems. The prize will be awarded based on content.

Early Career Paper Competition: This new competition is open to authors from industry, government agencies, and post-doctoral candidates, with less than 10 years of professional experience, and who are not full-time students or faculty members. The first-named author on the paper will be the qualifying author. These papers will be reviewed in the same manner as all other contributed papers, and the prize will be awarded based on content and presentation.

IEEE Transactions MTT Special Issue

Authors of all papers presented at IMS2023 can submit an expanded version of their paper to a special symposium issue of the *IEEE Transactions on Microwave Theory and Techniques*.

IEEE Microwave and Wireless Technology Letters

Up to 50 of the best papers at the Symposium will be published in a special issue of *IEEE Microwave and Wireless Technology Letters*, at the authors' discretion.

Details at www.ims-ieee.org

Technical Areas

Electromagnetic Field, Device, and Circuit Techniques

1. **Field analysis, guided waves, and computational EM** – Novel guiding, radiating, and electromagnetic structures; new analytical techniques and numerical methods for such structures, and new computational EM methods, incl. EM-coupled multiphysics modeling
2. **Circuit and system CAD algorithms** – Linear/nonlinear simulation and design optimization techniques; behavioural modeling (excl. PAs); statistical approaches; surrogate modeling; space mapping; model order reduction; uncertainty quantification in simulations; stability analysis; non-EM related multiphysics simulations
3. **Instrumentation and techniques for guided and over-the-air measurements** – Measurement techniques from microwave to THz for materials, linear and nonlinear devices, circuits, and systems; calibration and de-embedding techniques, measurement uncertainty, and over-the-air measurement methods and novel instrumentation

Passive Components and Packaging

4. **Planar passive components and circuits, excl. filters** – Novel planar transmission-line components; artificial transmission lines, metamaterial structures, and high-impedance surfaces; planar couplers, dividers/combiners, multiplexers, resonators, and lumped-element approaches
5. **Planar passive filters** – Planar passive filters, including lumped elements, theoretical filter and multiplexer synthesis methods
6. **Integrated passive circuits and filters** – Design and characterization of silicon integrated, III-V integrated passive components and filters, including IPDs
7. **Non-planar passive components, filters, and other circuits** – Transmission line components, resonators, filters and multiplexers based on dielectric, waveguide, coaxial, or other non-planar structures
8. **Tunable passive circuits and active filters** – Tunable and active filters, tunable phase shifters and couplers
9. **Microwave acoustic, ferrite, ferroelectric, phase-change, & MEMS components** – Surface and bulk acoustic wave devices including FBAR devices, bulk and thin-film ferrite components, ferroelectric-based devices, and phase change devices and components. RF microelectromechanical and micromachined components and subsystems
10. **Packaging, MCMs, and 3D manufacturing technologies** – Component and subsystem packaging, assembly methods, multi-chip modules, wafer stacking, 3D interconnect, and integrated cooling; package characterization; novel processes related to inkjet printing, 3D printing, or other additive manufacturing techniques

Active Devices and Circuits

11. **Semiconductor device technologies and modeling** – RF to THz devices on III-V, silicon, and other emerging technologies, incl. 2D devices); MMIC and Si RFIC manufacturing, reliability, failure analysis, yield, and cost; linear and nonlinear device modeling (CAD, compact, physics-based, empirical) including characterization, parameter extraction, and validation
12. **HF/VHF/UHF circuits, technologies, and applications** – Advances in passive and active circuits (incl. PAs), components, and systems that operate in the HF, VHF, and UHF frequency ranges ranges (<1 GHz)
13. **Signal generation, modulators, frequency conversion** –CW and pulsed oscillators in silicon and III-V processes including VCOs, DROs, YTOs, PLOs, and frequency synthesizers, frequency conversion ICs in silicon and III-V processes, such as IQ modulators, mixers, frequency multipliers/ dividers
14. **Microwave and millimeter-wave low-noise amplifiers, variable-gain amplifiers, and receivers** – LNAs, VGAs, receivers, detectors, integrated radiometers, and low-noise circuit characterization
15. **Low-power (<10 W) amplifiers, below 30 GHz** – Advances in discrete and IC power amplifier devices and design techniques based on Si and III-V devices, demonstrating improved power, efficiency, and linearity for the microwave band (1-30 GHz)
16. **High-power (>=10 W) RF and microwave amplifiers, below 30 GHz** –Advances in discrete and IC power amplifier devices and design techniques based on III-V and LD-MOS devices, demonstrating improved power, efficiency, and linearity for the microwave band (1-30 GHz); power-combining techniques for SSPA and vacuum electronics
17. **Millimeter-wave and THz power amplifiers** – Advances in IC power amplifier circuits, design techniques, and power combining based on Si and III-V compound semiconductor devices demonstrating improved power, efficiency, and linearity for millimeter-wave and THz bands; vacuum electronics for millimeter-wave
18. **Linearization and transmitter techniques for power amplifiers** – Power amplifier behavioral modeling; linearization and pre-distortion techniques; envelope-tracking, out phasing, and Doherty transmitters for III-V and silicon technologies
19. **Mixed-signal, wireline, and signal shaping circuits** –High-speed mixed-signal components and subsystems, including: PLLs, TDCs, ADCs, DACs, DDSs, and supporting circuits to interface these to the analog world
20. **Integrated transceivers and phased-array chips for beamformers and imaging** – Design and characterization of complex III-V ICs, silicon ICs, heterogenous systems in the RF to mm-wave band including narrowband and wideband designs; innovative circuits and sub-systems for communications, radar, imaging, and sensing applications; Integrated on-chip antennas and on-package antennas
21. **Terahertz and photonic integrated circuits** – Design and characterization of THz active circuits; THz circuits for communications, radar, imaging, and sensing applications; Interaction between microwaves, THz waves, and optical waves for the generation, processing, control, and distribution of microwave, mm-wave, and THz signals; nanophotonics, nanoplasmonics, and nano-optomechanics

Systems and Applications

22. **Wireless power transmission** – Energy harvesting systems and applications, rectifiers, self-biased systems, combined data and power transfer systems
23. **Sensing and RFID systems** – Short range wireless and RFID sensors, gas and fluidic sensors; passive and active tags from HF to millimeter-wave frequencies; RFID systems including wearables and ultra-low-power
24. **Microwave and millimeter-wave wireless subsystems and systems** – Technology advances combining theory and hardware implementation in microwave/millimeter-wave subsystems such as beamformers; microwave and millimeter-wave (<100 GHz) communication systems, incl. 5G – 6G, with hardware implementation for terrestrial, vehicular, and indoor applications, point-to-point links, radio-over-fiber links, cognitive and software-defined radios applied to (massive) MIMO, full-duplex technologies, shared and novel spectrum use, novel modulation schemes, and channel modeling
25. **Radar and imaging systems** – RF, millimeter-wave, and sub-THz radar and imaging systems, automotive radars, sensors for intelligent vehicular highway systems, UWB and broadband radar, remote sensing, radiometers, passive and active imaging systems, radar detection techniques, and related signal processing
26. **Airborne and space systems** – Technologies and systems for remote sensing for earth observation; positioning, navigation, and timing; space exploration, human spaceflight and space transportation; satellite communications including 5G, 6G applications involving aerospace platforms; communication and sensor systems for UAVs, HAPSs, airplanes, and satellites
27. **MHz-to-THz devices, circuits, and systems for biological and healthcare applications** – Electromagnetic field interaction at molecular, cellular, tissue and living systems levels; devices, circuits, and systems for characterizations of biological samples; microwave-enhanced chemistry; instrumentation and systems for biomedical diagnostic and therapeutic applications, incl. MRI and microwave imaging; wireless, wearable, and implantable devices for health monitoring
28. **AI/ML for RF to mmWave** – AI/ML algorithms implementations, and demonstrations for: spectrum sensing; mobile edge networking; MIMO and array beam operations and management; design and optimization; in-situ sensing, diagnostics, control, reconfiguration of MHz to THz communication and sensing circuits and systems

Emerging Technologies

29. **Quantum devices, circuits, and systems** – Quantum devices and circuits (incl. cryogenic RF circuits); algorithms, interfaces, and systems for quantum computing and quantum sensing applications
30. **Model-based system engineering** – Applications or demonstrations of model-based system engineering (MBSE) applied to system architecture, behavioral analysis, simulation, performance analysis, and test of RF systems, over the whole product life cycle; applications areas such as aerospace, wireless systems, EMC, and automotive
31. **SubTHz and THz Systems** – SubTHz and THz systems, incl. space and sub-THz architectures for 6G communication systems with hardware implementation
32. **Other innovative MHz-to-THz systems and applications**

MAKING WAVES

AmpliTech on TV

AmpliTech designs, develops and manufactures custom leading-edge RF components for the commercial, satcom, space and military markets. These designs cover frequencies from 50 kHz to 44 GHz. Learn more in this video.

AmpliTech
www.youtube.com/watch?v=BTWWk_ZoSUA

Mathematical Tools of the Trade Poster by AR

AR's updated Mathematical Tools of the Trade Poster provides a reference for EMC engineers to use on a daily basis in the lab or at the desk.

AR RF/Microwave Instrumentation
https://bit.ly/3QmJDLm

Video for Ethernet Transformers

iNRCORE's discrete Ethernet Transformers are ruggedized in transfer molding or pour-filled construction to meet MIL-PRF-21038 environmental requirements. They support various Ethernet protocols, including AFDX (Avionics Full Duplex Switched Ethernet), TTE (Time-Triggered Ethernet) and IEEE 802.3x, including PoE (Power over Ethernet).

iNCORE
https://youtu.be/OLbIRSsdB6M

MCV Microwave Launches New Website

MCV Microwave launched a powerful website with dynamic product tables with filtered product search for frequency, bandpass, power, etc., plus downloadable data sheets.

MCV Microwave
www.mcv-microwave.com

New High Power Coupler Selection Guide

MIcable introduces their new HIGH POWER COUPLER selection guide. Search the directional and dual-directional couplers in the range of 0.3 to 18 GHz. The power handling of standard product is up to 400/600 W. Widely applied in testing, communication, instrumentation, power amplifier, transmitter and other high-power applications.

Fujian MIcable Electronic Technology Group Co., Ltd.
www.micable.cn

The Knowles Family of Microwave Products Has Expanded

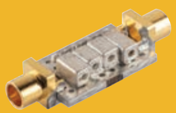

Advantage allows the user to build a balanced circuit essential for ultimately constructing balanced amplifiers, switches, phase shifters, mixers and other key microwave building blocks. Learn more in the latest catalog.

Knowles Precision Devices
www.knowlescapacitors.com/Support/Catalogs

Mini-Circuits' Deer Park Location Opens High-Frequency Technology Center

Mini-Circuits' Deer Park office has expanded to now include a 10,000 square-foot, open-concept floorplan that features a 3,500-square-foot class 100k cleanroom environment, extra-large workstations for team members, common meeting space, plus a fully-stocked kitchen and lunch area.

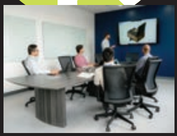

Mini-Circuits
https://bit.ly/3oYCKEF

Free Rohde & Schwarz Wireless Communications Calculator

The free calculator covers the most important standards including 5G NR, LTE, Wi-Fi and Bluetooth. Just select the wireless communications standard and band of interest. The calculator provides the channels and related frequencies, in numerical and graphical format, as well as the maximum UE power.

Rohde & Schwarz
https://bit.ly/3ASeKdi

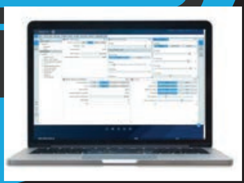

B2B RF Connector Solutions Product Portfolio

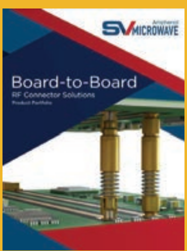

SV Microwave has released their latest product portfolio featuring RF connector solutions, with a focus on making a board-to-board (B2B) connection using SV's SMP and SMPM series connectors.

SV Microwave
https://svmicrowave.com/images/uploaded/Board%20to%20Board%20Brochure_FINAL.pdf

NEW PRODUCTS

FOR MORE NEW PRODUCTS, VISIT WWW.MWJOURNAL.COM/BUYERSGUIDE
FEATURING VENDORVIEW STOREFRONTS

COMPONENTS

Passive Multiplier

VENDORVIEW

Accepting input signals between 73 and 110 GHz at +17 dBm, model SFP-03310-UEB is a passive ×3 multiplier that produces THz signals with 0 dBm amplitude. When combined with a sweeper or a synthesized signal source, the multiplier preserves the stability and accuracy of the source. Typical harmonic suppression is 20 dB. The input and output signals pass through WR-10 and WR-03 waveguides ports with UG-387/U-M anti-cocking flanges. Dimensions are 0.75 × 0.75 × 0.75 in.

Eravant
www.eravant.com

Programmable Attenuator

VENDORVIEW

MIcable has developed a programmable attenuator MDA004080-50E covering 0.4 to 8 GHz. The user can control the attenuator via USB/Ethernet with 1 dB step or down to 0.1 dB option, 0.2 dB accuracy, 50 dB attenuation dynamic range over the whole band. The user can control this unit through the GUI user-friendly software or by programming through the DLL dynamic link library file. Custom designs are available with frequency range from 0.5 to 40 GHz.

Fujian MIcable Electronic Technology Group Co., Ltd.
www.micable.cn

45 to 1220 MHz 1:1 Balun

The MRFXF0072 balun is a high performance balun that gives your CATV amplifier or EQ circuit optimized performance. The part offers a unique feature rarely found in three wire baluns, including DC bias of 400 mA through the ground pin. The MRFXF0072 offers > 20 dB typ. return loss, ±0.5 dB amplitude match and less than 0.7dB IL. Drop it in and see great performance. It is offered in a std 0.230 × 0.280" surface-mount package and is pin to pin compatible.

MiniRF
www.minirf.com

0.5 to 20 GHz Directional Couplers

Pulsar introduces three new 0.5 to 20 GHz SMA directional couplers with 6-, 10- and 20-dB coupling. All three have 15 dB minimum directivity, 1.50:1 maximum VSWR and 25 W maximum power handling. The CS06-25-436/20 is 6 dB with an insertion loss of 1.80 dB maximum, the CS10-25-436/20 is 10 dB with an insertion loss of 1.40 dB maximum and the CS20-25-436/20 is 20 dB with an insertion loss of 0.90 dB maximum. Dimensions are 4.4 × 0.70 × 0.40 in.

Pulsar Microwave Corp.
www.pulsarmicrowave.com

50 GHz Attenuators

VENDORVIEW

RFMW announces design and sales support for XMA Corp's 8582-6150-xx series of 2.4 mm, 50 GHz Attenuators. The XMA coaxial attenuators are available in standard dB values of 3, 6, 10, 20 and 30 dB and handle up to 1 W of power. Low VSWR provides high performance with minimal additional through path insertion loss.

RFMW
www.rfmw.com

High-Power Lowpass Filters

RLC Electronics' high-power lowpass filters are designed for high-power systems in the frequency range of 100 to 8000 MHz. These filters are designed to handle 2500 W average under extreme temperature and altitude conditions, while offering low loss (0.15 dB typical) and 1.5:1 VSWR (maximum). RLC filters offer you the flexibility of choosing your cutoff frequency, number of sections and connector type (N, SC, HN, 7/16) for a truly custom high-power lowpass product.

RLC Electronics
www.rlcelectronics.com

CABLES & CONNECTORS

BNC In-Series Adapters

VENDORVIEW

HASCO's straight coaxial adapters offer performance from DC up to 6 GHz. HASCO offers In-Series adapters in precision, general purpose, low PIM and coax-to-waveguide adapter options. Their coax adapters come in BNC, N, TNC, SMB, SMA, SSMA, 3.5, 2.92, 2.4, 1.85 and 1.0 mm connector configurations, operating up to 110 GHz.

HASCO
www.hasco-inc.com

AMPLIFIERS

Solid-State Power Amplifier

VENDORVIEW

The AMP2073-3 from Exodus Advanced Communications is a solid-state power amplifier (SSPA) that operates from 2 to 10 GHz. It delivers a CW/pulsed saturated output power of 15 W with a power gain of more than 40 dB. This Class A/AB power amplifier has spurious levels of less than -60 dBc and harmonics of -20 dBc. It is equipped with built-in protection circuits and provides extensive monitoring parameters.

Exodus Advanced Communications
www.exoduscomm.com

X- & Ku-Band SSPAs

Kratos General Microwave's cutting-edge, field-proven SSPAs are designed and built for the harshest environment conditions, including hostile temperatures, shock, vibration, moisture, altitudes and G-forces. The custom and off-the-shelf SSPAs in X-Band and Ku-Bands, utilize the latest GaN and GaAs technologies and provide high power density in a compact footprint to meet critical space and weight requirements in high frequencies.

Kratos General Microwave
www.kratosmed.com

CW Immune ERDLVA

VENDORVIEW

Quantic PMI Model ERDLVA-218-CW-75MV is a CW Immune ERDLVA that operates from 2 to 18 GHz and has a TSS of -42 dBm, a log slope of 75 ± 10 mV per dB and a rise/recovery time of 25 ns/500 ns. This ERDLVA has SMA female connectors and is 2.90" × 2.30" × 0.50".

Quantic PMI
www.Quantic PMI-rf.com

New**Products**

MMIC Power Amplifier

VENDORVIEW

Qorvo's QPA0506 is a MMIC power amplifier fabricated using Qorvo's QGaN25 0.25 µm GaN on SiC production process. Covering 5 to 6 GHz, the QPA0506 typically provides 36 dBm of saturated output power and 18 dB of large-signal gain while achieving 53 percent power-added efficiency. The QPA0506 can support a range of bias voltages to optimize power and PAE to system requirements. The QPA0506 is matched to 50 ohms with a DC blocked input and a DC grounded output.

Qorvo
www.qorvo.com

SOFTWARE

Modelithics COMPLETE Library

VENDORVIEW

Modelithics announced the release of the latest version, v22.2, of the Modelithics COMPLETE Library for use with the Cadence® AWR Design Environment® Platform. This version adds nearly 50 new models for various components to the Modelithics COMPLETE Library. With these additions, the Modelithics COMPLETE Library now includes over 825 models that represent over 25,000 passive and active RF/microwave components. This collection of simulation models comprises surface-mount RLC components, diodes, transistors, amplifiers, attenuators, filters, couplers and other system components.

Modelithics Inc.
www.modelithics.com

INSTRUCTION

RF Technology Certification

BESSER ASSOCIATES

RF Technology Certification is an online course designed for professionals who need a solid background in RF and wireless technology and products. The four-part program provides the student with a thorough understanding of RF analytical tools, communication signals, RF devices and test instruments. The program was developed by Besser Associates, a worldwide leader in RF and wireless training.

Besser Associates Inc.
www.besserassociates.com

MATERIALS

3D Material

Radix™ 3D printable dielectric is the first 3D material featuring a dielectric constant of 2.8 and low loss characteristics at microwave frequencies. These printable dielectric

MICRO-ADS

New**Products**

materials give RF designers unprecedented design freedom in creating new components, eliminating the need to consider typical manufacturing constraints. The Radix™ material is designed for use on a scalable, high-resolution printing process, offering the industry a way to manufacture dielectric components like gradient index (GRIN) RF lenses and other complex geometries at scale.
Rogers Corp.
www.rogerscorp.com

TEST & MEASUREMENT

Cryogenic Test Dewer

CMT is manufacturing cryogenic component test dewers, optimized for testing cryogenic components at either 4K or 13K, depending upon the model. The dewer design offers flexibility to configure the cold plate for testing different types of cryogenic components. The 12 removable side plates can be easily modified to quickly add RF connections. Includes a 66-pin hermetic DC connector for temperature sensors DC wiring to internal components, two KF25 vacuum port connections for vacuum pump and gauges. Additional custom configurations are available.
Cosmic Microwave Technology
www.cosmicmicrowavetechnology.com

Base Station Emulator

VENDORVIEW

The NOFFZ base station emulator ensures that IoT cellular interfaces can be easily validated in the laboratory or tested end-of-line. It creates precisely customizable cellular mobile environments for test and characterization requirements from 2G to 5G. The BSE can then be used to perform a wide variety of functional tests, typically testing topics such as handover scenarios between different technologies, data upload and download or outage scenarios.
NOFFZ Technologies GmbH
www.noffz.com

Digital Oscilloscope

Rigol's StationMax DS7000 digital oscilloscope with real-time spectrum analysis, 3 and 5 GHz bandwidths, 20 Gsa/s sample rate, 2 Gpts memory depth, 1 million wfms/s, 8 to 16 bit resolution, 15.6" multi-touch display, new UltraVisionIII platform.
Rigol
www.rigolna.com

The SM435B RF Analyzer

Signal Hound's SM435B is a high performance 43.5 GHz spectrum analyzer and monitoring receiver with 110 dB of dynamic range and 1 THz/sec sweep speeds. The SM435B offers 160 MHz instantaneous bandwidth (IBW) calibrated I/Q capture, available through block transfer of a 2-second I/Q buffer over USB 3.0 to the PC. The SM435B comes with a signed calibration certificate, a printed packet of calibration data and Spike™ Software.
Signal Hound
www.signalhound.com

Next-Generation Digitizers

VENDORVIEW

Three new digitizer cards from Spectrum Instrumentation raise the standard of PC-based instrumentation performance: The cards are capable of streaming acquired data over the PCIe bus at an impressive 12.8 GB/s—nearly twice as fast as any other PCIe digitizer currently on the market. It means they can continuously run at their maximum sampling rate of 6.4 GS/s, with 12-bit resolution, streaming this massive data to CPUs or CUDA GPUs for real-time processing.
Spectrum Instrumentation GmbH
www.spectrum-instrumentation.com

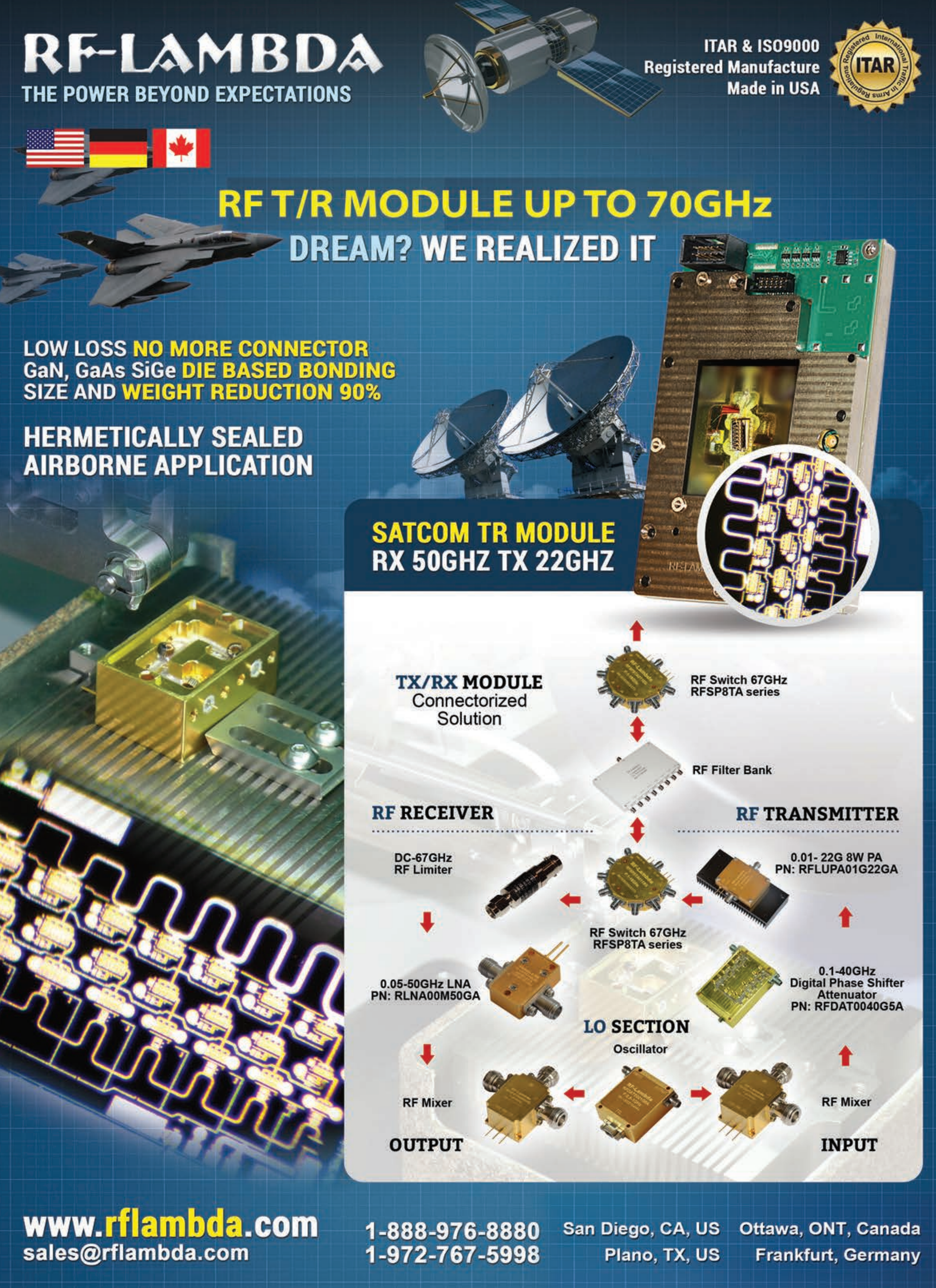

RF-LAMBDA
THE POWER BEYOND EXPECTATIONS
ITAR & ISO9000
Registered Manufacture
Made in USA
ITAR
Registered International Traffic in Arms Regulations
RF T/R MODULE UP TO 70GHz
DREAM? WE REALIZED IT
LOW LOSS NO MORE CONNECTOR
GaN, GaAs SiGe DIE BASED BONDING
SIZE AND WEIGHT REDUCTION 90%
HERMETICALLY SEALED
AIRBORNE APPLICATION
SATCOM TR MODULE
RX 50GHZ TX 22GHZ
TX/RX MODULE
Connectorized
Solution
RF Switch 67GHz
RFSP8TA series
RF Filter Bank
RF RECEIVER
RF TRANSMITTER
DC-67GHz
RF Limiter
0.01- 22G 8W PA
PN: RFLUPA01G22GA
RF Switch 67GHz
RFSP8TA series
0.05-50GHz LNA
PN: RLNA00M50GA
0.1-40GHz
Digital Phase Shifter
Attenuator
PN: RFDAT0040G5A
LO SECTION
Oscillator
RF Mixer
RF Mixer
OUTPUT
INPUT
www.rflambda.com
sales@rflambda.com
1-888-976-8880
1-972-767-5998
San Diego, CA, US
Plano, TX, US
Ottawa, ONT, Canada
Frankfurt, Germany

Review by: Patrick Hindle

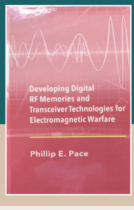

Bookend

Developing Digital RF Memories and Transceiver Technologies for Electromagnetic Warfare

Phillip E. Pace

This book provides a thorough treatment of the latest developments in digital RF memory (DRFM) technology and its role in maintaining dominance over the electromagnetic spectrum. Part I discusses the use of advanced technology to design transceivers for spectrum sensing using unmanned systems to dominate the electromagnetic spectrum. Part II discusses artificial intelligence and machine learning to enable modern spectrum sensing and detection signal processing for electronic support and electronic attack. Another key subject is examination of counter-DRFM techniques.

DRFM and transceiver design details and examples are provided along with the MATLAB software allowing the reader to construct their own embedded DRFM transceivers for unmanned systems. It examines the design tradeoffs in developing multiple, structured, false target synthesis DRFM architectures and aids in developing counter-DRFM techniques and distinguishes false target from real ones.

Phillip E. Pace is a distinguished professor (emeritus) in the Department of Electrical and Computer Engineering at the Naval Postgraduate School and has taught as an adjunct professor at Southern Methodist University in addition to working as a senior scientist at L3Harris Technologies. Pace provides a comprehensive book of about 900 pages covering this topic thoroughly from semiconductor technologies to sensing to algorithms. This is an excellent book on the subject and very organized including examples, equations and graphics.

If you are looking for a comprehensive book on the subject with advanced level details including equations and algorithms, this is a perfect book to read. It is well written and organized with very good figures/graphics, references, equations and examples to explain the concepts that are covered.

ISBN 13: 9781630816971
ePub: $119
Hardcover: $159
Copyright: 2022
To order this book, contact:
Artech House
685 Canton St.
Norwood, MA 02062
800-225-9977
or
16 Sussex St.
London, SW1V 4RW, UK
+44 (0)20 7596 8750

E LEARNING CENTER

Presented by: Microwave Journal

NEW

9/13
5 Ways Our Filters Are Extending the Norm for Peak Performance

Sponsored by: RFMW, Knowles

9/14
Impacts of Solder Reflow on High Bandwidth RF Connectors: Everything's great until you apply solder!

Sponsored by: Samtec

9/20
Matching mmWave Radar Software Models to PCB Antenna Measurements

Sponsored by: Rogers Corporation

Now On Demand
Radar and Radio Systems Coverage Optimization

Sponsored by: Altair

microwavejournal.com/events/2176

ONLINE PANEL SERIES

9/8 UWB Location and Security Applications

Register to attend at mwjournal.com/webinars

FEATURED eBooks

mwjournal.com/ebooks

AdvertisingIndex

Sales Representatives

Eastern and Central Time Zones
Michael Hallman
Associate Publisher
(NJ, Mid-Atlantic, Southeast, Midwest, TX)
Tel: (301) 371-8830
Cell: (781) 363-0338
mhallman@mwjournal.com

Shannon Alo-Mendosa
Northeastern Reg. Sales Mgr.
(New England, New York, Eastern Canada)
Tel: (781) 619-1942
Cell: (978) 501-9116
salomendosa@horizonhouse.com

Submitting ad material?
Visit: www.adshuttle.com/mwj
(866) 774-5784
outside the U.S. call +1-414-566-6940

Pacific and Mountain Time Zones
Brian Landy
Western Reg. Sales Mgr.
(CA, AZ, OR, WA, ID, NV, UT, NM, CO, WY, MT, ND, SD, NE & Western Canada)
Tel: (831) 426-4143
Cell: (831) 713-9085
blandy@mwjournal.com

International Sales
Richard Vaughan
International Sales Manager
Tel: +44 207 596 8742
rvaughan@horizonhouse.co.uk

Ed Kiessling
(781) 619-1963
ekiessling@mwjournal.com

Germany, Austria, and Switzerland (German-speaking)
WMS.Werbe- und Media Service
Brigitte Beranek
Tel: +49 7125 407 31 18
bberanek@horizonhouse.com

France
Gaston Traboulsi
Tel: +44 207 596 8742
gtraboulsi@horizonhouse.com

Israel
Dan Aronovic
Tel: +972 50 799 1121
aronovic@actcom.co.il

Korea
Young-Seoh Chinn
JES MEDIA, INC.
Tel: +82 2 481-3411
corres1@jesmedia.com

China
Shenzhen
Jenny Li
ACT International
jennyl@actintl.com.hk

Shanghai
Linda Li
ACT International
Tel: 86-021-62511200
lindal@actintl.com.hk

Wuhan
Sky Chen
ACT International
skyc@actintl.com.hk

Beijing
Cecily Bian
ACT International
Tel: +86 135 5262 1310
cecilyb@actintl.com.hk

Hong Kong, Taiwan, Singapore
Floyd Chun
ACT International
Tel: +86-13724298335
floydc@actintl.com.hk

Japan
Katsuhiro Ishii
Ace Media Service Inc.
Tel: +81 3 5691 3335
amskatsu@dream.com

Corporate Headquarters: 685 Canton Street, Norwood, MA 02062 • Tel: (781) 769-9750

FABS and LABS

CAES Gets Additive RF

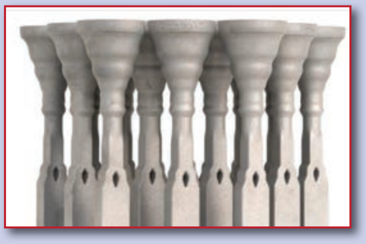

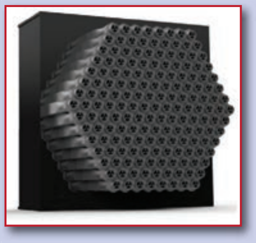


Waveguide components have been made the same way for decades, but new additive manufacturing techniques have been developed to bring innovation to these products. In April of 2021, CAES announced a strategic alliance to bring additive manufacturing and 3D printing technology to U.S. customers with an exclusive license to SWISSto12's patents, trade secrets and product designs. A year later, CAES celebrated the opening of its state-of-the-art RF additive manufacturing (AM) operations in Exeter, N.H. The facility is 3500 square-feet and the largest 3D printing facility for RF in the U.S. The laboratory is outfitted with state-of-the-art equipment dedicated to 3D printing of RF technology and has been identified as a leading facility to provide AM services by top U.S. aerospace and defense prime manufacturers.

The proprietary printing and metal finishing offers the highest achievable RF performance on the market for AM. The SWISSto12 process has been qualified for space applications (ESA) and provides improved RF performance, with a post processing technique that improves the surface roughness (reduces loss) to realize 5x better performance than unprocessed pieces.

The operations consist of dedicated equipment for 3D-printed RF technology design and manufacturing, including a qualified laser powder bed fusion machine, associated process support equipment, proprietary metal finishing and plating line and complete RF testing capability. Full environmental testing facilities are also available on site.

The Additive Manufacturing Room currently has one EOS M290 printer and can accommodate future printer expansion. The low volume AM Post processing/plating line has a small setup using the SWISSto12 CAES proprietary post processing and plating IP for prototyping. The full Production AM post processing/plating line is under construction and expected to be installed in September 2022. These lines are currently producing prototype and demonstrator hardware and expected to be qualified in November 2022. Outside printing services, taking advantage of larger powder bed formats and various materials, have also been qualified for maximum flexibility and higher volumes.

CAES and SWISSto12 primarily work with Al alloys (AlSi10Mg and AlSi7Mg) but also have experience with Titanium and INVAR along with a strong SWISSto12 heritage with plated plastics (PEEK and PEK). Parts can currently be made as large as 31 x 16 x 20 in. The tolerances can be controlled down to 1 mil so products can operate up to V-Band frequencies. Lead times can be reduced by about 50 percent, with full design to delivery in about three months compared to traditional manufacturing.

AM provides maximum design flexibility in achieving shapes that traditional manufacturing techniques cannot make and can significantly reduce the number of connections/parts, size and weight. Parts can be designed to provide multiple functions in a single assembly. In most cases, AM manufactured parts can provide greater integrated functionality in a monolithic structure while reducing system complexity, providing a higher level of performance, reduced number of parts and mass reduction of 20% to 50%. CAES also has the capability to add active components to the assemblies to create a complete integrated subsystem or system design.

CAES has a long history of innovation and now their AM facility opens an era in designing and producing high performance RF structures that will revolutionize the way aerospace parts are constructed. AM offers the A&D markets improved system performance plus reduced size, weight and time to market.

https://caes.com

WERLATONE
ENGINEERING EVOLVED

HIGH POWER DIRECTIONAL COUPLERS

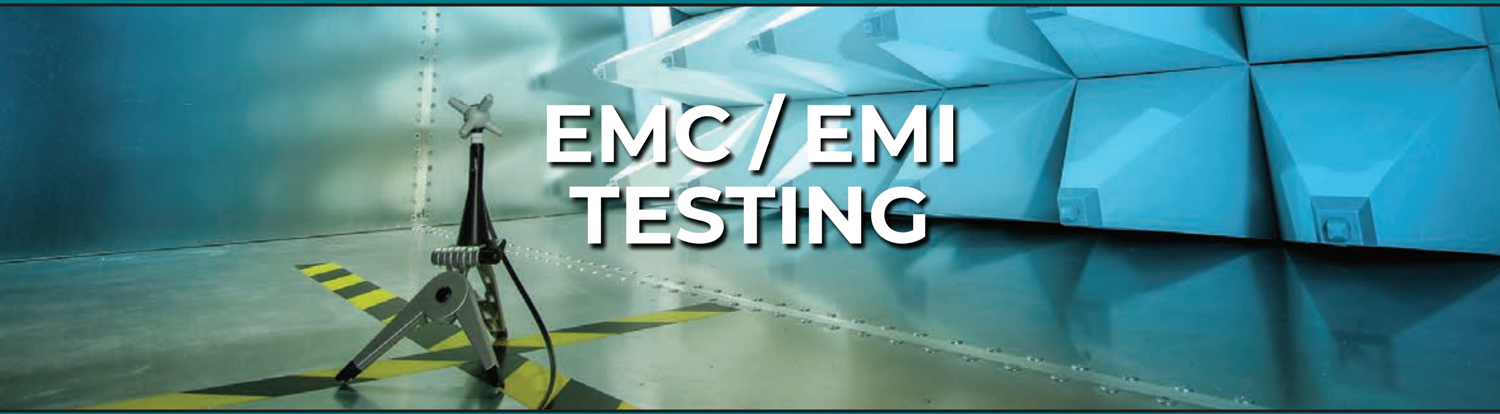

Up to 1000:1 Bandwidth ✦ Low Insertion Loss ✦ *Mismatch Tolerant*® Designs

Model	Type	Frequency (MHz)	Power (W CW)	Coupling (dB)	Insertion Loss (dB)	Connectors	Size (inches)
C8730	Dual	0.009-250	500	40	0.40	N-Female	10.5 x 3.0 x 2.0
C8731	Dual	0.009-250	1000	40	0.40	N-Female	10.5 x 3.0 x 2.0
C11462	Dual	0.009-400	500	40	0.45	N-Female	6.7 x 2.28 x 1.69
C8510	Dual	0.009-1000	500	40	0.45	N-Female	6.7 x 2.28 x 1.69
C5047	Dual	0.01-100	4,000	50	0.15	7/16-Female	10.0 x 4.16 x 3.5
C1979	Dual	0.01-100	10,000	60	0.10	LC-Female	2.0 x 6.0 x 4.5
C5086	Dual	0.01-250	250	40	0.50	N-Female	5.2 x 2.67 x 1.69
C5100	Dual	0.01-250	500	40	0.40	N-Female	10.5 x 3.0 x 2.0
C5960	Dual	0.01-250	1,000	50	0.40	N-Female	10.5 x 3.0 x 2.0
C1460	Dual	0.01-250	2,000	50	0.15	N-Female	10.0 x 3.0 x 2.0
C4080	Dual	0.01-250	3,500	50	0.20	N-Female	10.0 x 4.6 x 3.5
C11026	Dual	0.01-220	5,000	60	0.10	LC-Female	12.0 x 6.0 x 4.5
C8390	Dual	0.01-250	10,000	60	0.10	LC-Female	12.0 x 6.0 x 4.5
C5339	Dual	0.01-400	200	40	0.50	N-Female	5.2 x 2.67 x 1.69
C6047	Dual	0.01-400	500	40	0.50	N-Female	5.2 x 2.67 x 1.69
C2630	Dual	0.01-1000	100	40	0.60	N-Female	5.0 x 2.0 x 1.51
C6021	Dual	0.01-1000	500	40	0.45	N-Female	6.7 x 2.28 x 1.69
C6277	Dual	0.01-1000	500	50	0.45	N-Female	6.7 x 2.28 x 1.69
C11146	Dual	0.01-1000	500	43	0.45	SC-Female	6.7 x 2.63 x 2.20
C11047	Dual	0.01-1000	1,000	43	0.45	SC-Female	6.7 x 2.63 x 2.20
C11161	Dual	0.01-1000	1,000	50	0.45	SC-Female	6.7 x 2.63 x 2.20
C1795	Dual	0.1-1000	100	40	0.50	N-Female	5.0 x 2.0 x 1.51
C5725	Dual	0.1-1000	500	40	0.50	N-Female	5.2 x 2.28 x 1.69
C11077	Dual	0.1-1000	1,000	43	0.45	SC-Female	6.7 x 2.28 x 1.69
C3910	Dual	80-1000	200	40	0.20	N-Female	3.0 x 3.0 x 1.09
C5982	Dual	80-1000	500	40	0.20	N-Female	3.0 x 3.0 x 1.09
C3908	Dual	80-1000	1,500	50	0.10	7/16-Female	3.0 x 3.0 x 1.59
C6796	Dual	80-1000	5,000	60	0.20	1 5/8” EIA	6.0” Line Section
C8060	Bi	200-6000	200	20	0.40	SMA-Female	1.8 x 1.0 x 0.56
C8000	Bi	600-6000	100	30	1.10	SMA-Female	4.8 x 0.88 x 0.50
C10117	Dual	700-6000	250	40	0.20	N-Female	2.0 x 2.0 x 1.06
C10364	Dual	700-6000	500	50	0.20	7/16-Female	2.15 x 2.0 x 1.36
C10996	Dual	700-6000	700	50	0.20	7/16-Female	2.15 x 2.0 x 1.36
C11555	Dual	700-6000	1,000	50	0.20	7/16-Female	2.15 x 2.0 x 1.36
C10695	Dual	700-6500	500	50	0.20	7/16-Female	2.15 x 2.0 x 1.36

Werlatone, Inc. 17 Jon Barrett Road Patterson, NY 12563 845-278-2220 sales@werlatone.com www.werlatone.com

2022 MILITARY AND AEROSPACE

A Special Supplement to

Microwave Journal


ANALOG DEVICES
AHEAD OF WHAT'S POSSIBLE™
Complex Problems, Simple Solution
For mission critical applications, Analog Devices delivers proven, beamforming technology with trusted reliability when and where you need it most—from the unknown vastness of space to the unrelenting theater of war.
Optimized Form Factor
Enhance Speed to Market
Low Power, Minimal Heat Dissipation
Find your solution at analog.com/phasedarray

Proven mmWave RF Solutions that Connect, Protect and Power All the Systems Around You

GaN Solutions For Mission Critical Aerospace and Defense Applications

Part Number	Frequency Range (GHz)	Psat (dBm)	Gain (dB)	Supply Voltage (V)
QPD1016	DC-1.7	57	16.6	50
QPD1004	0.03-1.4	44	18	50
QPA2935	2.7-3.5	33	28.4	25
QPA0506	5-6	36.5	27.4	25
QPA1724	17.3-21.2	43	25	20

For additional Qorvo solutions, visit **www.qorvo.com.**

QORVO®

STAFF

Publisher: Carl Sheffres
Associate Publisher: Michael Hallman
Editorial Director: Patrick Hindle
Editor: Gary Lerude
Managing Editor: Jennifer DiMarco
Associate Technical Editor: Cliff Drubin
Editorial & Media Specialist: Kelley Roche
Associate Editor: Emma Lutjen
Multimedia Staff Editor: Barbara Walsh
Electronic Marketing Manager: Chris Stanfa
Senior Digital Content Specialist: Lauren Tully
Audience Development Manager: Carol Spach
Director of Production & Distribution: Edward Kiessling
Art Director: Janice Levenson
Graphic Designer: Ann Pierce

EUROPE
Office Manager: Nina Plesu

CORPORATE STAFF
CEO: William M. Bazzy
President: Ivar Bazzy
Vice President: Jared Bazzy

At the heart of the next generation electronic defense systems.

The next generation electronic defense systems demand effectiveness, reliability, power efficiency and affordability. You can count on CTT's thirty-seven years of experience in microwave amplification and subsystem integration to meet these demands.

CTT offers not only form, fit, function of microwave amplifier replacements for many mature systems, but also incorporates leading-edge technology components such as GaN and GaAs.

CTT has delivered production quantities of amplifiers with power levels of 10 through 600 Watts – and higher – for a variety of multi-function radar and EW applications.

CTT is well positioned to offer engineering and production technology solutions – including high-rel manufacturing – to infuse new technology into legacy systems for improved reliability and life cycle costs.

• AMDR • Shipboard Radar • AESA Radar • UAVs
• VLO/FLO Threats • New Land Radar • SAR • EW

More than 37 years ago CTT, Inc. made a strong commitment to serve the defense electronics market with a simple goal: **quality**, **performance**, **reliability**, **service** and **on-time delivery** of our products.

Give us a call to find out how our commitment can support your success. **It's that simple.**

Microwave Technology Leadership

- **Power Amplifiers**
  - **NEW GaN and GaAs Models**
  - Radar Bands up to 1kW
  - EW Bands up to 600W
  - Pulse and CW
  - Solid-State Microwave Power Modules
  - Rack-Mount Configurations
- **Subsystems**
- **SWaP-C Optimization**
- **Custom Engineered Options**

AS9100D
ISO 9001:2015

USA-based thin-film microwave production facility

CTT INC
A KRATOS Company

5870 Hellyer Avenue • Suite 70 • San Jose • California 95138
Phone: 408-541-0596 • Fax: 408-541-0794 • www.cttinc.com • E-mail: sales@cttinc.com

MEMS Oscillators Take On Hypersonic Challenges

Odile Ronat
SiTime Corporation, Santa Clara, Calif.

The unique capabilities of hypersonic flight present enormous challenges for timing system components, demands found nowhere else in a military's inventory. This article describes these challenges and how MEMS oscillators are better suited than quartz-based solutions for meeting the requirements.

Quartz-based timing components have provided timing references for aerospace and defense applications for decades. While quartz-based oscillators have been enhanced to mitigate their shortcomings, they still have inherent disadvantages that challenge their performance in next-generation defense systems such as hypersonic weapons.

The development of timing devices based on MEMS can be traced to the need to overcome the shortcomings of quartz crystal oscillators for mission-critical applications. Today's MEMS-based timing devices offer superior performance compared to quartz-based counterparts. MEMS is inherently reliable and rugged, making MEMS components well suited for the harsh operating environments encountered in aerospace and defense systems and, particularly, hypersonic weapons.

Hypersonic weapons pose unique challenges for the timing devices used in the mission computing, flight control, real-time signal processing and communications subsystems on the weapon. These challenges stem from the intimidating environment: extreme temperatures and pressures, vibration, shock and extremely high g-forces.

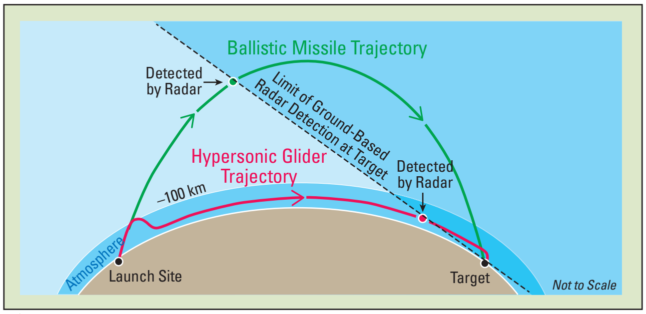

Fig. 1 The trajectories of hypersonic boost-glide vehicles vs. ballistic missiles. *Source:* Congressional Research Service, "Defense Primer: Hypersonic Boost-Glide Weapons."

Hypersonic Weapons Explained

Hypersonic weapons are ultra-fast, low-flying, agile and highly maneuverable vehicles that are capable of avoiding detection and defense systems. Although ballistic missiles travel at hypersonic speeds above Mach 5, they have set trajectories and limited maneuverability. Hypersonic missiles travel at speeds between 3000 and 15,000 mph—1 to 5 miles per second—which is up to > 25× faster than a commercial jet aircraft. These characteristics of high speed, maneuverability and unusual altitudes make them challenging for the best missile defenses until the last minutes of flight, which is often too late.

The two types of hypersonic weapons are hypersonic glide vehicles (HGVs) and hypersonic cruise missiles (HCMs). HGVs, also known as boost-glide vehicles, are typically launched from a ballistic missile, released at a specific altitude and speed and follow a flight path tailored to reach the target (see ***Figure 1***). HGVs are not generally powered once released, although a small propulsion system may be used to accelerate arrival at the target and provide directional control.

In contrast, HCMs are powered by air-breathing scramjet engines after being launched from a rocket or jet aircraft. They fly at high altitudes, although lower than HGV altitudes. HCMs have the dual advantages of hypersonic speed and relatively low altitude, enabling them to hit targets within a 600-mile radius in just a few minutes. Although HCMs fly at lower altitudes than HGVs, their hypersonic speeds make them difficult to detect and defeat, well beyond what most current surface-to-air missile systems can reach.

The scramjet used in the HCM is essentially a jet engine that produces thrust by the combus-

Reactel, Incorporated
Reacting First to All Your Filter Needs.
REACTEL, INC.
Let our Engineers show you what we can do in tight spaces!
High Performance, Rugged Packaging, Small Size and Weight
Great things *can* come in small packages. Reactel filters are ideally suited for the demanding environments that unmanned vehicles encounter.
Many manufacturers rely on Reactel to provide units which are:
• High performance
• Lightweight
• Low profile
Contact a Reactel engineer with your filter or multiplexer requirements. We can create a unit which will be the perfect fit for your applications.
REACTEL, INC.
REACTEL, INC
8031 Cessna Avenue • Gaithersburg, Maryland 20879 • Phone: (301) 519-3660 • Fax: (301) 519-2447
For general inquiries, please email reactel@reactel.com • Follow us on Twitter: @reacteljim
Go online to www.reactel.com to download your Reactel catalog today.
RoHS Compliant 2002/95/EC
Intertek
@reacteljim

tion of fuel and an oxidizer, the latter obtained by consuming atmospheric oxygen. This propulsion technology differs from typical rockets, which carry both fuel and the oxidizer in separate tanks or as a form of solid fuel. Air-breathing limits scramjets to lower altitudes, where the oxygen content is sufficient to maintain combustion. Practically, the scramjet engine must first be launched and then begins operating after reaching a specific altitude.

Scramjets have been in development since the 1950s; however, they've been extremely difficult to perfect, with the most successful results produced only since the 2000s. Even though scramjets are conceptually simple, their challenges are immense, primarily because of the low altitudes where they operate. The atmosphere generates enormous drag, and at very high speeds the resulting high temperatures require use of exotic materials, so the engine does not burn up. Combustion in the scramjet creates another thermal challenge: reducing the airflow speed into the engine, from higher hypersonic to slower supersonic speeds, and burning fuel creates extreme heating of the engine and nozzle. The electronic components used in a scramjet weapon must withstand these extreme temperatures.

Both types of hypersonic weapons create severe operating environments: high temperatures, thermal shock, vibration and high g-forces that the electronic components—radomes, antennas, RF front-ends, digital processing and timing—must withstand while meeting specified performance. The remainder of this article focuses on the reference clocks used for timing and local oscillators, comparing the performance of MEMS and quartz technologies to the key environmental stressors imposed by hypersonic weapons.

MEMS vs. Quartz

SiTime® introduced the first MEMS oscillator in 2006 and has continued to improve MEMS timing technology, adding temperature compensation and phase-locked loops (PLL) to reduce jitter and phase noise, integrating voltage regulators to reduce noise and eliminating frequency jumps at certain temperatures. SiTime now offers Endura® ruggedized oscillators engineered for harsh environments such as those encountered in hypersonic applications.

MEMS timing devices are designed to be free of spurious mode crossings with the fundamental mode and of resonator-induced activity dips. The MEMS device uses a single mechanical structure of pure, single-crystal silicon with a tensile strength of 7 GPa, about 14× higher than titanium's 330 to 500 Mpa. During the manufacturing process, SiTime uses a proprietary encapsulation technique called EpiSeal® to clean the resonator and hermetically seal it, which effectively eliminates aging. This manufacturing technique underpins the exceptional reliability of MEMS oscillators, which achieve significantly better failure rates than those of quartz oscillators (see ***Figure 2***). The mean time between failure (MTBF) of the Endura MEMS oscillator is 2.1 billion hours, approximately 50× greater than quartz-based oscillators.

With the hermetic EpiSeal process, contaminants are limited to low parts-per-billion (ppb), and an 1100°C anneal seals the Si crystal applied to the wafer in a high vacuum with extremely low or no impurities. The clean resonator cavity effectively eliminates resonator


CAES
PIONEERING ADVANCED ELECTRONICS
Enabling the World's Most Critical Missions
CAES technology pioneers the future of aerospace and defense electronics and underpins many of the world's most critical missions. Over the course of nearly 100 years, we have become the largest provider of analog and radiation-hardened technology to the United States aerospace and defense industry.
Connie, CAES Microelectronics Engineer, Colorado Springs, CO
CAES
Ted , CAES Rotary Joint Supervisor, Exeter, NH
caes.com

aging mechanisms (see ***Figure 3***). The typical 10-year aging specification for a representative SiTime Endura MEMS oscillator is ±360 ppb versus ±3000 ppb for quartz-based oscillators.

Quartz-based oscillators are typically housed in an open cavity, ceramic package with the IC and quartz resonator bonded to the package substrate using two types of adhesives. Each quartz device is trimmed to the desired output frequency using either ablation or by depositing metal onto the quartz resonator. The adhesives and metal trimming can be a source of contamination that ages the resonator through mass loading and reduces reliability.

Shock and Vibration

Endura MEMS-based oscillators are more resistant to shock and vibration, in part because MEMS resonators have

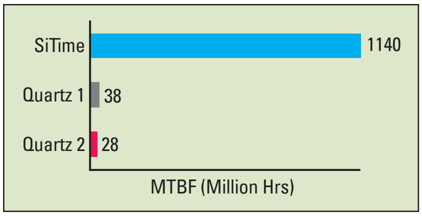

▲ Fig. 2 MTBF comparison of SiTime MEMS and quartz oscillators.

1000× to 3000× lower mass than quartz resonators. The acceleration imposed on the MEMS structure from shock or vibration results in lower force than on the quartz crystal, which will induce a lower frequency shift. This is illustrated in ***Figure 4***, which compares the phase noise of an Endura MEMS oscillator to several quartz temperature-compensated crystal oscillators (TCXOs). Subjected to random vibration with an RMS magnitude of 7.5 g over 10 Hz to 2 kHz, the MEMS oscillator has some 20 dB lower phase noise in this vibration frequency band. Integrating the phase noise over the vibration frequency band shows the undesirable integrated phase jitter (IPJ) of the MEMS oscillator increases by 1.2×, while the IPJ of the quartz TCXOs increased between 4.5× and 10× (see ***Table 1***).

Another measure of sensitivity to vibration is the frequency shift per g of applied sinusoidal acceleration, commonly termed the total acceleration sensitivity gamma vector and measured as ppb/g. ***Figure 5*** shows the gamma vector over three axes of 30 Endura MEMS units subjected to vibration frequencies at eight frequencies between 15 Hz and 2 kHz. The maximum observed value is only 0.00577 ppb/g, the best performance in the industry.

Shock resistance is a key requirement for hypersonic weapons and another area where MEMS outperforms quartz. SiTime shock tests Endura MEMS products to 30,000 g, significantly higher than most quartz products can achieve. To put this into perspective, a 155 mm howitzer projectile experiences a peak acceleration of 15,500 g over a 9 ms pulse. Using typical system design margins of 1.5× the expected environment, components used with 155 mm projectiles should be certified for 23,250 g.

Temperature Sensitivity

Recent advances in MEMS technology, especially the DualMEMS® architecture (see ***Figure 6***), provide benefits such as resilience to fast temperature ramps and low phase noise. The reso-

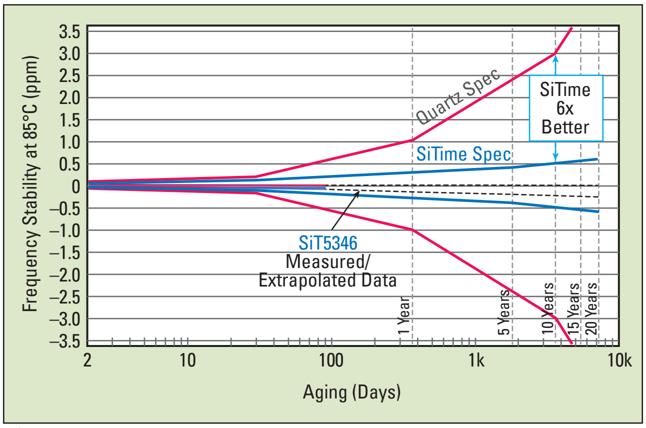

▲ Fig. 3 Aging specifications for MEMS and quartz-based oscillators.

nator and temperature sensor, shown on the left side of the block diagram, comprise the DualMEMS architecture. One resonator, the TempSense Resonator, serves as a temperature sensor, using its frequency versus temperature slope, and the other resonator, the TempFlat™ Resonator, provides a reference clock for the downstream PLL, designed to have a relatively flat frequency versus temperature slope. The ratio of frequencies between both resonators provides an extremely accurate measurement of resonator temperature, achieving 30 μK resolution. The tight thermal coupling between the resonators results from their proximity on the same die—within 100 μm—which achieves virtually no thermal gradient between the resonators.

In comparison, the temperature sensor in a quartz-based TCXO is integrated within an IC that sits below the quartz resonator on the substrate of the ceramic package. The spatial separation between the temperature sensor and the resonator enables a substantial thermal gradient between the two elements, introducing a frequency error when the oscillator is subjected to fast thermal transients.

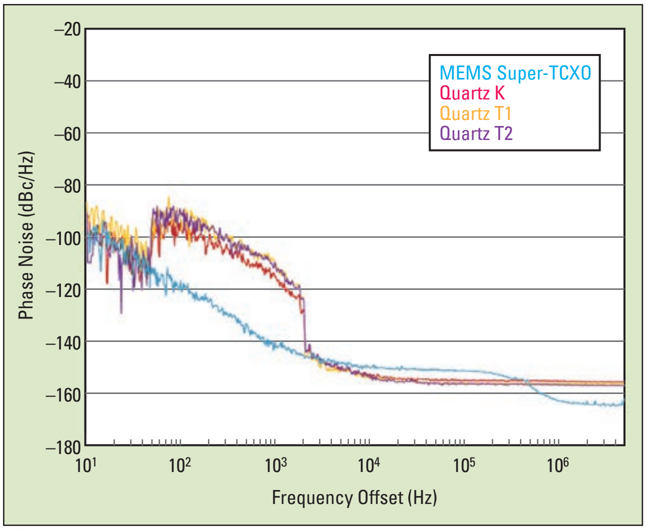

▲ Fig. 4 20 MHz oscillator phase noise with 10 Hz to 2 kHz random vibration.

TABLE 1 IPJ 10 HZ TO 10 KHZ RANDOM VIBRATION			
Oscillator	**Baseline (ps RMS)**	**With Vibration (ps RMS)**	**Increase**
MEMS	0.53	0.63	1.2x
Quartz K	0.54	2.42	4.5x
Quartz T1	0.58	3.93	6.8x
Quartz T2	0.44	4.43	10.1x

A key element of the MEMS temperature compensation architecture is the temperature to digital converter (see ***Figure 7***). This circuit generates an output frequency proportional to the ratio between the frequencies generated by the two resonators. It has 30 µK temperature resolution and up to 350 Hz bandwidth, enabling excellent close-to-carrier phase noise and Allan deviation (ADEV) performance.

ADEV is a time-domain measure of frequency stability. The advantage of ADEV over standard deviation is it converges for most noise types and is used for characterizing the frequency stability of precision oscillators such as TCXOs. Achieving good ADEV performance is critical for hypersonic weapons, as well as satellite communications and precision global navigation satellite systems.

Thermal Transients

The benefit of the DualMEMS architecture with fast thermal transients is shown in ***Figure 8***. The thermal tran-

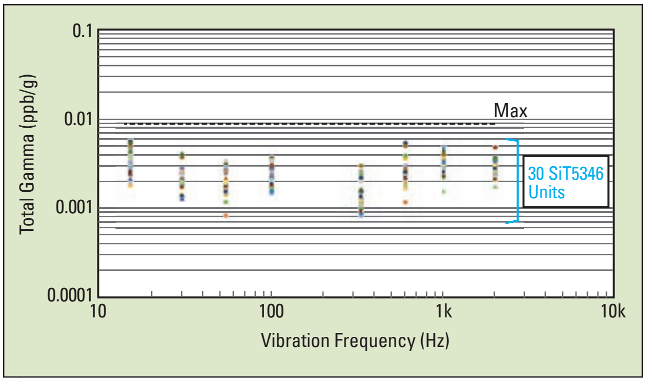

Fig. 5 MEMS oscillator acceleration sensitivity with vibration from 15 Hz to 2 kHz.

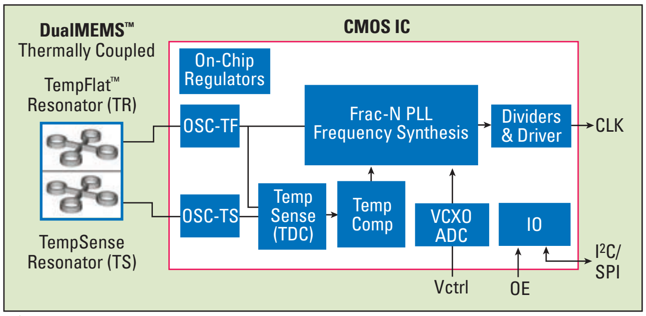

Fig. 6 DualMEMS oscillator architecture.

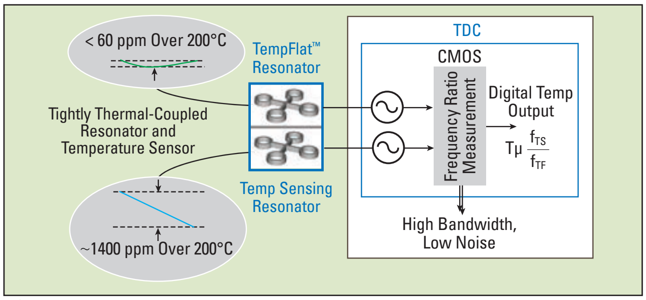

Fig. 7 Temperature to digital converter.

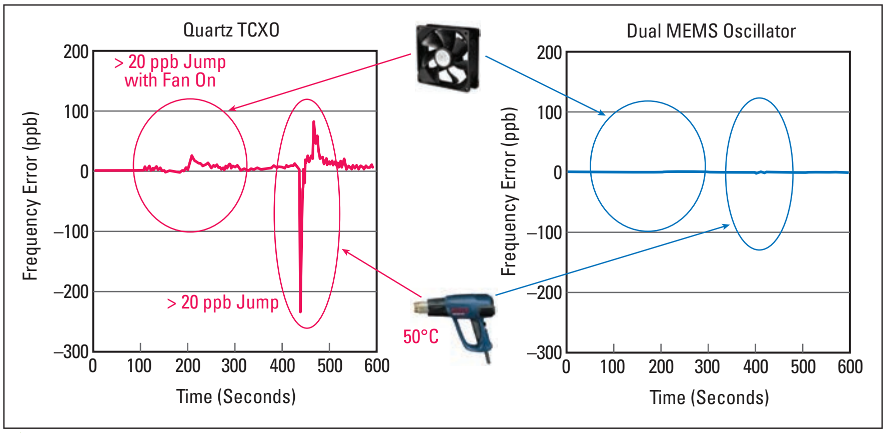

Fig. 8 Frequency error of TCXO and DualMEMS oscillators following thermal shock.

sients were created with a fan and heat gun applied to a DualMEMS oscillator and a ±50 ppb quartz-based TCXO. Following the application of heat, the quartz TCXO deviates 650 ppb peak-to-peak (from -450 to +200 ppb), exceeding its datasheet specification by 9×. The frequency change of the Endura DualMEMS oscillator is barely noticeable: 3 ppb or less, far below its specification of 100 ppb.

Rapid, turbulent airflow is a likely stress factor in hypersonic weapons and will cause die temperature changes, including fluctuations in heat flow from the oscillator to the environment. In extreme cases, this can cause vibration effects, which can be assessed from the ADEV. ***Figure 9*** compares the ADEV of quartz-based TCXO and MEMS oscillators, both subjected to airflow. The Endura MEMS oscillator has between 2× and 38× better performance than the quartz TCXO over ADEV averaging times between 1 and 100 s.

Power Supply Noise Rejection

In addition to external stresses such as vibration and changes to ambient temperature and airflow, the typical system stresses will also be present in hypersonic weapons. These include power supply noise, which can produce crosstalk from nearby data lines and switching regulators. The oscillator must maintain low phase noise and jitter in the presence of such noise.

Cutting-edge Connectivity

Providing innovative, reliable and customizable solutions that enable our customers to achieve mission success.

We Offer

- Technical excellence & broad market experience
- A comprehensive product portfolio providing customers with a single point of supply for a variety of Multi-Function RF Systems
- Vibration isolated and electronically compensated versions for Radar, or slaved to 1PPS for Communication or Multi-function Systems
- Designed into multiple military airborne radar systems
- Expertise in developing and producing reliable up- and down-converters and converter sub-systems that perform in rugged military environments
- Cost effective conversion techniques to reduce impact of in-band LO/image frequencies, simplifying filter requirements
- Very high dynamic range, phase and delay-matched multichannel Radar frequency converters in SWAP-optimized form factors

Up-and-Down Converters

Vibration Mitigated Frequency Sources

Direct and Indirect Synthesizers

more > smithsinterconnect.com

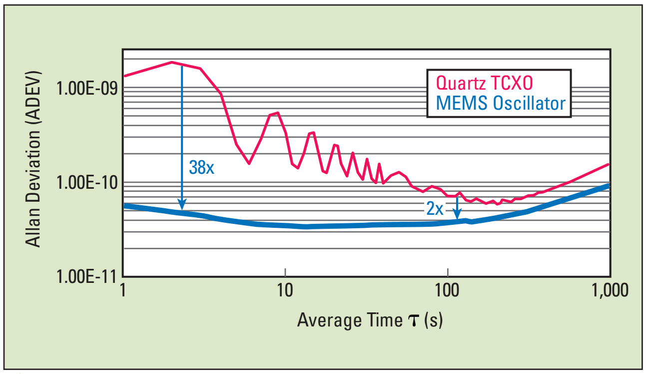

Fig. 9 The Allan Deviation of the MEMS oscillator vs. quartz-based TCXO, both with airflow.

Power supply noise rejection (PSNR) is a measure of the resilience of the oscillator to power supply noise. It is defined as the ratio of the jitter at the output (in ps) divided by the amplitude of the injected sinusoidal jitter on the supply pin (in mV). Normally, sinusoidal jitter is injected onto the supply pin with 50 mV amplitude. ***Figure 10*** shows the peak-to-peak jitter of a MEMS differential oscillator compared to quartz-based oscillators from six different suppliers. The injected power supply noise covers the frequency range from 20 kHz to 40 MHz. The low jitter demonstrated by the MEMS oscillator is achieved using multiple on-chip low-dropout regulators that isolate critical components, such as the voltage-controlled oscillator and the MEMS oscillator.

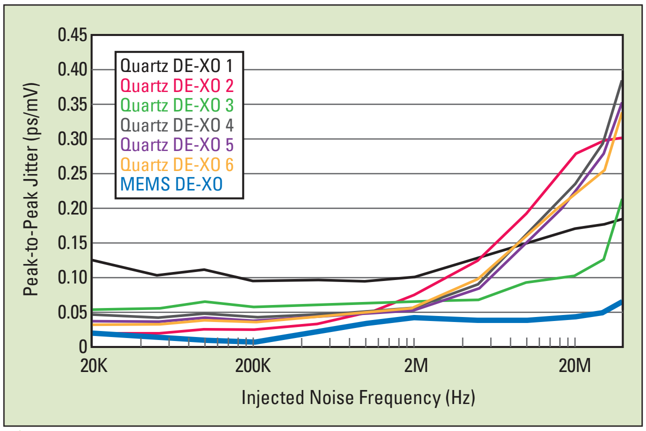

Fig. 10 PSNR of MEMS vs. typical quartz-based oscillators.

Summary

Hypersonic weapons have the potential to be among the most effective defense against adversaries due to their exceptionally high speed and maneuverability. Without careful design of the electronic subsystems, the harsh conditions caused by hypersonic speeds—very high temperature, rapid temperature change, extreme shock and vibration—can degrade if not destroy the components used in the weapon. For system timing and RF local oscillators, this article has demonstrated MEMS is superior to quartz-based oscillators and more capable of meeting the stringent performance and reliability requirements imposed by hypersonic environments. ■

EM-bridge Technology and Applications

Alan Thompson and Martin Thompson
Eureco Technologies Ltd., Ryde, Isle of Wight, U.K.

EM-bridge technology eliminates coaxial cable assemblies and their related issues from deployable antenna systems, providing more than a ten-fold reduction in RF attenuation and mass.

THE UBIQUITOUS COAXIAL CABLE

In 1880, Oliver Heaviside was granted a patent[1] in which he wrote: "My improvements have for objective to obtain perfect protection, and to render a circuit completely independent under all circumstances of external inductive influence. For this purpose, I use two insulated conductors for the circuit, and place one of them inside the other; thus, one conductor may be a wire, and the other a tube or sheath..." Heaviside's invention paved the way for the manufacture of a trillion miles of coaxial cable to carry countless messages and huge volumes of data. Heaviside also re-wrote Maxwell's equations and introduced the terms for conductance, impedance and inductance, with which all microwave engineers are familiar.

COAXIAL CABLE ISSUES

More than 132 years after Heaviside's invention, coaxial cables continue performing great work, but there are issues when using them in deployable direct radiating array (DRA) antennas on satellites. ***Figure 1*** shows an example of a large stepped-aperture DRA antenna[2-4] in the stowed and deployed states.

RF harnesses, comprising many long coaxial cables, are typically used in a beamforming network (BFN) to make signal path connections between transmit/receive (Tx/Rx) modules located in a central region of the satellite and the subarrays of radiating elements, which are located on deployable panels. When the antenna area exceeds 70 m^2, the total length of coaxial cable can exceed 1 km, and the attenuation in a coaxial cable BFN can be greater than 3 dB. Such high attenuation impacts the space mission through greater demands on the payload transmitter, power conditioning, batteries and solar panel subsystems.

Attenuation and mechanical flexibility of coaxial cables are mutually exclusive properties. To minimize attenuation due to conductor loss, the diameters of the inner and outer conductors must be increased, which rapidly raises the resistive bending torque and the mass of the cable.

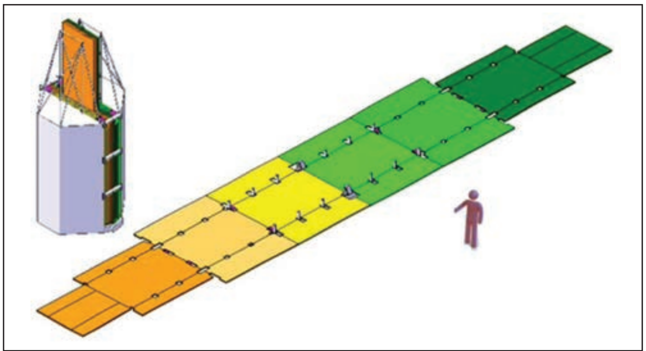

▲Fig. 1 A stepped-aperture array antenna, shown stowed and deployed.

Nonlinearities at the metal-to-metal contacts in the coaxial connectors and in the braid along the lengths of the coaxial cable, which feed the antenna subarrays, can cause severe passive intermodulation (PIM) issues.[5,6] PIM interference has a serious impact on the performance of high-power multi-frequency telecommunication systems, especially when the antenna is shared simultaneously by the transmitter and the receiver. Special coaxial connectors and assembly procedures are required to minimize PIM, which often prolongs final system testing and the delivery of space payloads.

BRIDGING THE GAPS

The authors have invented and patented[7] a means of bridging the gaps at the inter-panel junctions of deployable antennas that eliminates coaxial cables and their related issues from the BFN.

Figure 2 illustrates one example, in which folded sections of microstrip transmission line, each comprising a trace (1) and a ground plane (2) are separated by a dielectric substrate (3) in the normal manner. A flexible trace (4) and a flexible ground plane (5) are contained within their respective flexible dielectric bridges (6 and 7), which, in this folded (stowed) state, are in an arched form at the inter-panel junctions. A dielectric cover (8) keeps the flexible conductors close to their respective conductors in the microstrip.

During the deployment phase, the flexible parts unfold and slide over their respective traces and ground planes until the deployed state is reached (see ***Figure 3***). In this deployed state, the flexible trace, which is separated from

each of the microstrip traces by the dielectric, forms two series-branching, low impedance parallel-plate transmission lines, which are nominally a quarter-wavelength long at the operating frequency.

Similarly, the flexible ground plane, which is separated from each of the microstrip ground planes by the dielectric, forms series-branching, low impedance parallel-plate transmission lines that are nominally a quarter-wavelength long at the operating frequency. This arrangement forms an electromagnetic bridge (EM-bridge) between the two sections of microstrip line. An EM-bridge can also be used to connect other forms of planar transmission line, such as stripline.

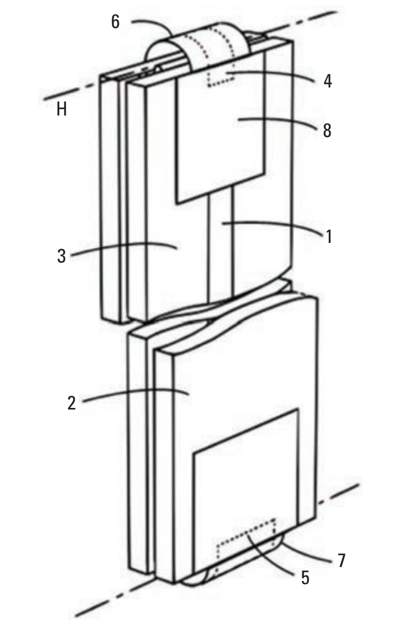

▲Fig. 2 Folded (stowed) microstrip.

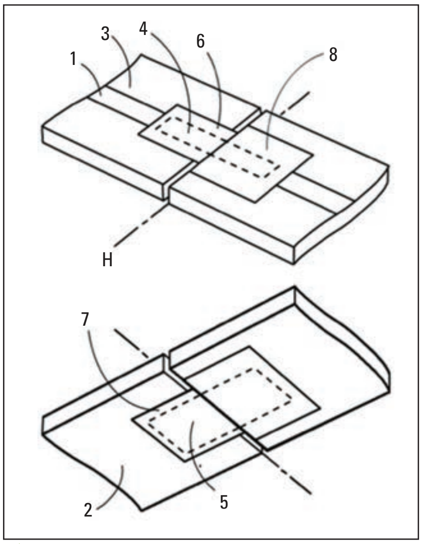

▲Fig. 3 Deployed microstrip.

SIMPLIFIED EQUIVALENT CIRCUIT

Figure 4 shows a simplified equivalent circuit of the EM-bridge. The characteristic impedance of each series-branching line (series stub) is much less than that of the planar transmission line to maximize bandwidth. Each series-branching transmission line is terminated in an open circuit, which is transformed to a short circuit at each bridge abutment by means of the impedance inverter property of the quarter-wavelength line. Therefore, each short circuit (or very low impedance) allows the flexible trace and flexible ground plane to facilitate an EM bridging function between the adjacent sections of planar transmission line.

Since there is no metal-to-metal contact within the EM-bridge, this potential source of PIM is eliminated.

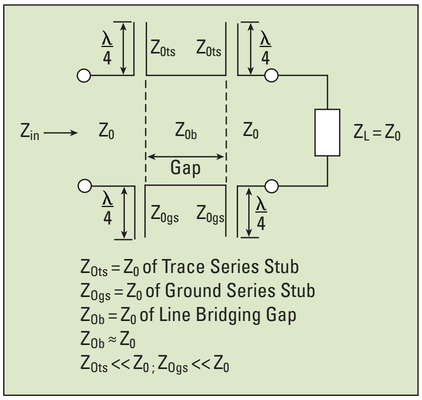

▲Fig. 4 EM-bridge simplified equivalent circuit.

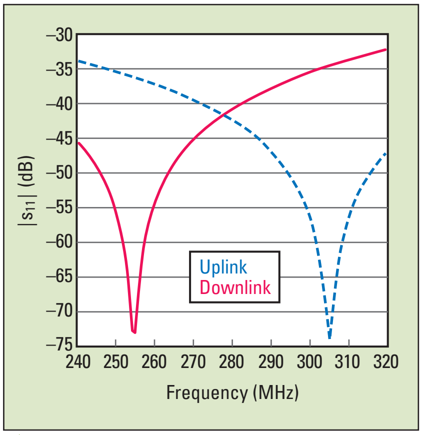

▲Fig. 5 Computed $|S_{11}|$ of the UHF satcom EM-bridges.

EM-BRIDGE SPACE APPLICATIONS

UHF Satcom

Large deployable parabolic reflector antennas are being considered for the payloads of the next generation of ultra-high frequency satellite communication (UHF satcom) systems, such as SKYNET 6. The EM-bridge technology enables deployable DRA antennas as an alternative means to form the required beam patterns. The Mathworks™ RF Toolbox™ enables a rapid analysis of the simplified equivalent circuit in Figure 4. Plots of $|S_{11}|$ and $|S_{21}|$ versus frequency are shown in ***Figures 5*** and ***6***, respectively, for EM-bridges in the uplink and downlink antennas. The computed $|S_{11}|$ and $|S_{21}|$ values are less than -45 dB and -0.0025 dB in the 30 MHz frequency bands, which are centered at 255 and 305 MHz, respectively.

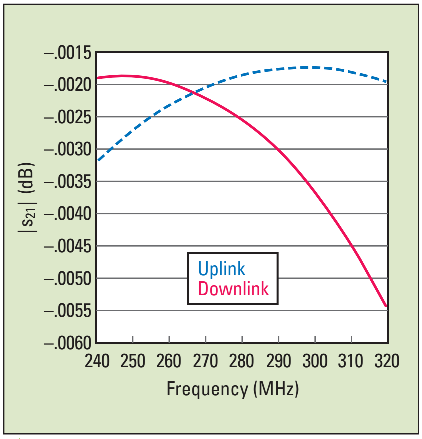

Fig. 6 Computed $|S_{21}|$ of the UHF satcom EM-bridges.

Fig. 7 UHF satcom EM-bridge breadboard.

Figure 7 is a UHF satcom EM-bridge breadboard, a first iteration design as part of the BFN required for the downlink antenna. A honeycomb structure, produced by additive manufacture (3D printing), forms a superstrate carrier to support the trace in each of the respective microstrip sections, which are mechanically connected via 3D-printed hinges.

In this EM-bridge design, beryllium copper strips are used for the flexible trace and flexible ground plane. The metal strips are mechanically secured in the first half and are free to slide between sheets of PTFE (Teflon®) in the second half of the assembly. Sheets of PTFE are also used in the first half to ensure that there is no metal-to-metal contact, avoiding a source of PIM.

When the EM-bridge is in the folded state, the beryllium copper strips store mechanical strain energy, which provides an assistive torque to aid the deployment of the antenna panel. Several EM-bridges are integrated within each of the deployable antenna panels, thus forming a sprung "piano-hinge" arrangement.

Figures 8 and ***9*** show measured $|S_{11}|$ and $|S_{21}|$ versus frequency for the

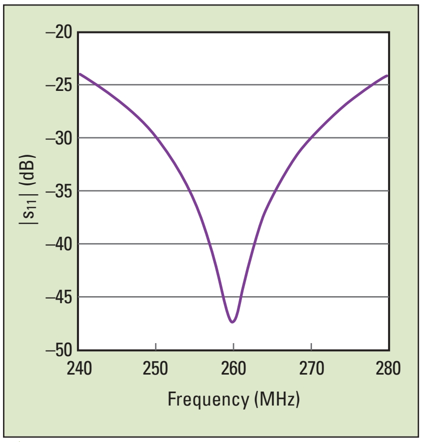

Fig. 8 Measured $|S_{11}|$ of the UHF satcom downlink EM-bridge.

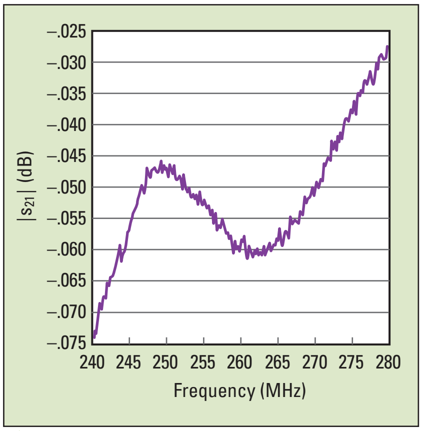

Fig. 9 Measured $|S_{21}|$ of the UHF satcom downlink EM-bridge.

first iteration of the downlink UHF satcom EM-bridge breadboard. The measured results indicate that the lengths of the flexible conductors should be increased to optimize performance at the downlink band center frequency of 255 MHz. Although the analysis of the simplified equivalent circuit provides a quick assessment of the reflection and transmission characteristics of the EM-bridge, it excludes discontinuities at the transitions of the coaxial connector test ports and the effects of evanescent modes, which account for the differences between the computed and measured results. Nevertheless, even this first iteration greatly outperforms an alternative coaxial cable assembly, both electrically and mechanically.

CubeSat Antennas

A CubeSat S-Band antenna typically uses a single microstrip patch radiating element mounted on the nadir-facing side to provide a circularly polarized radiation pattern for data link communication with ground stations. ***Figure 10*** shows a breadboard CubeSat antenna that uses EM-bridges to deploy four panels by means of the mechanical strain energy stored in the folded regions of the ground plane and to feed the deployed linearly polarized microstrip patch radiating elements.

A central phase-rotation BFN excites each of the radiating elements with the same amplitude, but with a phase difference of 90 degrees to produce a circularly polarized radiation pattern. This arrangement halves the S-Band transmitter power requirement, thus saving energy for use in on-board processing, or other mission needs.

COMSOL Multiphysics and the RF Module were used to design the BFN, the EM-bridges and the aperture-coupled microstrip patch radiating elements. ***Figures 11*** and ***12*** show measured $|S_{11}|$ and $|S_{21}|$ versus frequency for the 2.45 GHz EM-bridge, demonstrating excellent performance.

▲Fig. 10 CubeSat deployable antenna breadboard, shown stowed (a), deployed viewing the patch antenna side (b) and back, showing the antenna feed network (c).

SENSITIVITY ANALYSIS

Finite element analysis simulations are performed on the following error sources: 1) variations in the permittivity of the dielectric medium separating and insulating the flexible trace from the microstrip trace, 2) the presence of a void between the dielectric medium separating and insulating the flexible trace from the microstrip trace, 3) lateral displacement of the flexible trace with respect to the microstrip trace and 4) angular displacement of the flexible trace with respect to the microstrip trace.

To investigate these sources, simulations are performed on an EM-bridge designed to encompass the entire global navigation satellite system (GNSS) frequency spectrum (~1.1 to 1.7 GHz). The sensitivity simulations show that

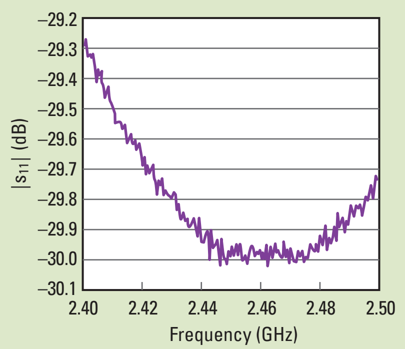

▲Fig. 11 Measured $|S_{11}|$ of the 2.45 GHz CubeSat EM-bridge.

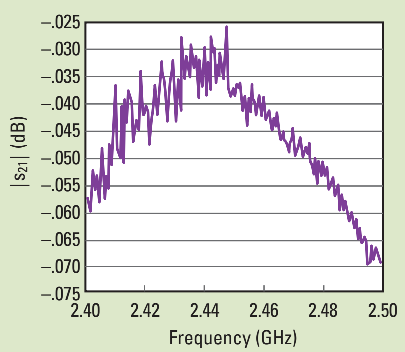

▲Fig. 12 Measured $|S_{21}|$ of the 2.45 GHz CubeSat EM-bridge.

www.islinc.com

THE FUTURE OF ADVANCED VIRTUAL RF FLIGHT TEST

IN CONTESTED/CONGESTED ENVIRONMENTS

The future RF environment for many advanced RF applications is both congested and possibly contested. Emulating this environment in field tests can be very costly and, in some cases, not feasible. ISL's RF Digital Engineering family of tools (RFView®) can greatly facilitate the entire life-cycle of advanced RF systems from development through sustainment for radar, electronic warfare (EW), ELINT, and other advanced RF applications. With ISL's RFView® hardware-in-the-loop (HWIL) solution, for the first time, actual flight hardware can be integrated into the high-fidelity mod&sim environment via RF analog or digital interface.

www.islinc.com/rfview

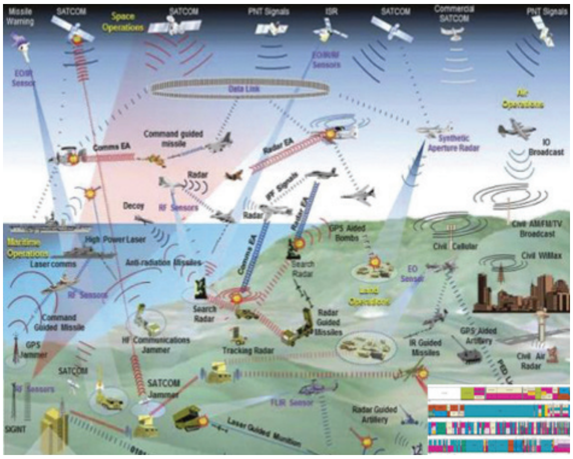

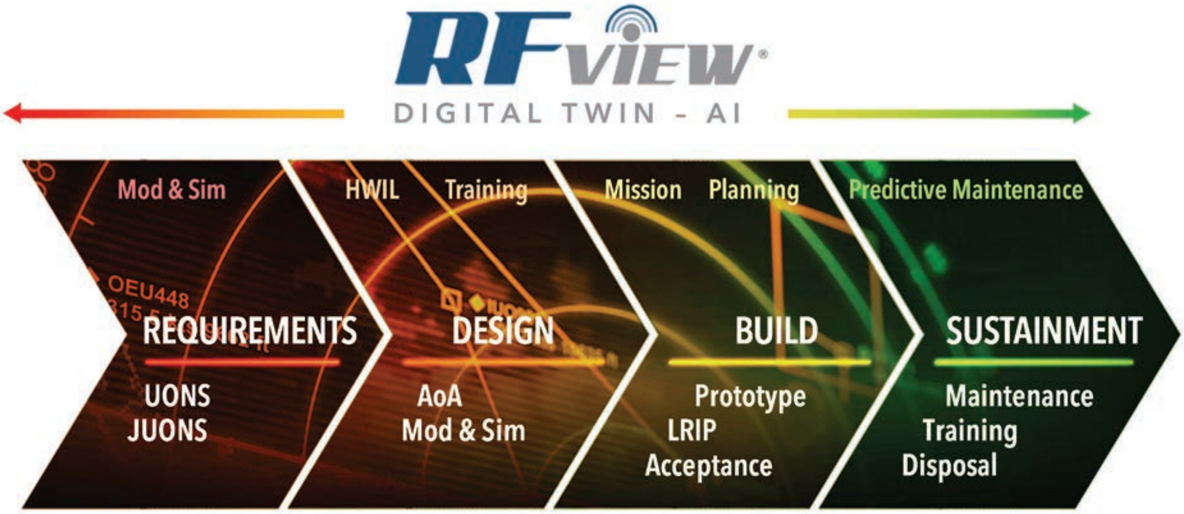

RFView®'s family of digital engineering tools support the entire product lifecycle from requirements and analysis-of-alternatives (AoAs), through design/protypting, test & evaluation (T&E), training, mission planning and sustainment. RFView® also provides a state-of-the art synthetic training environment for advanced AI machine learning (AI/ML) applications.

RFview® MODELING & SIM | RFview® HWIL | RFview® TRAINING | RFview® AI

RFVIEW® PHYSICS-BASED MOD&SIM ⟶ RFVIEW® HWIL (RTEMES) = AFRL SBIR SUCCESS STORY

the presence of a void in the parallel-plate region of the EM-bridge has the greatest effect on S-parameters, i.e., return loss and insertion loss. Nevertheless, manageable manufacturing tolerances ensure the effect of the void is not an issue.

Simulations show that radiation from the EM-bridge is essentially the same magnitude as that from a reference length of microstrip transmission line, i.e., radiation from the EM-bridge is small compared with the radiation from the BFN.

TECHNOLOGY READINESS LEVEL

Validation of an EM-bridge to technology readiness level TRL5/6 was performed by the University of Southampton in the U.K., using the test facilities at the National Oceanography Centre. The vibration tests were performed on a Bruel & Kjaer medium-force shaker and thermal testing was performed in a Weiss Technik UK temperature test cabinet.

A test specimen of the EM-bridge was subjected to a thermal and vibration test campaign to the levels required by the European Space Agency for CubeSat operations. A total of six thermal cycles were performed along with nine vibration test runs, comprising two modal surveys and a random vibration test in each of the three orthogonal axes. Deployment functional testing was performed 5x throughout the test campaign, all of which were successful, confirming that the EM-bridge had survived all the test environments.

OTHER SPACE APPLICATIONS

Other space applications for the EM-bridge include synthetic aperture radar antennas, GNSS antennas, radio telescope antennas, deployable feeds for illuminating reflector antennas, deployable booms and mechanical beam steering through ±80 degrees (eliminating a heavy rotary joint).

TERRESTRIAL APPLICATIONS

Radio Astronomy

A proof-of-concept transportable/deployable radio telescope (TDRT) was designed, built and tested during the COVID lockdowns. The DRA antenna uses an array of 120 microstrip patch radiators to form a 2.5 × 2.1 m^2 rectangular aperture in the deployed state. The H-plane linear arrays are fed by an E-plane feed network to give a Chebyshev weighting to the aperture excitation, which provides low sidelobes in the elevation plane to minimize the contribution of ground noise. A uniform aperture illumination in the azimuth plane maintains good efficiency.

The BFN uses an air substrate to eliminate dielectric loss and to reduce cost. The TDRT uses a stripline version of the EM-bridge, which has a measured insertion loss of 0.005 dB at the hydrogen line frequency of 1420.4 MHz, and thus it contributes < 1K to system noise.

In a traditional radio telescope, it is necessary to under-illuminate the parabolic reflector to reduce spill-over to the ground, which would otherwise increase the radio telescope's system noise temperature. Under-illumination reduces efficiency and degrades angular resolution.

Due to the higher efficiency and better (2x) angular resolution of the TDRT, it outperforms a traditional 3 m diameter radio telescope. The 2.5 × 1.2 m^2

flatpack form factor of the TDRT overcomes the transportation cost and handling difficulties associated with 3-m diameter dish antennas as well.

TDRT applications include outreach, university projects, teaching interferometry techniques and STEM activities for making transit observations of the sun, the galactic plane, Cygnus A and Cassiopeia A.

Curing of Composites

The current process of autoclave curing of carbon fiber composite parts in the aerospace, wind turbine and automotive industries is slow, energy intensive and expensive. Industrial closed-cavity microwave systems consume about 80 percent less energy than a comparable autoclave, with a 40 percent saving in cycle time. These systems, however, are susceptible to the generation of standing waves, causing hot and cold spots, which degrade the quality of the finished parts.[8]

The EM-bridge is an enabling technology in an agile robotic microwave system concept in which a lightweight robotic arm carries an antenna to apply microwave energy to the carbon fiber composite part. Artificial intelligence continuously interprets a thermal image of the composite part, identifying potential hot and cold spots and manages the deposition of energy to ensure that a uniform temperature distribution is maintained during curing the material.

SUMMARY

The EM-bridge is an enabling technology with the dual function of deploying antenna panels by means of stored mechanical strain energy and providing an extremely efficient transfer of EM energy across each inter-panel gap without recourse to metal-to-metal contact. Coaxial cables and related issues are eliminated from deployable structures. Passive intermodulation is minimized due to the absence of a metal-to-metal contact.

The technology readiness level has been validated to TRL5/6 for space applications, and to TRL7 in a TDRT. The EM-bridge is patented in 14 countries, with two other patents pending. There are opportunities for licensing, technology transfer and patent assignments. ■

ACKNOWLEDGMENT

The results presented are from a co-funded innovate U.K. project and activities performed through the Innovation Triangle Initiative and the Technology Transfer Program, funded by the European Space Agency.

References

1. O. Heaviside, *Improvements in Electrical Conductors, and in the Arrangement and Manner of Using Conductors for Telephonic and Telegraphic Purposes*, U.K. Patent No. 1407, 1880.
2. A. Thompson, J. Santiago-Prowald, P. Bensi and M. Aguirre, "A Stepped-Aperture Antenna Concept for Low Frequency SAR Missions," *Proceedings of the 30th ESA Antenna Workshop on Antennas for Earth Observation, Science, Telecommunication and Navigation Space Missions*, May 2008.
3. A. Thompson and M. S. Thompson, *Deployable Panel Structure for an Array Antenna*, U.S. Patent No. 8035573B2, 2011.
4. A. Thompson and M. S. Thompson, *Deployable Panel Structure*, UK Patent No. GB2455311, 2012.
5. M. Bayrak and F. A. Benson, "Intermodulation Products from Nonlinearities in Transmission Lines and Connectors at Microwave Frequencies," *Proceedings of the IEEE*, Vol. 122, No. 4, April 1975, pp. 361–367.
6. F. Arazm and F. A. Benson, "Nonlinearites in Metal Contacts at Microwave Frequencies," *IEEE Transactions on Electromagnetic Compatibility*, Vol. EMC-22, No. 3, August 1980, pp. 142–149.
7. A. Thompson and M. S. Thompson, *Deployable Radio Frequency Transmission Line*, U. K. Patent Grant GB2537885, 2017.
8. B. Nuhiji, M. P. Bower, T. Swait, V. Phadnis, R. J. Day and R. J. Scaife, "Simulation of Carbon Fibre Composites in an Industrial Microwave," *Proceedings of the 12th International Conference on Composite Science and Technology*, Vol. 34, Part 1, February 2020, pp. 82–92.

DC TO 50 GHZ

Hi-Rel Screening

For the Toughest Environments

- 50+ years of design and manufacturing experience
- Supply chain security—no EOL target
- Ceramic, plastic and bare die packaging formats
- Broad selection off-the-shelf + custom designs
- In-house upscreening for MMIC, core and wire, and LTCC components

Capable of meeting MIL requirements for:

Acceleration, fine leak, gross leak, HAST, HTOL, mechanical shock, thermal shock, and vibration. Additional screening available on request.

Mini-Circuits®

The Continuing Evolution of Radar, From Rotating Dish to Digital Beamforming

Jon Bentley and Jerome Patoux
Analog Devices, Wilmington, Mass.

Radar was a system only possible to conceptualize at the end of the 19th century, after the Scottish mathematician and scientist James Clerk Maxwell described the classical theory of electromagnetic radiation and German physicist Heinrich Rudolf Hertz first used an antenna to prove the existence of the electromagnetic waves predicted by Maxwell's equations. But the first real radar detection was in the early 20th century by Christian Hülsmeyer, a German physicist, with the equipment he called the Telemobiloscope. At the time, the equipment could detect the presence of a target but not its distance or speed.

The first radar system that was operational occurred a few decades later, and radar techniques progressed significantly during World War II, mostly for military applications. From there, radar continuously evolved to adjust to new threats and targets in diverse environments and to counter attempts to disable detection, such as jamming or to avoid detection, by more sophisticated targets.

The first modern radars used a rotating dish and high power amplifiers based on traveling wave tube technologies. They evolved with more sophisticated use of RF principles, such as Doppler effects, to estimate the range and speed of the target. German engineer and physicist Karl Ferdinand first showed phased array transmission in one direction in 1905. By World War II, American physicist Luis Alvarez had already developed rapidly steerable phased array radars; however, rotating dishes remained the main technology for several decades. In the 1980s, phased array systems were introduced, but not widely adopted due to size and little practicality, as they required data transfer to a computer to process the data and recreate the target. Phased array techniques only became practical with advances in electronics, largely highly integrated semiconductors that enabled the solid-state arrays developed at the end of the 20th century (see ***Figure 1***).[1]

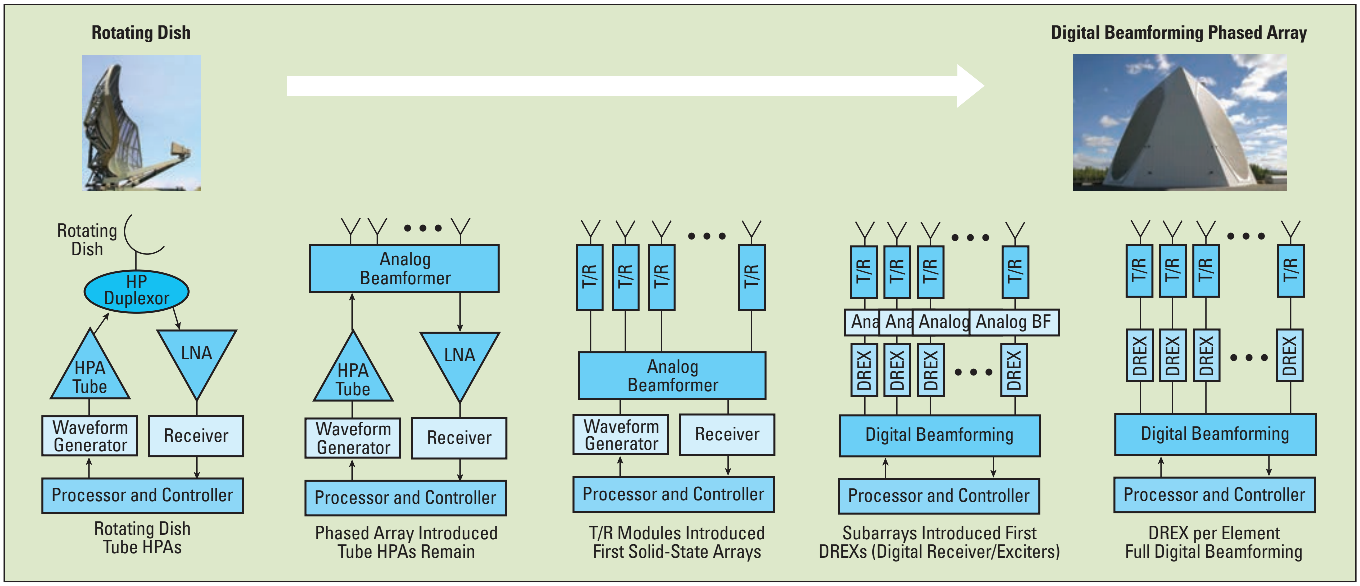

Fig. 1 Evolution of radar, from the rotating dish to the active phased array with digital beamforming.

ERA OF THE PHASED ARRAY

Active electronically scanned array (AESA) radar has enabled significant improvements in radar capabilities since the late 1990s, and they continue to evolve to larger and more sophisticated arrays. AESA radars use a "phased array" antenna: an array of antenna elements or radiators, each provided with a signal having a different phase shift, which creates one or more beams. The beams result from the constructive or destructive interference of the waves from each element: in-phase signals superpose and amplify in a particular direction. Designed with enough elements appropriately spaced, the beam can have a high gain main lobe in one direction and low sidelobes. By switching antenna elements or changing the relative phases among the elements, the beam can be steered to concentrate the energy in a different direction.

Modern radars resist jamming by changing the frequency of each pulse or using a chirp technique, which spreads the frequency across a wide bandwidth during a single pulse. Elevation and azimuth beams with Doppler processing of the received signals is the basis of 3D radar, where the location of an object and its speed are determined with a more accurate identification of the object—differentiating a bird from a drone, for example.

The evolution of radar is driven by the need to detect and quickly respond to more sophisticated threats. New threats harder to detect are always emerging, such as smaller targets like drones or drone swarms, hypersonic weapons and stealth fighters. The evolution also reflects the need to support air traffic control, weather formation monitoring, collision avoidance and autonomous cars, a few of many new applications. The common themes for improved performance are greater range, finer resolution, lower detection threshold, precise spatial envelope control, multiple frequency band coverage and mission convergence. Achieving these requirements relies on disruptive architectures and advanced electronics.

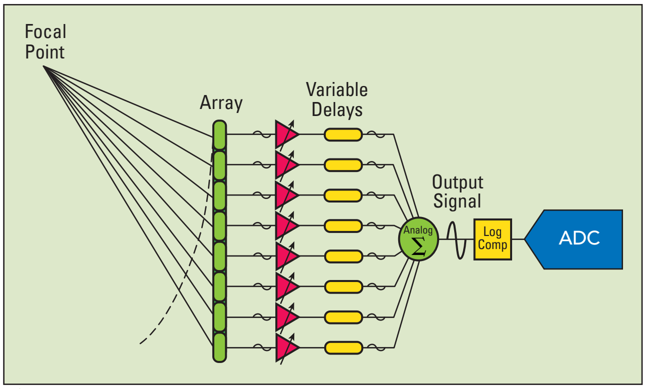

Fig. 2 Phased array using analog beamforming.

BEAMFORMING

AESAs use three beamforming techniques to create and manage multiple antenna beams: analog, digital or hybrid. The best approach depends on the tradeoffs to accomplish the system's mission. Today, the most popular architecture for advanced radar is a combination of analog and digital beamforming.[2] These hybrid architectures employ distributed mixed-signal converter nodes feeding RF beamforming subarrays. The trend is toward more mixed-signal nodes feeding smaller RF subarrays, as RF sampling moves toward the individual elements.

At higher frequencies and wider bandwidth, data throughput requires increased processing by the baseband processors, which increases power consumption. To mitigate this, the system can compromise converter performance by choosing lower bit resolution and power dissipation. However, this often yields undesirable signal quality, system performance and flexibility. So the tradeoff between digital processing bandwidth and acceptable cost and power will pace the adoption of wideband digital beamforming (DBF) at every element. However, large investments in semiconductor technology to improve data converter bandwidth and power efficiency will ultimately make wideband DBF at every element possible.

Radar performance improved dramatically with the transition from mechanical to AESA, and comparable improvements in performance will occur with the move from analog-to-digital beamforming as future systems become fully digital. With more converter channels located closer to the array elements, array gain improves the signal-to-noise ratio, although front-end adaptive RF signal conditioning is required to preserve the dynamic range in "blocker" environments. DBF enables flexibility: adjustments to a mission and supporting different missions, configured with system software. This multi-mission capability will enable system size and weight to be tailored for space-constrained systems, such as airborne.

Most current radar architectures in service today rely on analog beamforming (see ***Figure 2***). The traditional analog approach uses analog phase shifters to make fine adjustments for beam steering, realized with circuits that are practical and relatively inexpensive. The analog signal chains from the antenna elements are combined and converted to digital for processing. With larger arrays, the elements are usually grouped into subarrays, with multiple analog-to-digital converters in the system. These subar-

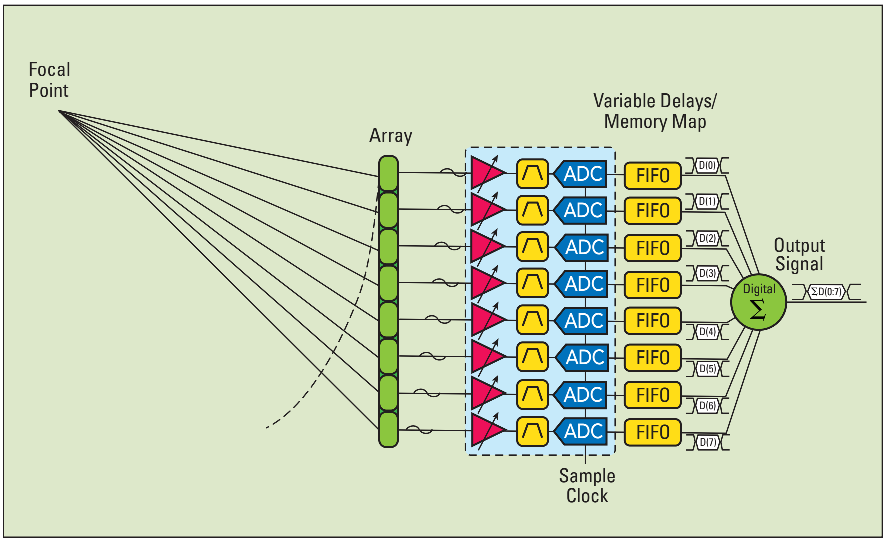

Fig. 3 Phased array with digital beamforming.

TABLE 1

DIGITAL BEAMFORMING TRADEOFFS

Benefits	***Challenges***
Flexibility • Digitally Applied Time Delays	Synchronization and Calibration
Multiple Simultaneous Beams • Faster Search • Improved Maximum Likelihood Estimation • Tracking Multiple Targets	LO Clock and DC Power Distribution
Adaptive Array Processing • Jammer Suppression	Hardware and SWAP-C Thermal Management
Noise Improvements	Dynamic Range (Noise, Linearity) Volume of Digital Data

rays currently provide the most practical implementation on the path to DBF: a hybrid architecture that significantly reduces the number of digital channels, associated data processing and power consumption.

As noted, the architecture offering the most flexibility and best performance, albeit with challenges, is full elemental DBF. With this architecture, a data converter processes the data from each element's front-end module (see ***Figure 3***), eliminating the analog beamforming layer. With DBF, many beams can be simultaneously formed and steered, the number limited only by digital signal processing (DSP) capacity. This architecture brings flexibility and arguably better reliability, with the attendant challenges from the amount of digital data to be processed, synchronizing multiple channels and minimizing the size, weight, power and cost (SWAP-C) of the array (see ***Table 1***).[3] Reviewing the benefits of DBF shown in the table:

- Digitally applied time delay overcomes pointing errors caused by analog phase shifters. Applying phase and amplitude digitally overcomes many of the errors caused by analog circuits.
- Multiple simultaneous receive beams enables an area to be searched more quickly. The maximum likelihood estimation of detecting a specific target is improved with additional processing techniques applied to the beams.
- Adaptive array processing can suppress jamming by nulling interfering sources. Increasing the number of digital channels increases the number of interfering sources that can be eliminated, although practical implementation of this capability has not yet been realized.
- Noise and dynamic range can be improved by combining distributed receiver channels with multiple waveforms.

However, DBF poses significant challenges, particularly with practical implementation:

- Synchronization and calibration of the multiple waveform generators and receiver channels is challenging, including channel-to-channel drift

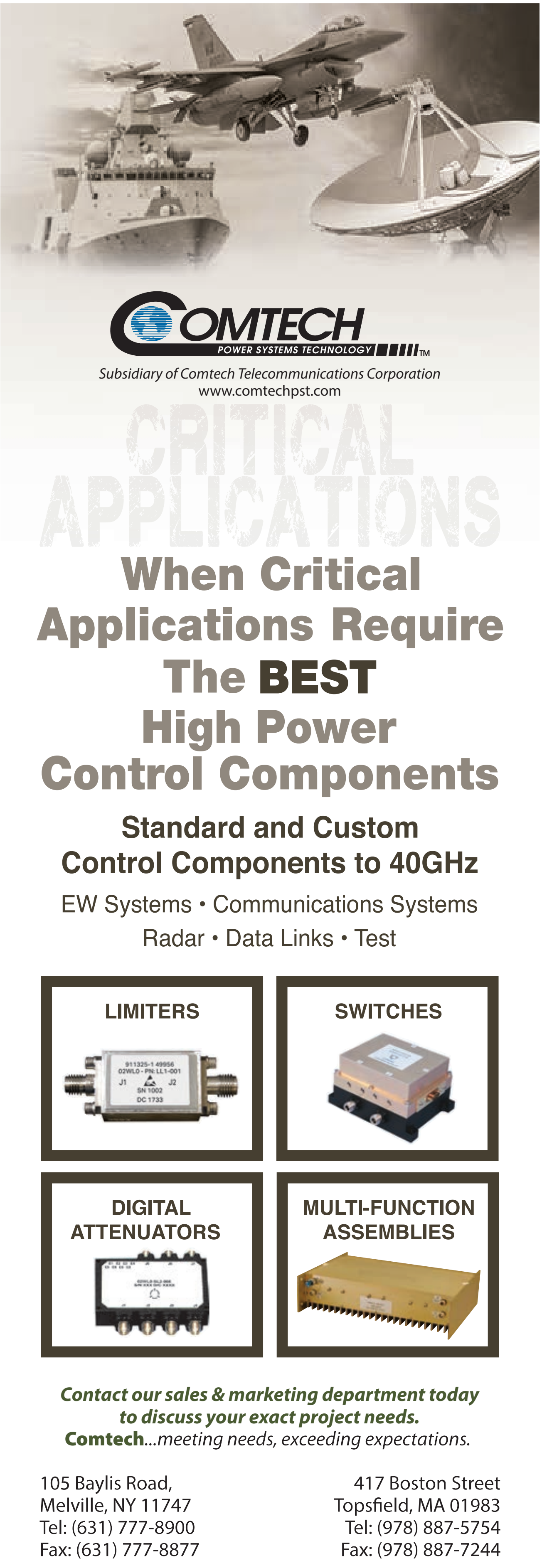

and calibration when first powered on.

- Routing the local oscillator and DC power distribution throughout the array can be complicated and difficult to implement.
- Hardware implementation and associated SWAP-C are increasingly challenging. The hardware cost, power consumption and thermal dissipation increase because signal processing is required at each element. The element spacing—a half wavelength or less to avoid grating lobes in the array—shrinks at higher frequencies, posing size constraints as each signal chain must fit within the area allotted to the element. The array thermal design must comprehend the added electronics at each element and the spacing constraints.
- Achieving the system dynamic range requires low noise and excellent linearity converters.
- The volume of digital data to be processed in real time taxes the capabilities of current processors, particularly with increasing radar bandwidth and using adaptive algorithms to suppress jamming.

Assessing these tradeoffs, DBF can be a cost-efficient architecture for L- and S-Band systems when used to achieve the highest performance with multiple simultaneous beams and ensure flexibility. However, as the operating frequency increases into X-Band and beyond, current semiconductor technology will not support the data rates and desired SWAP-C for full DBF architectures to be viable. Hybrid architectures are the most feasible AESA implementation, offering a practical combination of attributes.

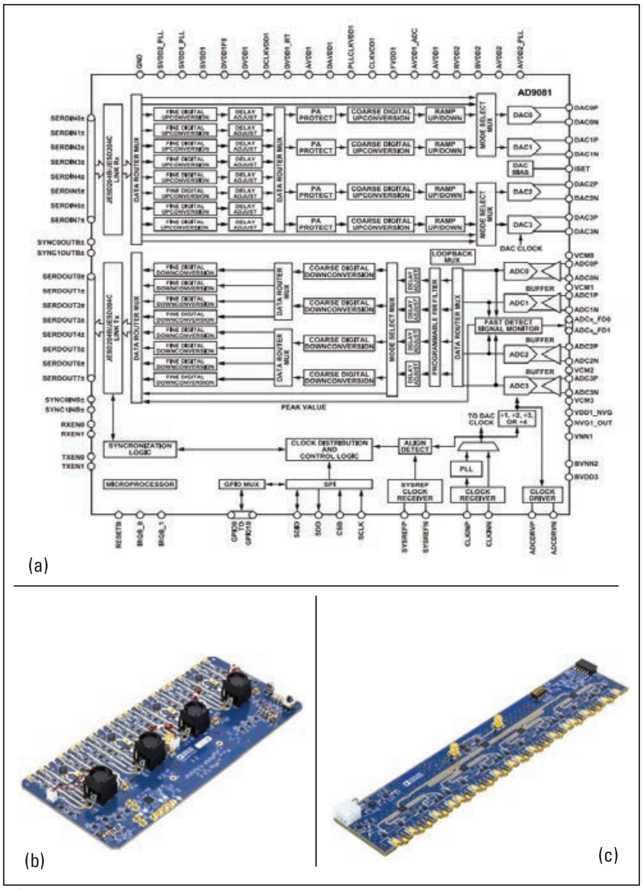

Fig. 4 AD9081 MxFE functional diagram (a) QUAD MxFE prototyping system (b) and 16 Tx/16 Rx calibration board (c).

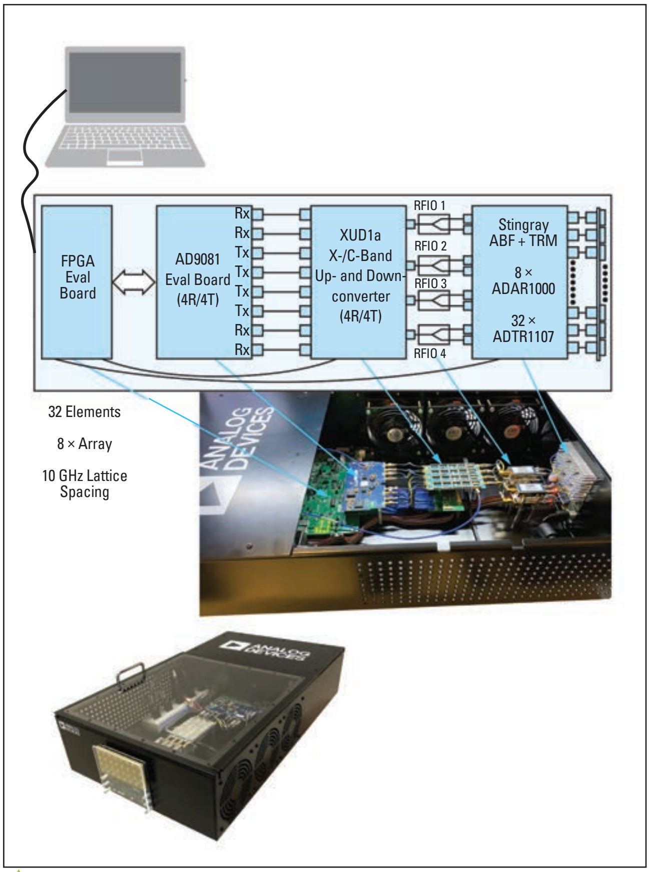

Fig. 5 X-/Ku-Band phased array prototyping system.

DEVELOPMENT PLATFORMS

Development platforms with high performance mixed converter front-ends (MxFE) can aid the design and implementation of a DBF array. They reduce engineering development and time to market for radar designers who need performance, optimized SWaP-C and high reliability. Using the high sampling rates of the latest generation data converters, the platforms support development of direct sampling receivers, shifting the design emphasis from the RF to embedded DSP on the converter. The DSP offloads the processing previously done by the FPGA, which maximizes the efficiency of system processing. These MxFE platforms can be used alone or as part of larger subsystem and system development solutions.

Analog Devices has developed a development platform for L-, S- and C-Band DBF phased arrays. The reference design has 16 transmit (Tx) and 16 receive (Rx) channels and contains four AD9081 MxFE direct RF sampling transceivers (see ***Figure 4a***). The MxFE's comprise RF front-ends, DSPs, high speed data interfaces and support circuitry including clocking, filtering and power. The Quad MxFE prototyping system is an evaluation platform for multi-chip synchronization, system level calibration, beamforming and other signal processing algorithms. A separate 16 Tx, 16 Rx calibration board (see Figure 4c) is also available to support developing system calibration algorithms to demonstrate power-up phase determinism as well as system performance improvements from a multichannel architecture. The Quad MxFE platform shows how noise and spurious improvements can

be achieved when combining channels, with measurements showing approximately 10 dB improvement in noise density and improved spurious performance, resulting in better dynamic range with the combined channel architecture.[4]

This platform helps AESA designers meet several needs: 1) validating new beamforming technology for phased array radar, 2) offering a reference design for a complete system solution and 3) providing a software platform for customers to develop proprietary IP before their own custom hardware is available. This platform represents a multichannel system environment that engineers can work with to extrapolate to larger phase arrays. All these features help reduce time to market.

The element spacing at L- and S-Band makes it feasible to fit the electronics of a direct RF sampling architecture into every element using current transceiver technology and direct sampling converters. As noted, this becomes challenging as the radar's frequency moves to X- and Ku-Band. Here, hybrid architectures are more practical.

For X- and Ku-Band frequencies, Analog Devices developed a second prototyping platform (see ***Figure 5***), which uses a 4:1 beamformer IC (BFIC) to reduce the receiver/exciter count by four and provide additional space for the RF electronics. The platform is a testbed for demonstrating hybrid beamforming and implementing system calibrations and beamforming algorithms.[5] It integrates eight, four-channel analog BFICs (ADAR1000) and 32 Tx/Rx modules (ADTR1107), one for each ADAR1000 channel. This is followed by RF up- and down-conversion between L-/S- and X-/Ku-Band (ADXUD1AEBZ), which feeds an AD9081 MxFE evaluation board. The platform also has a snap-on antenna board with 10 GHz lattice spacing.

SUMMARY

This article described the evolution of radar and the analog and DBF architectures used with AESAs. The benefits of full elemental DBF and the practicalities limiting their implementation have been compared to the hybrid subarray, which provides a practical option when DBF is not feasible.

Development platforms for both hybrid and DBF arrays facilitate the evaluation of disruptive concepts and technologies and shorten development cycles. Analog Devices has developed two such platforms for systems from L- to Ku-Band. They can help designers gain system insights that lead to better designs and shorter development time.■

References

1. R. Cariou, "Le Traitement Du Signal Radar: Détection et interprétation de l'écho radar," Dunod, web: www.dunod.com/sites/default/files/atoms/files/9782100577972/Feuilletage.pdf
2. P. Delos, "An interview with Analog Devices Discussing RF Electronics for Phased Array Applications," 2019.
3. G. Stimson, H. Griffiths, C. Baker and D. Adamy, "Advantages of Digital Beamforming," *An Introduction to Airborne Radar*, Third Edition, Institute of Engineering and Technology, 2014, pp. 133.
4. P. Delos, M. Jones and H. Owens, "A Measurement of Distributed Direct Sampling S-Band Receivers for Phased Arrays," pp. 5-7
5. P. Delos, S. Ringwood and M. Jones, "Hybrid Beamforming Receiver Dynamic Range Theory to Practice," pp. 1-2.

TESTING & SCREENING EEE-INST-002 COMPLIANT SPACE COMPONENT

IN-HOUSE SPACE UPSCREENING

Launch Prep

Mil-Spec or Equivalent Qualifications

- 30+ years of space-level screening and testing
- 7500+ components and custom capabilities
- EEE-INST-002 compliant workflows

Standard Capabilities

Burn-in, thermal cycling and shock, vibration*, radiographic inspection*, destructive physical analysis (DPA)*, mechanical shock, hermeticity with accompanying acceptance test procedure (ATP).

*While Mini-Circuits performs most of its testing and upscreening in-house, we use specialist partners for a limited selection of tests.

Military-Grade 5G Pushes Coexistence Boundaries with Radar and Satellite

Nancy Friedrich
Keysight Technologies, Santa Rosa, Calif.

Coexistence grows as radar and satellite systems use the same or nearby frequency bands with 5G, creating the need to assess coexistence and mitigate potential interference as new 5G networks are deployed.

5G cellular promises new applications for military and government communications, including high-definition video; 3D or augmented reality; ultra-reliable, low latency communications; and massive machine-type communications. These capabilities will enhance intelligence, surveillance and reconnaissance, command and control and supply chain procurement and logistics. With new bands specified for 5G, however, coexistence with existing services poses a dual-edged challenge. Radar and satellite systems using the same or nearby frequency bands can reduce the capacity in 5G systems, while 5G can impair radar performance and damage satellite ground stations. Only by assessing and mitigating the potential impact among 5G, radar, satellites and other systems, can all these coexisting systems deliver their intended performance.

For example, in the U.S., the spectrum between 3.1 and 3.5 GHz is shared between federal and non-federal radio location services, with federal services having the primary allocation or priority. Similarly, both C-Band and extended C-Band frequencies are used for fixed satellite services and 5G, with potential interference issues between them.

WHAT IS COEXISTENCE?

Coexistence refers to the situation when two or more signals have the right to occupy the same or nearby spectrum. Usually, one of the services has priority. Radar typically has priority over 5G. If there's a conflict, the 5G transmitter must shut off or move to a different frequency. With satellite systems, 5G interference can be severe: receiver front-ends in ground stations are highly susceptible to interference from high-power 5G base stations.

5G operating bands are currently grouped into frequency ranges below 6 GHz (FR1) and mmWave spectrum around 28 or 39 GHz (FR2). To provide the bandwidth for 5G, new operating bands have been allocated, with most of the initial deployments in the 3.6 to 3.8 GHz and 26 to 27.5 GHz bands and more bands planned. The 5G services in these bands must coexist with the downlink range used by satellite ground stations, from 3.4 to 4.2 GHz, and the military satellite bands from 27.5 to 29.5 GHz and the fixed satellite service downlinks from 37.5 to 40 GHz.

Some of these coexistence issues are unique to the U.S., according to a report published by the Congressional Research Service.[1] The re-

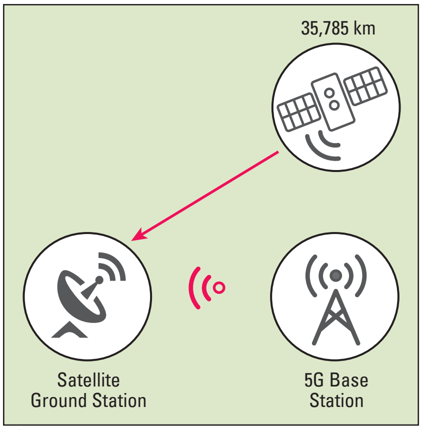

Fig. 1 5G base stations can interfere with the sensitive receivers in satellite ground stations if they use nearby spectrum.

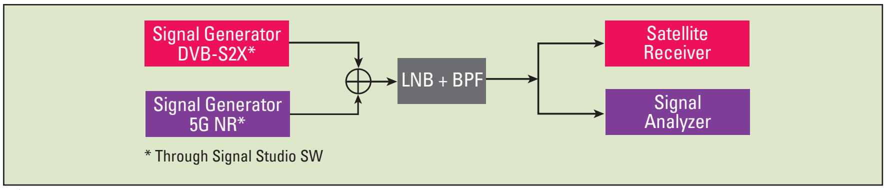

Fig. 2 Test setup for assessing the coexistence performance of a satellite receiver in the presence of 5G signals.

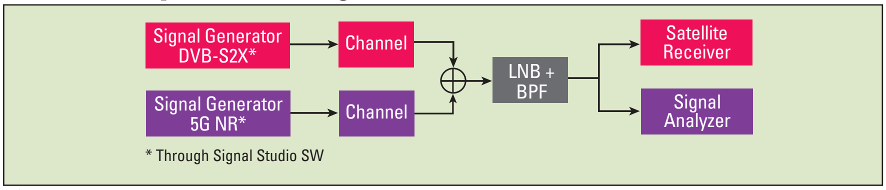

Fig. 3 Emulators add channel effects to coexistence lab testing.

port says, "Although Department of Defense (DOD) uses certain mmWave frequencies for high-profile military applications such as advanced extremely high frequency satellites that provide assured global communications for U.S. forces, it extensively uses sub-6 frequencies—leaving less sub-6 availability in the United States than in other countries. The Defense Innovation Board (DIB) advised DOD to consider sharing sub-6 spectrum to facilitate the build-out of 5G networks and the development of 5G technologies used in the sub-6 band."

The solution to these challenges is spectrum sharing, which makes coexistence conflicts likely.

IMPACT OF COEXISTENCE

Coexistence is a concern when two or more signals have the right to occupy similar spectrum. However, the signals don't have the right to interfere with each other. For communication systems, coexistence issues may degrade the service by decreasing the data throughout or totally disrupting the link, which will create a financial problem from higher operating costs and lower revenue. Ensuring coexistence can be challenging, as the respective systems have different functions, designs, signal characteristics and locations.

Several approaches can be used to minimize potential problems: The frequency regulator, such as the FCC, can define guard bands and frequency spacing between services. Services can be required to maintain minimum distances from transmitters. As an example, the minimum separation between shipborne radars and terrestrial 5G base stations can be defined. Transmit power can be restricted—indoors versus outdoors, for example—and antenna type, angle and elevation defined to restrict the level and direction of the radiated power.

Arguably the most challenging is the coexistence of 5G with satellite systems (see ***Figure 1***). Satellite ground stations have sensitive RF front-ends designed to receive the low-level signals from satellites orbiting at 35,785 km. The low noise amplifier in the receiver can be overloaded by nearby terrestrial sources, such as the much higher-power 5G signals from base stations—both operating in C-Band.

HOW TO MEASURE

The potential of coexistence interference can be assessed in the lab using a tailored test system that enables adjusting parameters such as signal strengths, center frequency, frame structure, modulations, etc. (see ***Figure 2***). In the figure, which shows the satellite-5G example, the signal generator provides the satellite DVB-S2X signal, using software to create the digital video that is downloaded to the hardware.

Some common metrics are used to assess signal quality and the impact of coexistence. One is error vector magnitude (EVM), with units of percent or dB. This measures the difference between a measured symbol and a reference (theoretical) symbol in I and Q. As the demodulation of a signal in the receiver becomes poorer, the EVM increases. A perfect signal will have 0 percent EVM.

The 3GPP standard for 5G details the EVM requirements for various modulations, with the modulation changed to maximize what the channel can support. With lower noise and distortion, the channel can support higher-order modulation, which transmits more symbols in a given time. QPSK is the lowest order and accommodates the highest EVM. As the channel quality improves, the modulation steps to 16-, 64- and 256-QAM.

As 5G is deployed, coexistence will remain a prominent concern, extending from consumers to militaries and governments as private 5G networks are rolled out on bases, in government facilities and conflict zones. In addition to satellite networks, the coexistence risk will need to be assessed for military radar and non-5G communications systems.

Typically, coexistence problems cause service disruptions or performance degradation. Often, however, the consequences remain unknown until a problem occurs. To avoid surprises, a best practice is to prototype scenarios in the lab and look for coexistence issues. Once systems are deployed, 24/7 monitoring in the field can help identify sporadic issues and lead to resolution.

DIGITAL TWINS

Digital twin technologies can be used to plan for and simulate coexistence scenarios. Scalable channel emulators can support up to 64 channels and 400 MHz bandwidth and will cover mmWave bands with external hardware for up- and down-conversion. Emulators work with various software packages to implement 3GPP 5G and custom channel models. These systems can simulate Doppler shift and delay in the channel, which adds more realism to lab tests (see ***Figure 3***).

When designing and deploying a new 5G network, a "crawl-walk-run" approach is recommended to identify and mitigate coexistence issues (see ***Figure 4***). Begin with software to create a digital twin and model the current transmitters and receivers and see the effects from the new system. Hardware

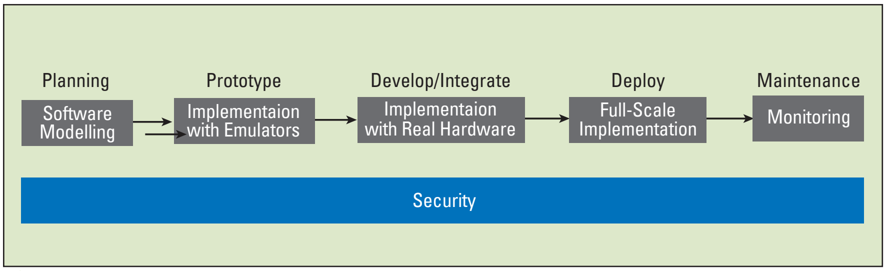

Fig. 4 Recommended development flow, beginning with software modeling.

prototyping follows, using available devices and systems with commercial off-the-shelf (COTS) hardware emulators to mimic a small-scale system in a lab or anechoic chamber. COTS emulators enable the frequency, bandwidth and power to be varied, which may identify corner cases where coexistence issues arise.

Outside the lab, plan field testing with deployed 5G, tactical or public safety networks and radar or satellite ground stations. Field tests can measure transmit power, signal strength, EVM, throughput with modulation and MIMO, latency, block error rate and beamforming quality. In some cases, drones can be used for fly testing to determine 3D coverage, measuring signal strength, signal quality and throughput.

SUMMARY

To assure the performance of a military or government 5G network, coexistence must be planned and assessed up and down the stack from layer 1 to 7. Testing must span from the chipset to the full network and include multiple RF channels, carrier mechanisms, data protocols and waveforms, such as 3GPP 5G New Radio, pre-5G and custom OFDMA. When assessing the impact of coexistence issues, consider these questions:

- How will the interfering waveforms interact?
- How much suppression is required, in-band and out-of-band?
- How much guard band is necessary?
- What metrics should be used to assess impact?
- Is lab testing sufficient or should it be supplement with field test?

With the ability to assess the coexistence of networks and services, issues can be identified and resolved to achieve reliable communications. Many approaches are available from the lab to the field to assess potential issues that may degrade the performance of military and government systems. Once deployed, ongoing monitoring will reveal new coexistence issues, safeguarding the 5G network and, more importantly, the individuals depending on its performance. ■

Reference

1. Congressional Research Service, "National Security Implications of Fifth Generation (5G) Mobile Technologies," April 5, 2022, Web: sgp.fas.org/crs/natsec/IF11251.pdf.

Heterogeneous Integration Enables Direct Conversion RF to Digital Processing at the Tactical Edge

Tony Trinh
Mercury Systems, Andover, Mass.

By integrating commercially developed processing and high speed digitization at chip scale, new microelectronic devices are advancing the capabilities of defense systems.

The 21st century electronic battlefield is rapidly evolving, this is especially true for systems operating within the RF spectrum. We face adversaries using stealthy techniques and deploying advanced weapons. Countering those techniques and weapons requires extremely low latency responses from intelligent, adaptive applications. Practically, that requires a "quantum leap" in RF processing at the tactical edge.

While an injection of new technology is needed, it is not sufficient. Long-term success requires a continual process moving innovation from commercial electronics into defense systems. Sustained success also requires the technology innovations delivered to defense programs come from trusted and secure sources. Security threats from semiconductor tampering are like those from software breaches and are more difficult to detect.

Fortunately, a dynamic answer to the RF edge processing challenge comes from an adaptation of system-in-package (SiP) technology: the RFSiP. An RFSiP combines multifunction processing with the latest analog-to-digital and digital-to-analog converter (ADC/DAC) capability. Establishing technology partnerships among industry leaders, a high performance mixed-signal SiP is feasible at one-fifth the size of a small, printed circuit board (PCB).

NEXT-GEN RADAR AND EW

Electronic warfare (EW) systems are moving to ever-higher levels of complexity. Radars now use pulse widths lasting only nanoseconds. In addition to single frequency bursts, frequency hopping signals are across the RF spectrum. Other radar countermeasures include dynamically changing waveforms and patterns. To reliably detect these stealthy signals, EW systems must use higher sampling rates to continuously monitor the expanding bandwidths and frequency spectrum. 5 GSPS is no longer considered a high sampling rate; the bar is 50 GSPS.

For the EW system, detection is just the first step. It must be followed by effective responses created with low latency. This capability requires real-time processing for signal analysis and countermeasure generation, tightly coupled with the ADCs and DACs. The new generation of applications requires high data conversion rates with powerful processing to keep up with incoming signals.

One illustrative example is radar spoofing, where the EW system detects, alters and replays the radar's pulses to create false and deceptively moving targets. This only works when the response latency is low, so the emitter radar does not perceive a time lag in the return pulse. In addition to maximizing rapid pulse detection and response, EW effectiveness depends on generating high spectral density across multiple channels, making high fidelity as critical as low latency.

Active radars have similar requirements. For example, a multifunction active electronically scanned array puts tremendous demands on embedded processing, as the radar must dynamically shift from surveillance of long-range threats to tracking and jamming short-range targets. The mode flexibility required can only be achieved when all available data is processed in real time.

New application areas add additional processing requirements. Cognitive radar applies artificial intelligence (AI) techniques to extract information about a target from a received signal, then uses the information to improve transmit frequency, waveform shape and pulse repetition frequency. Similarly, cognitive EW applies AI to identify patterns in the detected data to develop effective responses. Both cognitive radar and cognitive EW must execute their AI algorithms in near real-time. To do so, graphics processing units (GPUs) are added to RF processing, complementing the FPGAs that perform signal analysis and creation. Using many core processors is not the answer. While they can execute billions of instructions per second, they are not designed for low power consumption. They also need mixed-signal ICs and FPGAs for the RF interfaces, so a complete system requires a PCB.

Until recently, these multiple processing methods required distinct semiconductors, often assembled in a multi-board system. For RF applications, moving data from the ADC and DAC to centralized computing challenges data fidelity and latency. The current generation of converters are generating data bandwidths that overwhelm system interconnects, with transmission times that don't support low latency radar and EW responses. This forces substantial data reduction before the central processor. To overcome these limitations, system architectures must move away from a centralized computing model to processing where the data is—at the tactical edge. Fortunately, new packaging technology helps solve that challenge.

INTEGRATION AND SWaP

RF edge processing requires multiple, tightly integrated functions working together to capture, analyze and manipulate a data stream in real time. Latency requirements favor ADCs and DACs that implement direct digital conversion. Efficient processing of the digital bit stream requires pipelined operations by some combination of FPGAs, GPUs and general-purpose processors. The components must connect via high bandwidth interconnects with low latency and be supplied with the required power. Everything must be assembled within a package small enough to be near the antenna.

The technology solution for RF edge processing comes from the commercial electronics market, which continually drives process and packaging technology with hundreds of billions of dollars in R&D investments every year. The mantra of commercial electronics is increasing functionality while miniaturizing, reducing power consumption and costing less. The much smaller defense industry can capitalize on the commercial investment by adopting and adapting new technologies to the unique requirements of defense applications. By leveraging commercial technology, the defense electronics industry can convert the basic research and invention cycle to adopting, adapting and maintaining the technology advantage over adversaries.

The commercial microelectronics industry is adopting heterogeneous integration (HI) of SiP technology. This capability assembles small semiconductor functions, called chiplets, on a small piece of Si. Each chiplet performs a specific function, such as the RF front-end, data conversion, digital signal processing, digital I/O or the dozens of functions in a mixed-signal data flow. Every chiplet is an individual semiconductor—even as complex as multicore processors. The chiplets can be combined and connected in many ways, each combination has a high performance subsystem or system optimized for an application. HI enables the multifunction, pipelined dataflow to be packaged into a SiP, much smaller than a PCB.

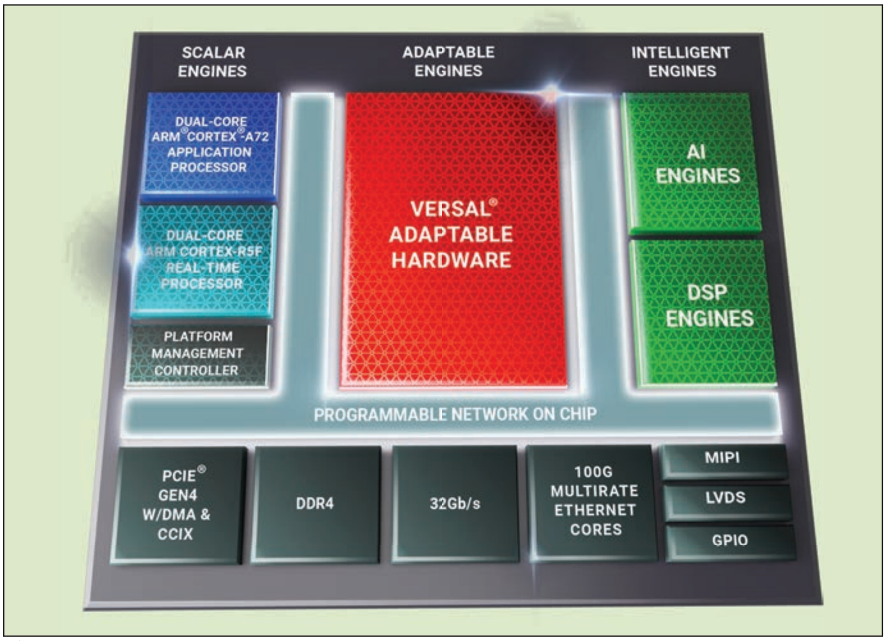

▲ Fig. 1 AMD-Xilinx Versal AI Edge ACAP functional block diagram.

Fig. 2 Mercury Systems' custom microelectronics packaging center in Phoenix.

HI SiP FOR RF EDGE PROCESSING

A SiP created by Mercury Systems for RF sensor data processing will illustrate the concept and capability. The RFS1140 is one of a family of RFSiPs reflecting the practice of adopting technology from the commercial world and tailoring it for defense systems.

Processing Chiplet

The RFSiP's processing chiplet is a new semiconductor architecture, an adaptive compute acceleration platform (ACAP). The Versal® AI Edge ACAP from AMD-Xilinx is a heterogeneous processor, fabricated with 7 nm technology and incorporating three compute engines, much more than an FPGA or MPSoC. Each ACAP includes scalar processors, programmable logic and vector processors, all connected by a high bandwidth network-on-chip (see ***Figure 1***).

Multiple compute engine types are designed into the ACAP because no single style of processing can optimally perform all the tasks involved in a sophisticated edge application. Scalar processors, functioning like traditional CPUs, are ideal for complex decision-making and control. The AI Edge ACAP has four of these: two low-power ARM® Cortex®-R5F real-time processors and two full-power domain Cortex-A72 cores, supported by a system memory management unit. Programmable logic, also referred to as adaptable engines, adds flexibility to handle diverse and computationally demanding algorithms. Included are FPGA structures, with 1.5x the lookup tables (LUTs) of a Virtex chip, as well as programmable I/O and a customizable memory hierarchy of block RAM and UltraRAM. Vector processors, called intelligent engines, are optimized for advanced signal processing such as linear algebra and matrix math, which are well suited for 5G wireless systems and AI inference. The chip contains two types: DSP engines, which function like traditional digital signal processors, and AI engines, like advanced GPUs, which comprise vector processors for fixed and floating-point operations, a scalar processor and dedicated program and data memories. A single Versal ACAP chip provides 400 AI engines, 1968 DSP engines and more than 900,000 FPGA LUTs.

Data Converters

The processing in the RFSiP is combined with the extremely fast ADCs and DACs of the Electra-MA from Jariet Technologies. Each RFSiP has two of these low-power transceivers, yielding four ADC receive channels and four DAC transmit channels. All operate to 64 GSPS and can directly digitize frequencies through 36 GHz and operate in the first Nyquist zone to 32 GHz.

Power Converter

A Ferric power converter is a die power regulator that supports high current density. Three of these are used within the RFSiP, taking a single supply voltage and generating all the voltages needed by the other components. This power management architecture simplifies the RFSiP's integration into larger systems.

SiP Integration

The AMD-Xilinx, Jariet and Ferric chips and 4 GB of DDR4 memory are integrated on an organic substrate in a 50 x 50 mm^2 area. A high bandwidth interconnection, including a dedicated bus, moves data between the Jariet data converters and the Versal ACAP. This advanced RF capability is delivered in a package optimized for SWaP-C. The individual die are attached using thermal compression bonding and assembled in Mercury Systems' dedicated microelectronics facility in Phoenix (see ***Figure 2***).

ENABLING RF EDGE APPLICATIONS

Equivalent to multiple PCBs in currently deployed systems, the RFS1140 is a single, small package SiP. It enables tactical edge processing in very constrained spaces and lowers overall system cost. With direct digitization at extremely high sampling rates, the RFSiP enables systems to detect and monitor stealthy signals. By eliminating the down-conversion to an intermediate frequency, direct digitization achieves extremely low latency, even at 64 GSPS data rates. The RFSiP supports the processing requirements for tracking potential targets, including those moving at hypersonic speeds, and generates low latency responses. The AMD-Xilinx Versal ACAP in the SiP has an extensive set of heterogeneous math processing engines with both the processing power and flexibility needed by AI-based cognitive radar and EW applications.

Through close collaboration with the technology teams at Mercury, AMD-Xilinx, Jariet and Ferric, the SiP concept was adopted and rapidly adapted for RF edge processing. The SiP design approach enables future generations of semiconductor technology created by commercial R&D to rapidly upgrade defense systems while maintaining the same physical form factor.

TRUSTED SOURCING ESSENTIAL

Advanced microelectronics can give our forces a technical advantage on the battlefield. A key element to maintain that advantage is ensuring the trust and security of the microelectronics supply chain. The risks of a compromised supply chain are clear. Semiconductor tampering is extremely difficult to detect and can include hidden "backdoors" and remotely operated "kill switches." While many cybersecurity discussions focus on software threats, semiconductor vulnerabilities may pose greater risks to DOD programs.

Scalable manufacturing operations within the U.S. are essential to the rapid deployment of secure microelectronics for defense programs. Organizations committed to the delivery of trusted solutions start with investments in processes and manufacturing capacity, followed by DMEA accreditation. Employing standardized design architectures and interfaces reduce technical and schedule risks and the likelihood of cost overruns, as well as ensuring trust and security in the supply chain.

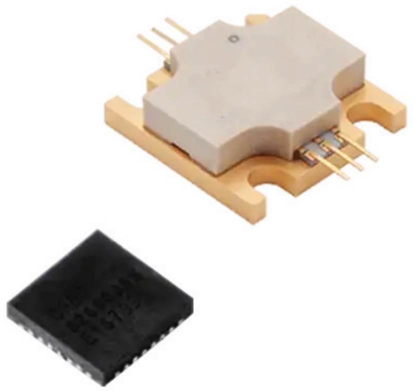

Choosing the Right GaN Package for Long Pulse Radar Modes

Wolfspeed
Durham, N.C.

A key objective when designing radar, electronic warfare and communications systems is to achieve the best range possible within the limited space available. RF GaN technology is best suited to provide the required power density, as well as high temperature and high voltage operation, for demanding applications. In many pulsed radar systems, the carrier frequency of the pulses is constant, but the pulse repetition interval (PRI) and the pulse width vary. A longer PRI and low duty cycle offer better unambiguous measurement range or range resolution. However, lower PRI, higher duty cycle and greater pulse width deliver more power per pulse and, therefore, longer range.

Modern marine and air surveillance radars continually change operating modes by changing PRIs and pulse widths to suit the different requirements of target search, acquisition and tracking. Increasingly, defense and commercial applications prefer multimode radar, adding communication and electronic warfare capabilities to active electronically scanned array (AESA) systems. AESAs with thousands of transmit and receive elements for beam steering add to the power density demand from designs.

The output power of a GaN HEMT power amplifier (PA) varies with pulse width and duty cycle (see ***Figure 1***). The output power decreases as duty cycle or pulse width increase, assuming everything else in the test remains the same. The effect of duty cycle and pulse width on output power must be considered during the PA design.

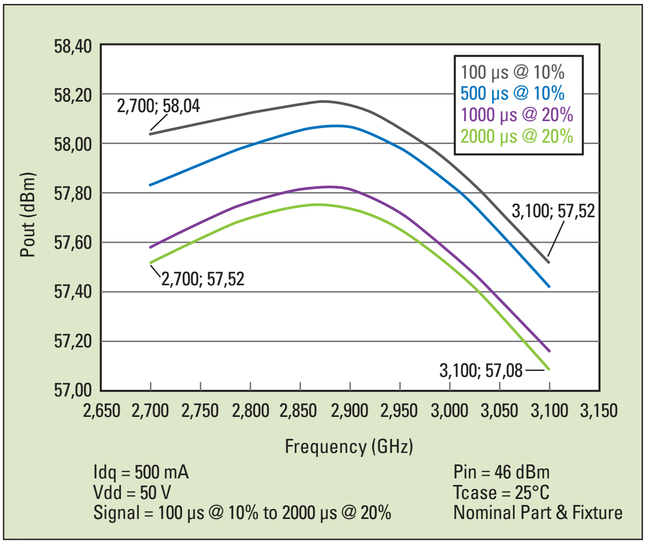

Fig. 1 Output power vs. pulse width and duty cycle.

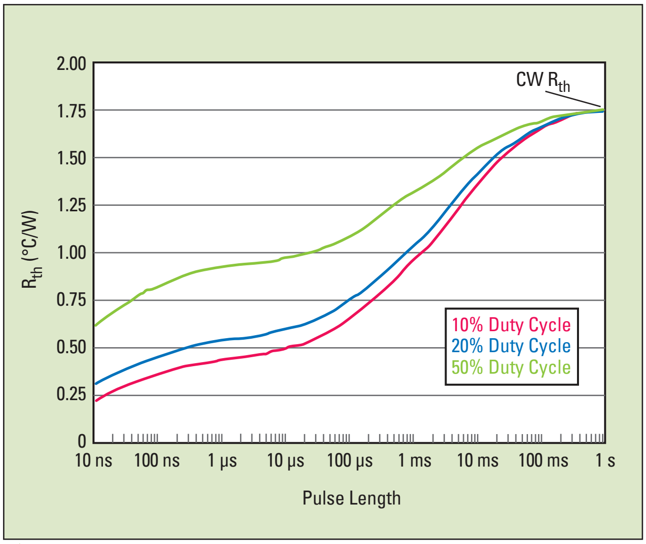

Fig. 2 R_{th} vs. pulse length and duty cycle.

THERMAL RESISTANCE

The variation in output power and power-added efficiency reflects the variation in the junction-to-case-thermal resistance, $R_{\theta jc}$, of the RF GaN device with pulse width and duty cycle. $R_{\theta jc}$ limits the maximum power dissipation and output power before the device reaches its maximum junction temperature, T_j. Although $R_{\theta jc}$ increases with increasing pulse width and duty cycle (see ***Figure 2***), it approaches a fixed value for large pulse widths irrespective of the duty cycle. This ultimate value is the CW thermal resistance.

When designing a multimode radar, the correct values of $R_{\theta jc}$ must be used, as device reliability or lifetime (mean time to failure), is determined by the power dissipated and resulting junction temperature. The peak junction temperature determines design feasibility and what thermal management solutions are needed. The peak junction temperature is proportional to the case temperature, the dissipated power and the thermal resistance, as given by Equation 1:

$$T_j = T_c + \left(P_{diss} \times R_{\theta jc}\right) \quad (1)$$

To determine T_j, we must determine $R_{\theta jc}$ and P_{diss}. Thermal resistance (in °C/W) is calculated as the difference in temperature (ΔT in °C) between two surfaces—here the junction and case—that support a fixed <

$$R_{\theta jc} = \frac{\Delta T}{P_{diss}} \text{ in } °C/W \quad (2)$$

In Equation (1), T_c can be measured using infrared microscopy; however, measuring T_j to calculate ΔT is more complex. A physical model created using a software tool such as ANSYS and a finite element method simulation is used to correlate the case temperature measurement to the junction temperature.

To find P_{diss} it is necessary to calculate P_{dc}:

$$P_{dc} = 100 \times \left(\frac{P_{out}}{\text{Efficiency}}\right) \quad (3)$$

and from this:

$$P_{diss} = P_{dc} + P_{in} - P_{out} \quad (4)$$

Calculate the peak junction temperature by inserting these values into Equation (1).

QFN MOUNTING OPTIONS

Designers often choose surface-mount packages such as QFN because they result in a compact PA stage. However, these are typically designed for applications with pulse widths between 100 and 500 µs and duty cycles less than 20 percent. The trend toward multimode and longer pulse operation increases the power dissipation, requiring consideration of package constraints to ensure adequate thermal management.

A common thermal solution for QFNs has been using plated-through vias filled with conductive epoxy that connect the top-surface device mounting layer through the RF ground layer to the chassis (see ***Figure 3***). Via arrays are typically used for power dissipation up to 30 W, with pulse widths under 500 µs and duty cycles less than 20 percent. A high density of vias is needed to dissipate the additional heat generated by new, longer pulse radar designs. Another option is to use a Cu coin embedded in the printed circuit board (PCB). While this may require a thicker multi-layer board to support the coin, with higher processing cost, it performs significantly better thermally for long pulse designs that approach CW (see Figure 2).

Using the same device with a fixed P_{diss}, thermal simulations were run using the via array and embedded coin board designs. In both cases, while the device thermal resistance is independent of the device mounting configuration, the case-to-fixture thermal resistance is not. ***Table 1*** shows a remarkable difference in the fixture temperature, $T_{fixture}$, needed to achieve a desired case temperature, T_{case}. To maintain T_{case} = 85°C with a CW signal, the via array requires an unrealistic fixture tem-

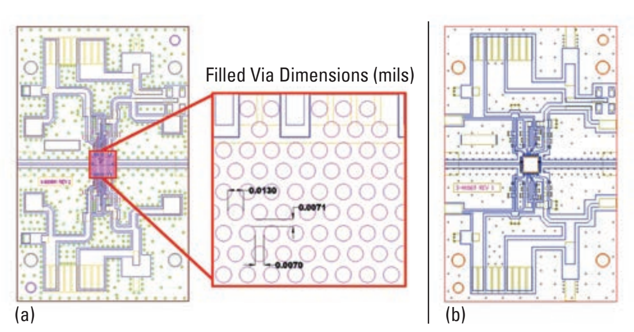

Fig. 3 Via array (a) and embedded Cu coin (b) thermal paths.

perature of –52°C, compared to 29°C with the embedded Cu coin.

For high-power aerospace and defense applications, metal-ceramic packages that can be mounted directly on the heatsink are recommended. The device thermal resistance, R_{th}, of the ceramic package is higher than that of the surface-mount option. Unlike metal-ceramic packages, SMT options require the PCB to be included in the thermal path. Since the PCB thermal resistance could be of the same order as the device, it can add a significant temperature differential to the cooling requirements.

PAs FOR RADAR

Wolfspeed offers a 25 W GaN MMIC PA for radar systems in the 5.2 to 5.9 GHz range. The 28 V PA is available in both 5 x 5 plastic QFN (CMPA5259025S) and 440219 metal-ceramic flange (CMPA5259025F) packages. To maintain the same 85°C case temperature, the fixture temperature should be 23°C for the QFN "S" model and 70°C for the metal-ceramic "F" model (see ***Table 2***).

Wolfspeed
Durham, N.C.
www.wolfspeed.com/products/rf/

TABLE 1

THERMAL ANALYSIS OF VIA ARRAY AND EMBEDDED COIN DESIGNS

Cooling Method	*Signal Condition*	$T_{fixture}$ (°C)	$T_{case(peak)}$ (°C)	$T_{j(peak)}$ (°C)	*Junction to Case* R^{th} (°C/W)	*Case to Fixture* R^{th} (°C/W)
Via Array	500 µs @ 10%	72	90.3	147.6	0.478	0.15
Via Array	500 µs @ 20%	58.8	89.7	147.6	0.483	0.26
Via Array	1 ms @ 10%	72	96.2	156.3	0.501	0.20
Via Array	1 ms @ 20%	58.8	94.8	155	0.502	0.30
Via Array	**CW**	**-51.6**	**85**	**146.6**	**0.513**	**1.14**
Embedded Coin	500 µs @ 10%	79.4	89.9	147.7	0.482	0.09
Embedded Coin	500 µs @ 20%	73.7	89.4	148.4	0.492	0.13
Embedded Coin	1 ms @ 10%	79.4	94.7	156	0.511	0.13
Embedded Coin	1 ms @ 20%	73.7	93.5	155.4	0.516	0.17
Embedded Coin	**CW**	**28.7**	**85**	**150.3**	**0.544**	**0.47**

TABLE 2

THERMAL COMPARISON OF GAN PA PACKAGE OPTIONS

Device	$T_{fixture}$ (°C)	T_{case} (°C)	$T_{j(max)}$ (°C)	P_{diss} (W)	*Package* R^{th} (°C/W)	*Fixture to Case* R^{th} (°C/W)	*Effective* R^{th} (°C/W)
CMPA5259025S	23.3	85	155.2	32.4	2.17	1.90	4.07
CMPA5259025F	70	85	172.4	29.3	2.99	0.51	3.49

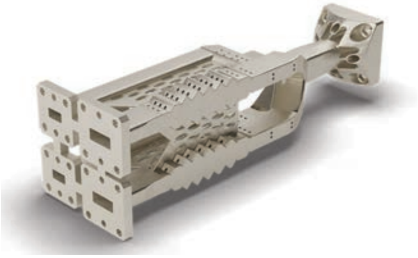

Ka-Band Dual-Polarized Diplexers

SWISSto12 SA
Renens, Switzerland

3D printing has revolutionized the production of passive waveguide and antenna components. This manufacturing technology enables the combination, for the first time, of low fabrication cost, short fabrication cycles, reduced mass and high performance in a monolithic assembly. If the building material is a metal alloy, the fabricated device is already RF conductive and can withstand demanding environmental conditions such as found in space, naval or airborne applications. 3D printing is now accepted by the aerospace and electronic warfare industry and its use is expected to keep growing in the coming years.

▲ Fig. 1 Basic DPD with ports on the bottom (a) and a multi-beam GEO cluster (b).

SWISSto12 pioneered the development of metal 3D printed passive components. The company developed a proprietary chemical treatment to reduce the surface roughness of the printed parts. Without this treatment, the surface finish is too rough, which results in high insertion loss. The SWISSto12 process multiplies conductivity by a factor of 3x to 5x, depending on the material selected for the finish. SWISSto12 offers two finishing options: raw aluminum and copper-silver.

KA-BAND DUAL-POLARIZED DIPLEXERS FOR SATCOM

Ka-Band dual-polarized diplexers (DPDs) are five-port waveguide devices used in satellite communications to feed an antenna aperture, typically a feed horn, with two circular polarizations (RHCP and LHCP) and two frequency bands. The uplink is around 30 GHz, the downlink around 20 GHz. A DPD requires precise manufacturing to meet Ka-Band performance requirements, yet the satcom industry is pushing for cost reduction because these systems often target the final user or are integrated in multi-beam arrays in quantities of hundreds. SWISSto12's 3D printing process simultaneously meets both requirements: performance and cost.

Examples of SWISSto12 DPDs are shown in ***Figure 1***. The DPD consists of two diplexers to combine and separate the two frequency bands and one dual-band septum polarizer for converting linear to circular polarization. Using 3D printing to fabricate these building blocks achieves the required fabrication tolerances and reduced cost. Further cost optimization is possible since

TABLE 1 TYPICAL SWISSTO12 DPD SPECIFICATIONS				
	Option 1		Option 2	
	Downlink	Uplink	Downlink	Uplink
Frequency Band (GHz)	19.2 – 21.2	29 – 31	17.7 – 21.2	27.5 – 31
Return loss (dB)	> 20	> 20	> 20	> 20
Insertion loss (dB)	< 0.25	< 0.2	< 0.25	< 0.2
Polarization	LHCP & RHCP	LHCP & RHCP	LHCP & RHCP	LHCP & RHCP
In-Band Isolation (dB)	> 25	> 25	> 25	> 25
Cross-Polarization Discrimination (dB)	> 28	> 28	> 28 (≈75% of Band) > 25 (Full band)	> 28 (≈75% of Band) > 25 (Full band)
Isolation Tx/Rx (dB)	> 90	> 80	> 90	> 80
Port	WR42 or WR51	WR28 or WR34	WR42 or WR51	WR28 or WR34
Mass (g)	75			
Size	Footprint: 35 x 35 mm, Height: < 150 mm Optional Footprint: 25 x 25 mm			

the devices can be produced in quantity, up to 50 per printing run. 3D printing of these DPD building blocks enables customization of the interfaces and footprint without significant non-recurring engineering.

SWISSto12 currently offers DPD options for two downlink and uplink bands (see ***Table 1***). Each DPD is available with a square or circular flange, and each has two size options: standard (35 mm x 35 mm footprint) and compact (22 mm x 22 mm). ***Figure 2*** shows the return loss, in-band isolation and isolation between transmit (Tx) and receive (Rx) measured at the rectangular ports of four identical samples (option 1 in the table). The performance is comparable to conventionally fabricated DPDs and highly repeatable, since the parts do not require any assembly. ***Figure 3*** shows the cross-polarization discrimination of a DPD with a monolithically integrated antenna. Highlighting this point, other components such as the antenna or a monopulse tracker can be added to the DPD without significantly increasing fabrication cost.

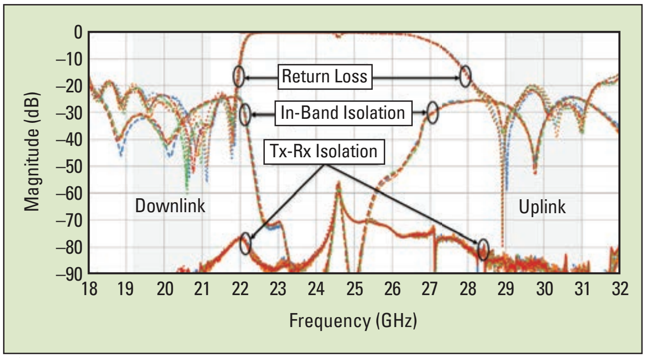

Fig. 2 Measured return loss, in-band isolation and Tx-Rx isolation of four identical DPDs (option 1 in Table 1).

THE SWISSto12 PROCESS

SWISSto12's process comprises the following steps:

- 3D printing using selective laser melting followed by thermal cycling for stress relief
- Basic post-processing: cleaning and machining the mechanical interfaces
- Surface treatment: chemical polishing for roughness reduction and plating. SWISSto12 products are always chemically treated for roughness reduction and insertion loss improvement. The basic process provides competitive loss, while the copper-silver finish process provides the lowest possible loss.
- Assembly and RF test. Assembly may include helicoils, sealing or integration into a more complex system. Various tests can be performed, depending on customer requirements.

SWISSto12 products, including DPDs, are currently found on multiple platforms, from large GEO satellites to small CubeSats in space and navy ships on Earth. The 3D fabrication process has been qualified to MIL and GEO standards and complies with the European Cooperation for Space Standardization laser powder bed fusion techniques for space applications, issued in 2021.

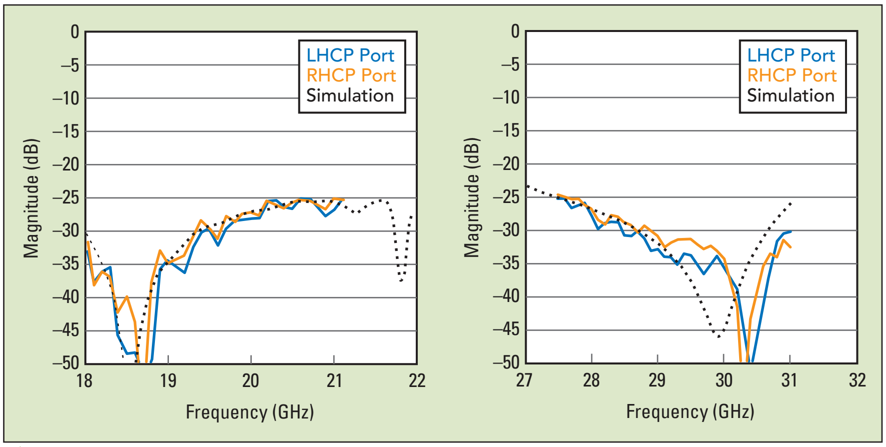

Fig. 3 Measured cross-polarization of the DPD with integrated feed horn (option 2 in Table 1).

SWISSto12 SA
Renens, Switzerland
www.swissto12.com
sales@swissto12.ch

Modular HTOL Burn-In System Offers Low-Cost Per Channel

With the increasing complexity of RF systems, more components are becoming part of the RF block diagram. While reliability concerns focus on the power amplifier, any components subject to high RF drive must be qualified. The modular architecture of the Accel-RF HTOL Burn-In System provides the flexibility to qualify multiple device types at a low-cost per channel and minimal lab footprint.

The rack configuration has all power supply control and power control unit (PCU) modules embedded and controlled through the LIFETEST software and system controller. Auto biasing for gate/base and drain/collector levels, maximum allowable levels and on/off sequencing are programmable in the PCU setup. Each device being tested is independently sourced and controlled, with temperature control and monitoring done independently and individually per device channel. Temperature setting and control are managed through the LIFETEST software with continuous updates and control possible.

The HTOL Burn-In System enables high channel capacities with an expandable tray design, using chilled water to remove heat. The system design offers a range of DC bias options, from high-resolution, low-power supplies for small devices—GaAs HBT or SiGe—to high current supplies for high-power RF devices—GaN or LDMOS. Numerous frequency bands and RF drive levels are supported.

Founded in 2003, Accel-RF helped enable industry adoption of compound semiconductor transistors and MMICs in space, military and commercial markets. It supplies reliability test systems to top-tier semiconductor and aerospace/defense users in the U.S., Europe and Asia. Accel-RF is the only provider of fully integrated, scalable, turnkey systems that provide dynamic, multi-dimensional, RF, DC and temperature testing with a single platform.

Accel-RF
San Diego, Calif.
www.accelrf.com

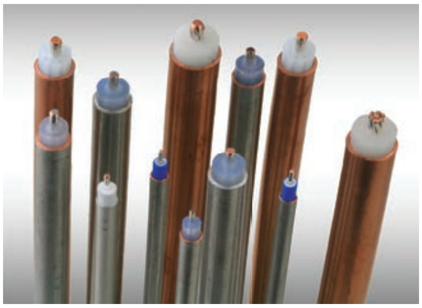

Semi-Rigid and Flexible Cable Family

EZ Form has one of largest offerings of semi-rigid cables for military and aerospace programs, with 27 active semi-rigid cables qualified to MIL-DTL-17 and listed on the Qualified Products List of the U.S. Defense Logistics Agency. This extensive range of semi-rigid cables includes copper and aluminum jacketed versions in 0.020, 0.034, 0.047, 0.086, 0.141 and 0.250 in. diameters, available unplated or with silver, tin or tin-lead plating. Except for the 0.25-in. diameter cable, the upper frequency range is 20 GHz; the 0.25-in. diameter is rated to 18 GHz. These semi-rigid cables are easily bent to a finished shape, maintaining its set after bending and making it well-suited for either automated bending equipment or hand forming.

EZ Form also offers more flexible cables with performance comparable to the MIL-C-17 semi-rigid family. The EZ-Flex 401, 402 and 405™ series handles like RG flexible cables and offers double shielding, low leakage, low VSWR, lower weight, flexibility and durability. This family includes 50 and 75 Ω options with outer diameter from 0.086 to 0.25 in. Frequency coverage extends to 60 GHz with the smallest diameter (0.086 in.) cable.

A third family of cables offered by EZ Form is the EZ-Flex Formable™, which is easily shaped by hand. The cable has a copper-tin composite outer conductor which provides the same 100 percent shielding as the solid jacket of a semi-rigid cable, yet it is easily bent by hand. The EZ-Flex Formable cables can be used with the same type of solder-on connectors used with semi-rigid cable, providing similar RF performance without complicated manufacturing.

EZ Form Cable
Hamden, Conn.
www.ezform.com/mil-dtl-17-qpl/

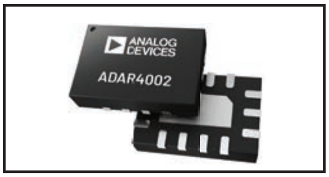

ADAR4002 0.5-19 GHz Broadband Bi-Directional Single-Channel TTD

VENDORVIEW

The ADAR4002 is a low-power broadband single-channel true time delay unit (TDU). The TDU covers the frequency range of 0.5 to 19 GHz. The TDU has two programmable modes; 508 ps with 4 ps resolution and 254 ps with 2 ps resolution. The built-in 6-bit DSA has 31.5 dB of attenuation range. The ADAR4002 is designed to provide flexible digital control through either a SPI interface or a shift register to enable daisy chaining multiple chips together. The ADAR4002 contains memory for 32 beamstates. The memory combined with on-chip sequencers, allows a fast memory advance via the UPDATE pin.

Analog Devices Inc.
www.analog.com/en/products/adar4002.html

Cernexwave Coaxial Circulators and Isolators

VENDORVIEW

Cernexwave's coaxial circulators and isolators are an ideal solution for broadband or narrowband signal control at a wide range of power levels. They can be tailored to the exact frequency and power you need while maintaining low insertion loss and high isolation. They can also customize the input and output ports to fit perfectly in your system. The model COIU2U40916-01 coaxial isolator has a frequency range of 225 to 400 MHz with 16 dB isolation and can handle over 50 W of power.

Cernexwave
www.cernexwave.com

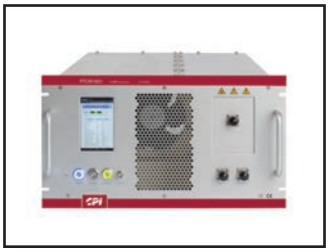

Instrumentation Amplifiers That Deliver Power for EMC HIRF Testing

VENDORVIEW

TMD Technologies Division of Communications & Power Industries (CPI) launches higher-power K- and Ka-Band traveling wave tube modular instrumentation amplifiers. The new PTCM1017 and PTCM1027 amplifiers feature higher gain and efficiency performance when compared to solid-state amplifiers. With frequency coverage of 18 to 26.5 GHz and 26.5 to 40 GHz, both amplifiers offer power output exceeding 100 W CW and can also be pulsed using an internal grid modulator. The amplifiers are optimized for applications including EMC, radiated immunity, communications, electronic warfare, radar and RF component testing.

Communications & Power Industries LLC (CPI)
www.cpii.com/product.cfm/16/165

USA-Built GaN SSPAs for EW: 2 to 18 GHz, 8 to 100 W

Engineered specifically to meet the stringent requirements imposed by many modern system designs, CTT's GaN power amplifiers, built in the U.S., perform a wide range of functions making them ideal for applications in cutting-edge multifunction EW systems. Three models include: AGM/060-5056, 2 to 6 GHz, 100 W power out; AGX/0218-3946, 2 to 18 GHz, 8 W power out; AGX/0318-4656, 3 to 18 GHz, 40 W power out. TTL on/off options and rack-mount configurations are also available. CTT can provide replacements for amplification products formerly produced by Amplica, Avantek Inc., Celerity and Watkins-Johnson Company.

CTT Inc.
www.cttinc.com

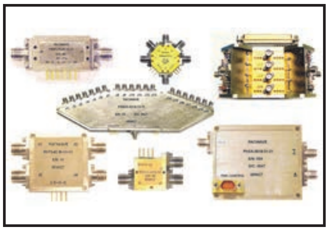

High-Power RF PIN Diode Switches & Assemblies

These 10 MHz to 40 GHz RF PIN Diode switches and assemblies ensure accurate test and measurement of multiple RF components used in radar systems, electronic warfare systems, ground-based communications systems and more. All units feature integral TTL and field-replaceable connectors for easy removal so units can be dropped into designs to interface directly with pins, saving considerable space. Single pole switches are available from one to 24 throws.

dB Control
www.dBControl.com

Unprecedented Power Across the Ka-Band

VENDORVIEW

Increase your radar's accuracy with this GaN-based HPA that delivers 8 W of power through the operating frequency band. Leverage more power without additional size and weight—this HPA comes in a compact, robust, MIL-STD-810F rated package. If your goal is to develop a truly powerful radar system, ERZIA delivers the performance and reliability you need.

ERZIA
www.erzia.com/products/hpa/734

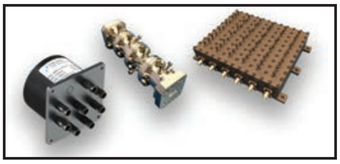

High Performance Passive Components

VENDORVIEW

Exceed Microwave provides custom high performance passive microwave component designs up to 110 GHz for defense, space and commercial applications. Exceed Microwave is AS9100 certified and ITAR registered, providing high-quality, high performance passive components. They provide various types of designs, each with its own unique values and are designed and made in the U.S. Many of Exceed's designs offer extremely high Q factor, allowing very low insertion loss and high-power handling.

Exceed Microwave
www.exceedmicrowave.com

Exodus 26.5-40 GHz, 200 W SSPA

VENDORVIEW

Exodus Advanced Communications' 26.5 to 40 GHz, 200 W SSPAs are another industry first from Exodus. Designed for high field level EMC testing, Mil-Std 461(RS103) standards as well as other high-power applications. Exodus Model AMP4066B-LC is a 12U design providing outstanding power/gain flatness, forward/reflected power monitoring in both dBm and Watts, VSWR, voltage/current and temperature sensing for superb reliability and ruggedness. Unprecedented reliability compared to TWT's, 53 dB gain including gain control, and -20 dBc harmonics. 10, 20, 40, 60 and 100 W versions available.

Exodus Advanced Communications
www.exoduscomm.com

2-18 GHz 15 W High Gain Solid-State Broadband High-Power Amplifier

VENDORVIEW

MIcable announced the new 2 to 18 GHz, 15 W high gain solid-state broadband high power amplifier MPA-020180S42. With state-of-the-art GaN design technology, it has higher saturated output power while keeping higher P1dB and better linearity and can adapt to a variety of different signal modes such as continuous wave, pulse, wide instantaneous bandwidth signal, high-order modulation signal, etc.

Fujian MIcable Electronic Technology Group Co., Ltd.
www.micable.cn
sales3@micable.cn

2-18 GHz Reference Design Featuring HL9333 Harmonic Down-converter

HYPERLABS is proud to announce its newly redesigned 20 GHz harmonic down-converter IC packaged in a 4 mm QFN package. Boasting 18 GHz RF bandwidth and optimized for LO sampling rates from 100 MHz to 2.5 GHz, the HL9333 features excellent linearity, low noise and improved RF-IF conversion response that is considerably flatter than the previous generation HL9313 harmonic mixer. The HL9333, shown here in a 2 to 18 GHz reference design, is ideally suited for use in Nyquist folding receiver and other under-sampled broadband receiver systems.

HYPERLABS
www.hyperlabs.com/product/hl9333/

Rugged to the Core

iNRCORE has over 70 years of experience of customizing, designing and manufacturing military-grade magnetics, including pulse transformers, passive delay lines and active delay lines. These components are designed to comply with requisite military and industrial standards, and play a key role in supporting crucial platforms used by all branches of the armed forces. The team at iNRCORE brings the experience and expertise needed to provide customers with reliable solutions, regardless of production volumes. iNRCORE operates from AS9100-certified manufacturing facilities located in Bristol, Pa., and China.

iNRCORE
https://inrcore.com/about-us/

Insulated Wire Inc.

Insulated Wire (IW) serves a broad range of both military and commercial markets. These include telecommunications, data links, satellite systems, airborne electronic warfare and counter measures, missile systems, UAV applications, avionics and instrumentation, fire control systems, medical electronics and geophysical exploration.

Insulated Wire
https://iw-microwave.com/wp-content/themes/iw-microwave2017/img/IW-catalog2022.pdf

MILITARY AND AEROSPACE

COMPANY SHOWCASE

UK Designed and Manufactured Low Loss and Semi-Rigid RF and Microwave Cable Assemblies

Intelliconnect (Europe) Ltd, a specialist manufacturer of RF, waterproof and cryogenic connectors, can specify, design and manufacture custom RF and microwave cable assemblies, with a two to three week turnaround time for most projects. Applications include medical, satcom, military, aerospace, space, general microwave communications, test and measurement, research, rail traction, oil and gas and marine. Intelliconnect cables can be waterproofed to IP68 and offer special features including phase matching and ruggedized assemblies for use in harsh environments.

Intelliconnect Group

www.intelliconnectgroup.com

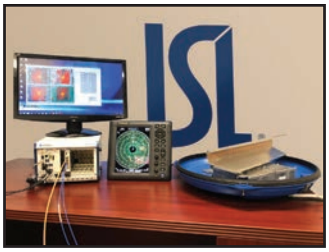

Virtual RF Hardware-in-the-Loop Flight Testing

ISL's real-time hardware-in-the-loop (HIL) RTEMES® system enables for the first time, virtual flight testing of advanced RF systems for radar, ELINT and electronic warfare applications. It supports multichannel RF systems from VHF to Ku-Band and is based on a cost-effective digital COTS transceiver/FPGA architecture. RTEMES® is designed to seamlessly integrate with ISL's RFView® RF Digital Engineering tools including high fidelity, physics-based modeling and simulation.

ISL

www.islinc.com

Directional Coupler Covers 26.5 to 40 GHz with 30 dB Coupling

VENDORVIEW

KRYTAR Model 264030 offers 30 dB of nominal coupling over the frequency range of 26.5 to 40.0 GHz (Ka-Band), in a compact and lightweight package. The coupler lends itself to wireless designs and many test and measurement applications within Ka-Band frequency. Ka-Band is used for many commercial and military satellite communications (satcom). Frequency sensitivity of ±0.5 dB, insertion loss of 1.3 dB, directivity greater than 12 dB, maximum VSWR is 1.7. Compact package measures 1.12 (L) x 0.40 (W) x 0.62 in. (H) and weighs 1.0 ounces.

KRYTAR

https://krytar.com/products/couplers/directional-couplers/

New 1 GHz OCXO Provides Ultra-Low Phase Noise

VENDORVIEW

To meet the increasing demand for high frequency OCXOs with ultra-low phase noise KVG's engineers have developed a 1 GHz OCXO. Using the advantages of a SC-cut crystal-based oscillator stage in combination with new analog frequency multiplication, the OCXO provides tight temperature stability and very good long-term stability. The 1 GHz OCXO comes up with excellent phase noise performance near the carrier with better than -112 dBc/Hz at 100 Hz as well as a very low noise floor below -155 dBc/Hz.

KVG Quartz Crystal Technology GmbH

www.kvg-gmbh.de/aktuelles/produktneuheiten/neuer-1-ghz-ocxo-mit-niedrigem-phasenrauschen-in-kleiner-bauform.html?lang=en

RF Power Sensors

VENDORVIEW

LadyBug Technologies' LB5944A, 44 GHz USB power sensor offers several features specifically designed for defense users. These include Option MIL, which prevents the storage of information inside the sensor; and Option SEC, a secure erase feature that allows sensitive users to erase any settings, offsets or data that have been stored within the sensor prior to the sensor leaving the secure environment. Additionally, the sensor utilizes LadyBug's patented active thermal stabilization which eliminates drift associated with accurate low-power measurements.

LadyBug Technologies

www.LadyBug-Tech.com

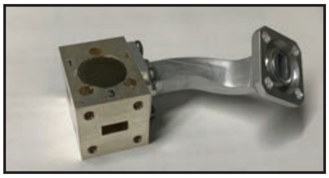

High Performance Components Since 1988

M Wave Design Corporation has been supplying low loss, high performance Ferrite and Waveguide components since 1988. The company specializes in high-mix, low volume microwave components. The unit illustrated above was a system design "afterthought" by its customer who ran out of space. We solid modeled and built the WR28 full-band circulator and waveguide run into their package constraints and "on time and in budget." M Wave Design Corporation designs and manufactures a broad range of custom passive microwave hardware from 100 MHz to 50 GHz.

M Wave Design Corporation

https://mwavedesign.com/

BAL-0032SSG 32 GHz Broadband Balun

The BAL-0032SSG is the industry's first surface-mount balun to support 32 GHz of instantaneous bandwidth. Hand-tuned for phase balance of better than 5 degrees and amplitude balance of better than 0.4 dB, the balun ensures signal integrity in high IBW applications that enable electronic warfare receivers to cover multiple frequency bands and multi-band radar solutions. Featuring a 10 MHz to 32 GHz frequency range, the balun delivers unmatched performance for next-generation data converters. Available now in an ultra-compact 5 x 9 mm package.

Marki Microwave
www.markimicrowave.com

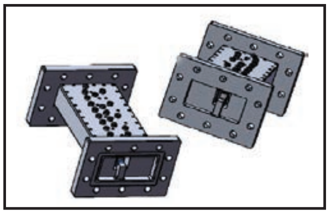

NEW 5G Filter for C-Band Satellite Receivers

MCV has designed a RED filter that will clear portions of the C-Band spectrum to support the growth of mobile data and 5G services in the U.S. and around the world for both the satellite communications and the wireless telecommunications market. McV RED 1 filter provides interference free signal covering 3200 to 4000 GHz with low loss and high attenuation on both sides and 40 dB rejection to 6.45 GHz. It is lighter and smaller than currently available models and equipped with CPR229 grooved interface (IP63 rating). Please contact sales@mcv-microwave.com for immediate delivery.

MCV Microwave
https://mcv-microwave.com

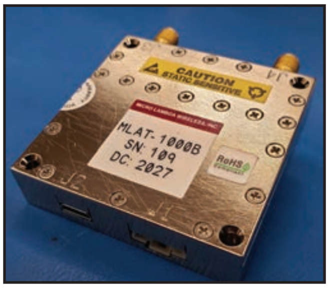

Micro Lambda Single-Channel Programmable Attenuators 10 MHz to 21 GHz

Micro Lambda Wireless, Inc offers the MLAT-Series single-channel programmable attenuators, ideal for a wide range of test equipment applications. They provide 0 to 30 dB or 0 to 60 dB attenuation in 0.5 dB steps over the 10 MHz to 21 GHz frequency range. All attenuators are housed in a compact package with SMA Female RF connectors. Controlled via USB or SPI, full software support provided, optional temperature ranges available.

Micro Lambda Wireless, Inc
www.microlambdawireless.com

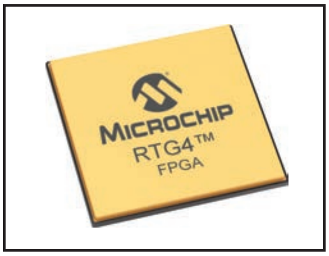

RTG4™ FPGAs – High-Speed QML Class V-Qualified FPGAs for Space

The company's wide range of radiation-tolerant (RT) FPGAs lets you select the right device to hit your power, size, cost and reliability targets, thereby reducing time to launch and minimizing cost and schedule risks. Building on a history of providing the most reliable, robust, low-power SONOS-, flash- and antifuse-based FPGAs in the industry, Microchip can offer you the best combination of features, performance and radiation tolerance.

Microchip Technology Inc.
www.microchip.com/rtg4

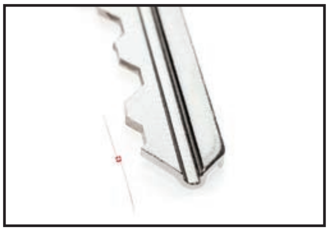

Microwave Components, Inc.

Microwave Components, Inc. (MCI) in Dracut, Mass., is a small, veteran-owned manufacturer of miniature air coils. MCI has been delivering custom, high Q, miniature air inductors to the aerospace, defense and space markets since 1978. Materials include: bare and insulated gold, copper, silver, gold plated copper, nickel copper alloy and aluminum wire. Inductances from 1 to 1000+ nH.

Microwave Components, Inc. (MCI)
www.mcicoils.com

RF Interference Mitigation Filter/ Amplifier

Overcome severe communication range issues caused by RF cosite interference on air-, sea-, and ground-based platforms with MPG's ICE3009 Filter/Amplifier. ICE3009 features a high dynamic range and agile filter/amplifier cascade to prevent receiver desensitization and to purify the transmit spectrum for fast frequency hopping VHF/UHF transceivers. ICE3009 features -55 dB selectivity (at 5 percent from F0), up to 10 dB receive gain, < 9 dB noise figure, +52 dBm receive input IP3 and up to 100 W RF transmit output power.

Microwave Products Group (MPG)
https://polezero.com/product/ice3009/

See Our VPX Transceiver Specs

VENDORVIEW

Norden's wideband VPX transceiver is used across military applications. It offers 2 to 18 GHz operation in a versatile OpenVPX platform. The NUDC2-18/1.3-2.3 includes internal LOs which provide an instantaneous IF bandwidth of 1 GHz and exceptional noise figure.

Norden Millimeter

https://nordengroup.com/wp-content/uploads/Norden-Transceiver.pdf

New Wearable SDR With Enhanced Ruggedization

Pixus Technologies announced a new compact implementation of its ruggedized enclosure line utilizing NI's Ettus Research™ brand software-defined radio (SDR). The new RB210 is a ruggedized version of NI's small form factor B210 SDR. It currently comes in an IP67 weather resistant style with options for full MIL grade implementations. The compact unit is approximately 87 tall x 156 wide and 300 mm long and weighs under 7 lbs. The RB210 features continuous frequency coverage from 70 MHz to 6 GHz.

Pixus Technologies

https://pixustechnologies.com/products/enclosure-system-solutions/specialty-small-form-factor-rugged-x310-other-2/specialty-small-form-factor-rugged-x310-other/

Filters, Multiplexers & Multifunction Assemblies

VENDORVIEW

Reactel manufactures a line of filters, multiplexers and multifunction assemblies covering up to 67 GHz. Reactel's talented engineers can design a unit specifically for your application, from small, lightweight units suitable for uncrewed flight or portable military systems to high-power units capable of handling up to 25 kW, connectorized or surface-mount.

Reactel

www.reactel.com

New SPINNER 1.00 mm RF Cable Connector

VENDORVIEW

The new 1.00 mm RF cable connector from SPINNER is especially suitable for use with UT-47 semi-rigid cable and are provided in standard or custom configurations with cable entries and soldering sleeves as well as a bulkhead, D-hole or four-hole panel mount version. SPINNER RF cable connectors are found in a wide range of applications such as communication infrastructure, medical, research, industrial, aerospace and defense, automotive and consumer products and must operate reliably even under the most difficult conditions.

SPINNER

www.spinner-group.com

Microwave Power Modules from Stellant Systems

Stellant Systems' M-1270 microwave power module (MPM) is a state-of-the-art amplifier used in threat simulators and search radar systems onboard common unmanned aerial vehicles and other high profile aircraft. Its extremely high-power output of 1 kW at 5 percent duty cycle from 9 to 10 GHz distinguishes it from the field. The MPM includes Stellant's L6134-54 mini-helix traveling wave tube driven by a low-power solid-state power amplifier contained within Stellant's proprietary power control unit.

Stellant Systems

www.StellantSystems.com

Designed for Durability. Engineered for Excellence.

Trexon solves the world's most challenging connectivity problems with relentless innovation, industry expertise and constant collaboration. Formed from the combination of top wire and cable companies, Trexon provides an expanding range of specialized products and solutions designed for rugged and specific conditions. The Trexon Engineered Products Group consists of the following industry leading companies; Cicoil, EZ Form Cable, The First Electronics Corporation, Hydro Group, Integrated Cable Systems and Power Connector Inc.

Trexon Company

https://youtu.be/n9ufNoBtJ9M

https://trexonglobal.com/engineered-products/

Sales Representatives

Eastern and Central Time Zones
Michael Hallman
Associate Publisher
(NJ, Mid-Atlantic, Southeast, Midwest, TX)
Tel: (301) 371-8830
Cell: (781) 363-0338
mhallman@horizonhouse.com

Shannon Alo-Mendosa
Northeastern Reg. Sales Mgr.
(New England, New York, Eastern Canada)
Tel: (781) 619-1942
salomendosa@horizonhouse.com

Pacific and Mountain Time Zones
Brian Landy
Western Reg. Sales Mgr.
(CA, AZ, OR, WA, ID, NV, UT, NM, CO, WY, MT, ND, SD, NE & Western Canada)
Tel: (831) 426-4143
blandy@horizonhouse.com

International Sales
Richard Vaughan
International Sales Manager
Tel: +44 207 596 8742
rvaughan@horizonhouse.co.uk

Germany, Austria, and Switzerland (German-speaking)
WMS.Werbe- und Media Service
Brigitte Beranek
Tel: +49 7125 407 31 18
bberanek@horizonhouse.com

France
Gaston Traboulsi
Tel: +44 207 596 8742
gtraboulsi@horizonhouse.com

Israel
Dan Aronovic
Tel: +972 50 799 1121
aronovic@actcom.co.il

Korea
Young-Seoh Chinn
JES MEDIA, INC.
Tel: +82 2 481-3411
yschinn@horizonhouse.com

China
Shenzhen
Jenny Li
ACT International
jennyl@actintl.com.hk

Shanghai
Linda Li
ACT International
Tel: 86-021-62511200
lindal@actintl.com.hk

Wuhan
Sky Chen
ACT International
skyc@actintl.com.hk

Beijing
Cecily Bian
ACT International
Tel: +86 135 5262 1310
cecilyb@actintl.com.hk

Hong Kong, Taiwan, Singapore
Floyd Chun
ACT International
Tel: +86-13724298335
floydc@actintl.com.hk

Japan
Katsuhiro Ishii
Ace Media Service Inc.
Tel: +81 3 5691 3335
amskatsu@dream.com

59TH WASHINGTON D.C.

AOC INTERNATIONAL SYMPOSIUM & CONVENTION

OCT. 25-27, 2022

REGISTER NOW AT 59.CROWS.ORG!

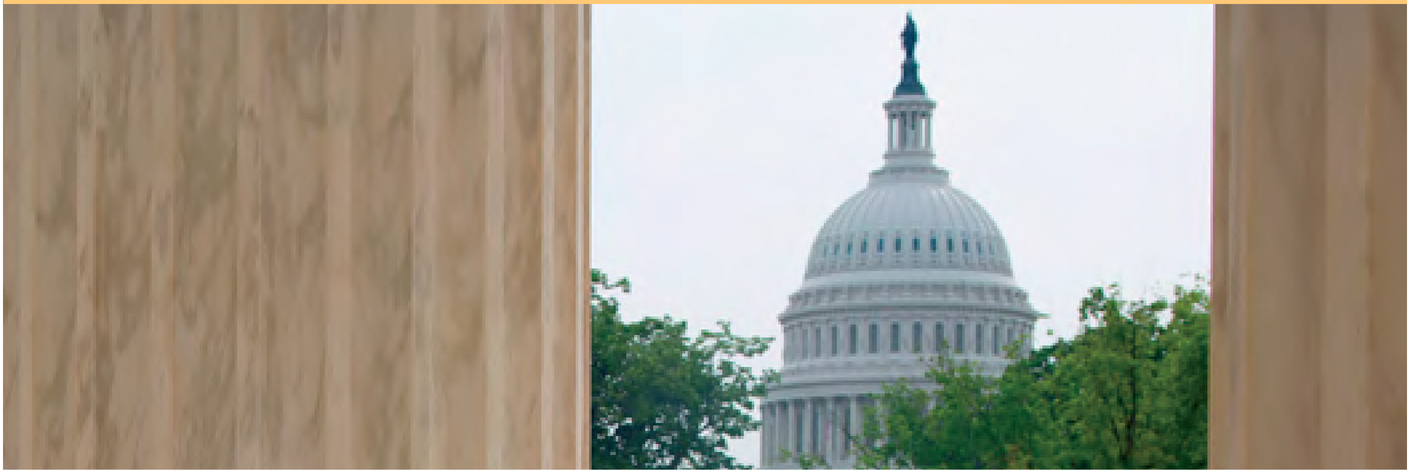

WHO SHOULD ATTEND

AOC 2022, the Association of Old Crow's Annual Symposium & Convention, brings together the *full spectrum of people* working in electromagnetic spectrum operations.

ACTIVE DUTY TO VETERAN

No matter what your mission, you need an advantage in the spectrum. A better understanding of the invaluable role of spectrum in military operations is imperative for success.

JUNIOR ENGINEER TO PRINCIPAL ENGINEER

You are the technology makers, the rapidly evolving designers. Through research and development, you are solving the problems and providing the solutions to the war fighters.

CASUAL TO PRO

The spectrum is part of your world and touches everything you do. You need to join our mission in order to gain the knowledge you need to drive decisions in your organization.

SUPPORT OUR MISSION • INFLUENCE OUR MISSION • LEARN OUR MISSION

59.crows.org

Host Sponsor

L3HARRIS

UHF TO KA-BAND

Defense Radar

For High-Sensitivity Surveillance & Acquisition

- In-stock and custom solutions (ITAR)
- Wideband, high power, low noise, high dynamic range
- 50+ years design and manufacturing experience
- Supply chain security—no EOL target

Long-Range Surveillance

Battlefield Management

Fire Control

Mini-Circuits®